
Electronic Thesis and Dissertation Repository

3-3-2023 8:30 AM

Vertebral Endplate Structural Defects: Measurement, Prevalence and Associated Factors

Aliyu Lawan, *The University of Western Ontario*

Supervisor: Battié, Michele C., *The University of Western Ontario*

A thesis submitted in partial fulfillment of the requirements for the Doctor of Philosophy degree in Health and Rehabilitation Sciences

© Aliyu Lawan 2023

Follow this and additional works at: <https://ir.lib.uwo.ca/etd>



Part of the [Anatomy Commons](#), [Medical Sciences Commons](#), [Radiology Commons](#), [Rehabilitation and Therapy Commons](#), and the [Research Methods in Life Sciences Commons](#)

Recommended Citation

Lawan, Aliyu, "Vertebral Endplate Structural Defects: Measurement, Prevalence and Associated Factors" (2023). *Electronic Thesis and Dissertation Repository*. 9147.
<https://ir.lib.uwo.ca/etd/9147>

This Dissertation/Thesis is brought to you for free and open access by Scholarship@Western. It has been accepted for inclusion in Electronic Thesis and Dissertation Repository by an authorized administrator of Scholarship@Western. For more information, please contact wlsadmin@uwo.ca.

Vertebral Endplate Structural Defects: Measurement, Prevalence and Associated Factors

Abstract

Objective: To synthesize current knowledge on the association of endplate structural defects (EPSD) with back pain (BP), improve EPSD measurement, and investigate EPSD prevalence, distribution, and association with age and body mass index (BMI).

Methods: In study 1, a systematic review was conducted on five databases for studies reporting on the association between EPSD and BP. Studies 2 and 3 used CTs and μ CTs of 19 embalmed cadavers to examine the diagnostic accuracy of common EPSD assessment methods, and to develop and validate a novel method. Study 4 used the novel method on 200 adult males' MRI to estimate EPSD prevalence, distribution, and association with age and BMI.

Results: Data from the 26 studies (11,027 subjects) on the association of EPSD with BP included in the systematic review were not pooled due to heterogeneity ($I^2=73\%$) relating to measurements and nomenclature, except for erosion, sclerosis and Schmorl's nodes (OR:1.53-1326). The common EPSD assessment methods had a sensitivity of 70.9%-79.5% and specificity of 57.5%-79.1% and certain phenotypes were absent or misclassified (e.g., wavy/irregular and erosion). A novel method was therefore developed, consisting of definitions and atlases of six EPSD phenotypes with good inter-rater reliability for EPSD presence (K=0.65-0.68) and improved sensitivity (71.0%-79.0%) and specificity (77.0%-87.0%). Inter-rater reliability for specific phenotypes was fair (K=0.52-0.55). Using the novel method, there was a high prevalence of EPSDs (45.6%), with erosion (17.6%) being the most common phenotype. EPSD occurred more in the upper lumbar regions ($\chi^2=41.68$) and on the caudal endplates ($\chi^2=9.28$) and were associated with greater age (OR:1.02, 95%CI:1.01-1.03) but not BMI (OR:1.00, 95%CI:0.98-1.03). Furthermore, age was associated with focal defects (OR:1.02, 95%CI:1.00-1.03) and erosion (OR:1.03, 95%CI:

1.01-1.04), while BMI was only associated with corner defects (OR:1.15, 95%CI:1.03-1.30).

Conclusion: The lack of standardized methods has impeded the understanding of EPSD and BP. Using a novel standardized assessment method, a developmental origin of Schmorl's nodes is supported, and focal and erosive defects appear degenerative in nature, while corner defects appear to have a biomechanical origin. The project has opened a new avenue for measurement and further understanding of EPSD and their etiology and clinical significance.

Keywords

Back pain, Schmorl's nodes, vertebral endplate, endplate defect, endplate irregularity, endplate lesion, endplate abnormalities, endplate assessment, endplate defect classification, endplate defect phenotypes, reliability, validity, psychometric properties, measurement methods

Summary for Lay Audience

Recent advances in medical imaging have allowed a clearer view of the endplate, a thin bony structure with rich blood and nerve supply, that is located at the interface between intervertebral discs and vertebrae of the spine. The endplate is now attracting attention as a possible source or contributor to back pain. Endplate structural defects (EPSD) are common, yet little is known of their causes and clinical consequences, and related measurements are varied and underdeveloped. Toward advancing the understanding of EPSD to help resolve questions about their occurrence, causes and clinical significance, we first investigated the importance of EPSD to back pain. We found that they are associated with pain, but problems due to underdeveloped methods of assessment make this finding uncertain, particularly for various types of EPSD. We, therefore, assessed the reliability and validity of common endplate assessment methods, which led to the development of an improved EPSD assessment method. The newly developed EPSD assessment method and data from a large population-based study of adult males (n=200) were used to assess EPSD prevalence, distribution and association with age and body mass index. We found that EPSD were very common in the adult male population, but occurrence varied by type, with erosion being the most common EPSD phenotype. EPSD occurred more at the upper lumbar levels and on the endplate below rather than above the intervertebral disc. EPSD were related to older age but not body mass index. However, findings differed by type of EPSD. Schmorl's nodes were not related to aging and may be developmental, while focal and erosive defects were related to older age, and corner defects to the body mass index. The project has provided a means to better identify EPSD to advance research on their prevalence, causes and consequences.

Co-Authorship Statement

This thesis contains material from one published manuscript (Chapter 2) and three manuscripts to be submitted for publication (Chapters 3, 4 and 5). Aliyu Lawan is the primary author of all chapters in this thesis with contributions from the following:

Chapter 2

J.C. Videman, Research Assistant, Faculty of Health and Rehabilitation Sciences, Western University.

M.C. Battié, Professor, Faculty of Health and Rehabilitation Sciences, and Western's Bone and Joint Institute, Western University.

Chapter 3

A. Leung, Associate Professor, Department of Medical Imaging, Victoria Hospital, London Health Sciences Centre

S. Leung, Radiologist, Department of Medical Imaging, Victoria Hospital, London Health Sciences Centre

J. Faul, MSc. Candidate, Anatomy and Cell Biology Department, Schulich School of Medicine and Dentistry, Western University

D.W. Holdsworth, Professor, Schulich School of Medicine, Western University

J. Udoh, Imaging Technician, Schulich School of Medicine, Western University

D.M. Bryant, Professor, Faculty of Health and Rehabilitation Sciences, Western University

M.C. Battié, Professor, Faculty of Health and Rehabilitation Sciences, and Western's Bone and Joint Institute, Western University.

Chapter 4

A. Leung, Associate Professor, Department of Medical Imaging, Victoria Hospital, London Health Sciences Centre

S. Leung, Radiologist, Department of Medical Imaging, Victoria Hospital, London Health Sciences Centre

J. Faul, MSc. Candidate, Anatomy and Cell Biology Department, Schulich School of Medicine and Dentistry, Western University

V.L. Cheung, Radiology Resident, Department of Medical Imaging, Victoria Hospital, London Health Sciences Centre

D. Wang, Radiologist, Department of Medical Imaging, Victoria Hospital, London Health Sciences Centre

K. Tay, Radiologist, Department of Medical Imaging, Victoria Hospital, London Health Sciences Centre

D.M. Bryant, Professor, Faculty of Health and Rehabilitation Sciences, Western University

M.C. Battié, Professor, Faculty of Health and Rehabilitation Sciences, and Western's Bone and Joint Institute, Western University.

Chapter 5

M.C. Battié, Professor, Faculty of Health and Rehabilitation Sciences, and Western's Bone and Joint Institute, Western University.

Acknowledgments

I would first like to thank my supervisor, Dr. Michele C. Battié for her trust, support, and exceptional mentorship over the last four years. Dr. Battié provided me with access to the Anatomy and Cell Biology Cadavers and the Twin Spine Study dataset, the possibility to participate in the International Society for the Study of Lumbar Spine, the International Forum for Back and Neck Pain Research in Primary Care, and encourage me to pursue several activities such as the Collaborative Specialization in Musculoskeletal Health Research at the Western's Bone and Joint Institute, participate in many international conferences, co-coordinate the PT field seminars, and co-supervised MPT project among others. Important to mention is the feeling of having not only a supervisor but a mother. Thank you so much for the opportunities you have provided. *Miyetti masim*

My sincere thanks to Dr. Andrew Leung and Dr. Dianne Bryant for serving on my candidacy examination and thesis committees, you both provided me with constructive feedback and advice during this project. My sincere appreciation to Western's Health and Rehabilitation Sciences and Bone and Joint Institute for providing me with knowledge through the courses I undertook and the financial support I received, through a Graduate Scholarship and CMHR grant. This work would have not been possible without the support I received from my collaborators, Western's Common Spinal Disorders Lab, Anatomy and Cell Biology, Roberts Research Institute, CANSpine lab and of course all the staff and professors that have provided relentless service over these years. Also, I would like to express gratitude to the donors and their families, and to the TSS participants without whom this project would not have been possible. My acknowledgment will not be complete without appreciating my previous teachers, supervisors and training and job organizations. I would like to appreciate my grandmother (Haj. Hafsat Addan-Giji), grandfather (Alh. Aliyu Musa Abubakar), mother (Haj. Fatima Goni), father (Alh. Baba Ladan), siblings and friends. Thank you for all the supports. To my wife, Dr. Hadiza Mohammed, words cannot express how grateful I am for having you, and for taking care of our two beautiful kids (Hafsat and Aliyu) while I am away on this mission. Thank you. Finally, to my kids, nieces, and nephews, I hope this will be an example to you of what passion, hard work, and support from family and friends can help you achieve. *A karshe ina godiya ga yan'uwa da abokai*

Table of Contents

| | |
|---|------|
| Abstract | ii |
| Summary for Lay Audience | iv |
| Co-Authorship Statement..... | v |
| Acknowledgments..... | vi |
| Table of Contents | vii |
| List of Tables | xi |
| List of Figures | xiii |
| List of Appendices | xv |
| List of Abbreviations | xvi |
| Chapter 1 | 1 |
| 1 Introduction: Background and Rational | 1 |
| 1.1.1 Objectives | 3 |
| 1.2 Introduction to the endplate and other relevant anatomy of the spinal column..... | 3 |
| 1.2.1 Vertebra..... | 4 |
| 1.2.2 Intervertebral disc | 5 |
| 1.2.3 Endplate | 5 |
| 1.3 Imaging modalities and applications to the endplate | 8 |
| 1.3.1 Computed Tomography | 8 |
| 1.3.2 Microscopic Computed Tomography | 9 |
| 1.3.3 Magnetic Resonance Imaging..... | 9 |
| 1.4 Theoretical Framework for EPSD in vertebrogenic pain | 12 |
| 1.4.1 Biomedical model | 12 |
| 1.4.2 The Pain Gate Control Theory | 14 |
| 1.4.3 Biopsychosocial model | 15 |

| | | |
|----------------|---|----|
| 1.5 | The Cadaveric and Twin Spine Study Samples | 17 |
| 1.5.1 | The Cadaveric Sample | 17 |
| 1.5.2 | The Twin Spine Study Sample..... | 17 |
| Chapter 2..... | | 19 |
| 2 | The association between vertebral endplate defects and back pain: A systematic review and meta-analysis | 19 |
| 2.1 | Materials and Methods..... | 21 |
| 2.1.1 | Search strategy and Databases | 21 |
| 2.1.2 | Selection criteria | 21 |
| 2.1.3 | Data extraction | 21 |
| 2.1.4 | Risk of Bias (Quality) assessment | 22 |
| 2.1.5 | Analysis..... | 22 |
| 2.2 | Results..... | 23 |
| 2.2.1 | Search and selection..... | 23 |
| 2.2.2 | Study characteristics | 25 |
| 2.2.3 | Meta-analysis | 37 |
| 2.2.4 | Quality assessment and GRADE of evidence..... | 40 |
| 2.3 | Discussion | 42 |
| Chapter 3..... | | 44 |
| 3 | Detection and characterization of Vertebral Endplate Structural Defects on CT: A Diagnostic Test Study | 44 |
| 3.1 | Materials and Methods..... | 46 |
| 3.1.1 | Materials | 46 |
| 3.1.2 | Image acquisition | 47 |
| 3.1.3 | Assessment of EPSD on clinical CT scans | 47 |
| 3.1.4 | Assessment of EPSD on μ CT (reference standard) | 48 |

| | | |
|-----------|--|----|
| 3.1.5 | Statistical Analysis..... | 49 |
| 3.2 | Results..... | 50 |
| 3.3 | Discussion..... | 57 |
| Chapter 4 | | 61 |
| 4 | Development and Validation of a novel Endplate Structural Defects Classification System..... | 61 |
| 4.1 | Materials and Methods..... | 63 |
| 4.1.1 | Materials..... | 63 |
| 4.1.2 | Image acquisition..... | 63 |
| 4.1.3 | Procedure..... | 64 |
| 4.1.4 | Statistical Analysis..... | 65 |
| 4.2 | Results..... | 66 |
| 4.2.1 | Instruction Manual: Endplate Structural Defects Classification Assessment..... | 69 |
| 4.2.2 | Scale evaluation..... | 70 |
| 4.3 | Discussion..... | 73 |
| Chapter 5 | | 76 |
| 5 | Endplate Structural Defects: Prevalence, Distribution and Association with Age and BMI in Adult Males..... | 76 |
| 5.1 | Sample and Methods..... | 78 |
| 5.1.1 | Sample..... | 78 |
| 5.1.2 | Data Acquisition..... | 79 |
| 5.1.3 | Endplate Structural Defect Evaluation Protocol..... | 79 |
| 5.1.4 | Data Analysis..... | 81 |
| 5.2 | Results..... | 82 |
| 5.2.1 | Prevalence of Endplate Structural Defects..... | 82 |
| 5.2.2 | Size of Endplate Structural Defects..... | 85 |

| | | |
|------------------|--|-----|
| 5.2.3 | Distribution of Endplate Structural Defects..... | 86 |
| 5.2.4 | Association of Endplate Structural Defects with Age and BMI..... | 87 |
| 5.3 | Discussion..... | 88 |
| Chapter 6 | | 94 |
| 6 | General Discussion and Conclusions..... | 94 |
| 6.1 | Distinct EPSD phenotypes are associated with Back Pain..... | 94 |
| 6.2 | Common EPSD assessment methods are limited by phenotypes represented..... | 95 |
| 6.3 | Introduction of a new EPSD classification and assessment method..... | 97 |
| 6.4 | EPSD phenotypes have distinct prevalence, distribution patterns and possible etiology..... | 98 |
| 6.5 | Study limitations..... | 99 |
| 6.6 | Conclusions..... | 100 |
| 6.7 | Significance..... | 101 |
| 6.8 | Future directions..... | 101 |
| References | | 103 |
| Appendices | | 119 |
| Curriculum Vitae | | 131 |

List of Tables

| | |
|--|----|
| Table 2-1: Sample characteristics of included studies, with endplate structural defect phenotype and back pain case definitions..... | 26 |
| Table 2-2: The frequency of endplate defects, proportions, and unadjusted and adjusted odds ratios (95% confidence intervals) as reported in each included study. | 30 |
| Table 3-1: Inter-rater reliability of endplate defect assessments by raters using Brayda-Bruno (B-B) et al and Feng et al methods. (Values are kappa coefficients (95% CI) for categorical variables and ICCs (95% CI) for continuous measurements.) | 51 |
| Table 3-2: Frequencies of endplate structural defects detected by Brayda-Bruno et al and Feng et al methods | 52 |
| Table 3-3: Frequencies of endplate structural defects categorized according to Brayda-Bruno et al and Feng et al methods and corresponding μ CT..... | 53 |
| Table 3-4: Sensitivity for the assessment of endplate structural defects for Brayda-Bruno et al and Feng et al compared to the reference standard (μ CT) for individual rater and the consensus rating. | 54 |
| Table 3-5: Correlation of clinical-CT endplate structural defects measurements with μ CT | 54 |
| Table 4-1: Inter-rater reliability of endplate structural defect assessments by raters. Values are kappa coefficients (95% CI) for categorical variables and ICCs (95% CI) for continuous measurements. | 70 |
| Table 4-2: Specificity and sensitivity for the assessment of endplate structural defects to the reference standard (μ CT) for individual rater. | 71 |
| Table 4-3: Sensitivity and specificity of non-dominant endplate structural defect assessments by raters. Values are kappa coefficients (95% CI) for categorical variables. | 72 |

| | |
|---|-----|
| Table 4-4: Correlations between dimensions of clinical CT and corresponding μ CT | 72 |
| Table 5-1: Intra-rater reliability the EPSD classification..... | 83 |
| Table 5-2: Size of endplate structural defect phenotypes (means and standard deviations or frequencies and percentages)..... | 86 |
| Table 5-3: Distribution of EPSD within the endplate (frequency (and percentage) of defects located solely or partially in part in the portion of the endplate noted)..... | 87 |
| Table 5-4: Distribution of EPSDs by endplate location (cranial vs caudal) and spinal region (upper vs lower)..... | 87 |
| Table 5-5: Association between EPSDs with age and BMI..... | 88 |
| Appendix A:- Table 0-1: Search strategy for each database..... | 119 |

List of Figures

| | |
|---|----|
| Figure 1-1: Human spinal vertebrae, highlighting the functional spinal units and endplate. Adapted from Wang et al (35) and retrieved from NYSORA (36) | 4 |
| Figure 1-2: A cadaveric Functional Spinal Unit with a corresponding schematic diagram showing vascular and neural supply to the endplate and intervertebral disc. Adapted from Crock et al (61) and Moore et al (37) | 7 |
| Figure 1-3: The lumbar vertebrae on CT, MRI (T1) and μ CT. Adapted from Fournier et al (78) and Carter (79) | 11 |
| Figure 1-4: Schematic representation of peripheral and central sensitization. Extracted from Latremoliere and Woolf (98)..... | 14 |
| Figure 1-5: Theoretical Model for Chronic Back Problems. Showing the interaction between various models (biomedical) and (biopsychosocial comprising biological, social and psychological factors) and theories (gate control theory and hospice movement) | 16 |
| Figure 2-1: Flowchart of study selection and inclusion..... | 24 |
| Figure 2-2: Forest plot for associations of each endplate defect type with various back pain definitions, with individual study and pooled estimates, and 95% confidence intervals. As can be seen from the high I^2 values, there was unacceptably high heterogeneity among all studies and those of particular endplate phenotypes to rely on the pooled estimates, with the exception of studies of <i>sclerosis</i> and <i>erosion</i> | 38 |
| Figure 2-3: Forest plot of the association of various back pain phenotypes with endplate defects with pooled estimates and 95% confidence intervals. As can be seen from the high I^2 values, there was unacceptably high heterogeneity among all studies and those of particular back pain phenotypes to rely on the pooled estimates, with the exception of studies of <i>back pain incidence</i> and <i>back pain frequency</i> . It should be noted, however, that the estimates for the latter came from one study. | 39 |

| | |
|---|----|
| Figure 2-4: Forest plot of the association of Schmorl’s nodes and various back pain phenotypes among general population samples with pooled estimates and 95% CIs. | 40 |
| Figure 2-5: Percentage distribution of the types of bias sufficiently and insufficiently assessed in the quality appraisal criteria of the included studies, specific to the study design used..... | 41 |
| Figure 3-1: Sensitivity of endplate structural defect phenotypes assessments on Clinical CT (Brayda-Bruno and Feng) to the reference standard (μ CT)..... | 55 |
| Figure 3-2: EPSD phenotypes observed on μ CT and corresponding CT | 57 |
| Figure 4-1: Assessment manual comprising of EPSD phenotypes, definitions, and atlases | 68 |
| Figure 5-1: EPSD phenotypes assessed using the new classification system..... | 84 |
| Figure 5-2: Distribution of endplate structural defect phenotypes by disc level. The numbers are percentages of all endplates assessed at each spinal level with the EPSD phenotype..... | 85 |

List of Appendices

| | |
|---|-----|
| Appendix A:- Table 0-1: Search strategy for each database..... | 119 |
| Appendix A:- Table 0-2: Prisma Checklist..... | 122 |
| Appendix A: Table 0-3: Evaluation guide comprising the μ CT, reference standard and CT, index test (Feng et al and Brayda-Bruno et al methods) assessments protocol. | 125 |
| Appendix A:- Table 0-4: STARD checklist..... | 129 |

List of Abbreviations

AM: Assessment Method
ANOVA: Analysis of Variance
Ant: Anterior
AP: Anterior Posterior
BMD: Bone Mineral Density
BMI: Bone Mass Index
BP: Back Pain
CI: Confidence Interval
CSF: Cerebrospinal Fluid
CT: Computed Tomography
DD: Disc degeneration
Def: Defect
Diam: Diameter
EPD: EndPlate Defect
EPSD: Endplate Structural Defect
FSU: Functional Spinal Units
LL: Left Lateral
LR: Right Lateral
MC: Modic Changes
MRI: Magnetic Resonance Imaging
MS: Motion Segment
Post: Posterior
Rad: Radiograph
RF: Radio Frequency
TD: Transverse diameter
TE: Time to Echo
TR: Repetition Time
TSS: Twin Spine Study
Vert: Vertebrae
 μ CT: microscopic Computed Tomography

Chapter 1

1 Introduction: Background and Rational

Back pain is the most prevalent musculoskeletal disorder throughout the world and one of the most common reasons for hospital visits in North America (1,2). According to the 2017 global burden of disease, back pain imposes more disability than any other disease or injury (3,4). It results in a high economic, psychological, and societal burden on affected individuals, their families and society. Despite the overwhelming burden of back pain and decades of back pain research, the pathoanatomy remains unknown in the vast majority of cases. Due to its obscure origin, back pain is mainly idiopathic (5). A biopsychosocial model with multidimensional approaches has been employed in research and management of back pain, with the biological aspect focused on identifying specific structural causes of the back pain. Historically, the biomedical model is traced back to the 19th-century model of nociception. The nociceptive process involved unique pain receptors being stimulated physically or chemically to produce a noxious stimulus that is transmitted to the central nervous system and perceived as pain (6). Against the background of the biomedical model, the contribution of the intervertebral disc to back pain has been questioned due to its sparse neural and blood supply. In fact, back pain preventive and treatment approaches targeting disc degeneration and pathology has resulted in little or no benefit (7–10).

The recent advances in imaging modalities have shifted attention to the long-neglected endplate, a thin mechanical interface between the intervertebral disc and the vertebral body, as a possible culprit in back pain. The endplate has a plentiful vascular and neural supply compared to the intervertebral disc. Furthermore, histologic evidence showed an increase in the density of blood and neural supply in the presence of endplate defects or adjacent disc degeneration (11,12). Endplate Structural Defects (EPSD) are common spinal imaging findings in both healthy and patient populations. However, most previous studies have investigated EPSD without differentiating types or referred to all EPSD as Schmorl's nodes (13), although it is now clear that Schmorl's nodes are not the sole vertebral EPSD. Schmorl's nodes were first described by Von Luschka in 1858 and later described in detail by Christian Georg Schmorl in 1927 (14). Since that time, Schmorl's nodes have been

referred to as focal endplate defects, local collapse of the endplate or endplate discontinuity, with or without subchondral bone involvement, (13,15) or protrusion of disc tissue through the endplate into the vertebral marrow (16). Schmorl's nodes are common, but the understanding of Schmorl's nodes is limited and remains conflicting. For example, the etiology of Schmorl's nodes remains a controversy. Several theories, including congenital and developmental (16–18), degenerative diseases (17,19), trauma (20–22), and autoimmune disorders (23), have been proposed to explain the development of Schmorl's nodes. Similarly, associations between Schmorl's nodes and disc degeneration and pathology (17,24,25), Modic changes, bone mineral density and back pain (20,26,27) remain conflicting. Several factors have been postulated as responsible for the inconsistencies, including differences in imaging modality, population studied (age and subject characteristics), and variations in the definition of EPSD terms. The reported prevalence rate of Schmorl's nodes has varied from 9% to 79% (17,26,28,29), with a higher prevalence from visual inspection from cadaveric spines than when acquired from Magnetic Resonance Images (MRI) in general population or patient samples.

Furthermore, when endplate defects are studied in general terms, including all observable phenotypes or definitions of EPSD, the prevalence widens from 6% to 97% (30,31). General terms include various EPSD that differ in topographical appearance, prevalence, and distribution, suggesting EPSD phenotypes have unique etiologies and may consequently differ in clinical presentation (12,32). For example, Schmorl's nodes are common in the upper spinal regions while endplate erosion and calcification are more common at the lower lumbar vertebrae (17,33), where the endplate is susceptible to a greater range of motion of flexion and extension (34). Yet, erosion is associated with demineralization while sclerosis is associated with mineralization.

However, as the study of EPSD advances, many problems have hindered progress in understanding the endplate. A study from the ISSLS Degenerative Spinal Phenotypes focus Group showed great disagreement among leading researchers and clinicians in naming and describing EPSD, and an overwhelming majority agreed with the need for standardized EPSD measurement and classification. Against this background, we reviewed the literature on the nomenclature and measurement methods of EPSD. The review highlighted 34

different terms used to describe EPSD but were never defined in most studies (65%). Of the 34 different terms used, some appeared to represent the same phenomenon, while the same terms were occasionally defined differently between studies. Similarly, majority (71.6%) of the studies reported no psychometric properties of the endplate measurements used. While the relatively few studies that reported psychometric properties, 14 (6.6%) reported only intra-rater reliability, 17 (8.1%) reported only inter-rater reliability, and 29 (13.7%) studies reported both, and no study reported a validation process or outcome of any measurement method. The review indicated the lack of common language for effectively communicating structural endplate findings.

In addition, the wide prevalence rates, and conflicting findings of EPSD reported in the literature may be due, in part, to the lack of standardized EPSD nomenclature and measurement methods. Also, without differentiating distinctly different EPSD phenotypes, their etiology and clinical outcomes will be obscured. Therefore, this thesis attempted to improve the understanding of the EPSD in spinal degeneration and back pain conditions by focusing on their measurement, classification, prevalence, distribution and association with age and BMI.

1.1.1 Objectives

The series of studies in this thesis aimed to:

1. Review the scientific literature on the association between EPSD and back pain, and where possible pool data for meta-analysis.
2. Determine the reliability and validity of common measurement methods for EPSD.
3. Develop and validate a novel EPSD classification system.
4. Determine EPSD prevalence, distribution patterns, and investigate associations with age and BMI using the novel classification system.

1.2 Introduction to the endplate and other relevant anatomy of the spinal column

The spinal column is typically composed of 24 vertebrae divided into cervical (n=7), thoracic (n=12), and lumbar vertebrae (n=5), as well as the sacrum and coccyx. Adjacent vertebrae are separated by an intervertebral disc, anchored through the vertebral endplate

inferiorly and superiorly. The Functional Spinal Unit, otherwise known as the spinal motion segment, comprises an intervertebral disc and its two adjacent vertebrae held together by ligaments and muscles and supplied by the interosseous nerves and blood supply. The disc, located anteriorly in the motion segment, and the facet joints, located posteriorly, allow for movement.

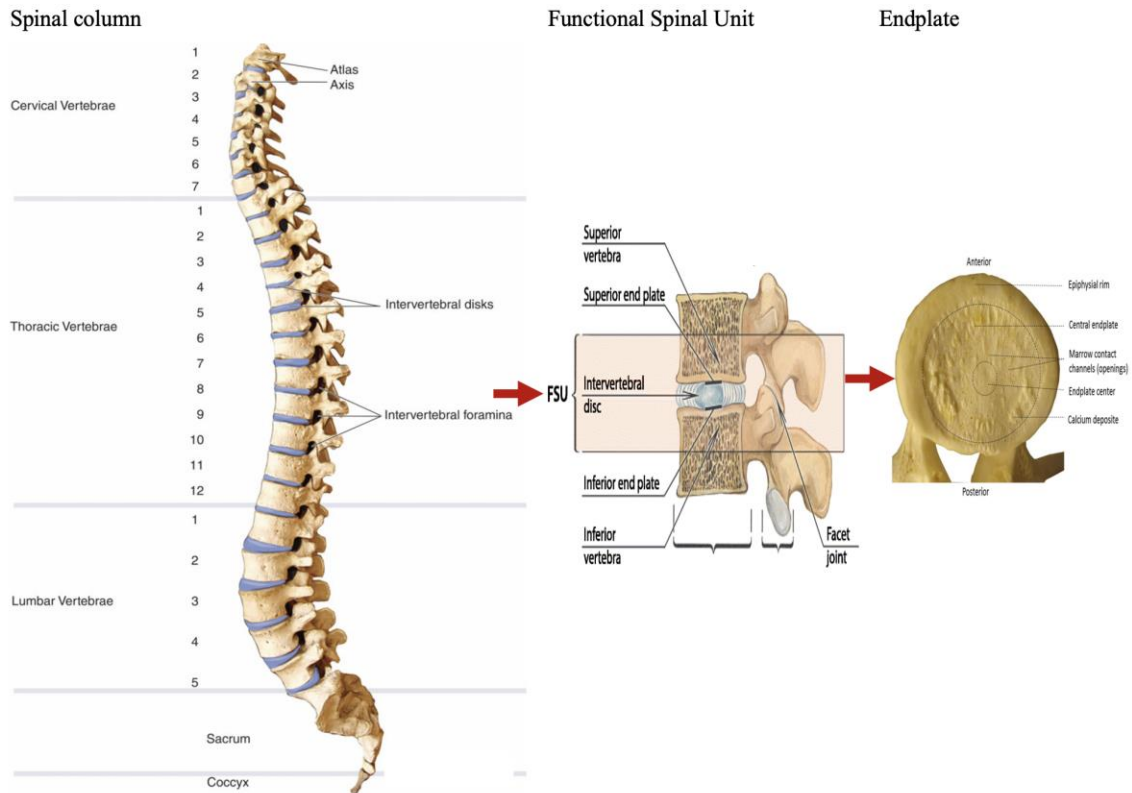


Figure 1-1: Human spinal vertebrae, highlighting the functional spinal units and endplate. Adapted from Wang et al (35) and retrieved from NYSORA (36)

1.2.1 Vertebra

Each vertebra consists of a vertebral body and vertebral arch, with pedicles, lamina, and a spinous process (Figure 1-1). The vertebral body is the largest component of the vertebra and is made up mainly of trabecular bone internally and enclosed externally by a thin layer of cortical bone except its superior and inferior which are covered by the endplates.

The vertebral arch is a circle of bone forming the bony canal through which the spinal cord or cauda equina passes. The vertebral arch is composed of the pedicles and the lamina. The

pedicles are short projections of bone from the posterior vertebral body, one on each side, that extend posteriorly to the transverse processes, while the lamina connect the transverse processes to the spinous process, completing the bony arch (37).

1.2.2 Intervertebral disc

The intervertebral disc consists of two main components, the *annulus fibrosus* and the *nucleus pulposus*. The annulus fibrosus is the most outer part of the disc, consisting of fibrous rings and concentric lamellae of fibrocartilage. The nucleus pulposus is the inner part of the disc, consisting of 88% water content at birth which is responsible for the flexibility and resilience of the disc. However, with increasing age and degeneration of the disc, the amount of water and nucleus matrix decreases, resulting in a loss of elasticity (38).

The intervertebral disc is a mechanically resilient tissue and is largely avascular. Although the outer 1/3 of the annulus fibrosus contains blood vessels, there is an average of 20 mm from one cell to its nearest blood supply (39). Thus, the intervertebral disc depends on diffusion of nutrients through the adjacent endplates (40,41).

1.2.3 Endplate

The endplate is a thin mechanical interface between the vertebral body and the intervertebral disc. It consists of two components, the cartilaginous and bony endplate (42). There are two endplates in each motion segment, which are cranial and caudal to each intervertebral disc. The *cartilaginous endplate* is formed in early life. It is a thin layer of hyaline cartilage with an average thickness of 0.6mm, which is thinner at the nucleus (40). The cartilaginous endplate has microscopic blood vessels during the development of the spine, which provide nutrition for the disc. During skeletal maturation, the cartilaginous endplate may undergoes progressive mineralization and eventually becomes absorbed and replaced by the bony endplate (43,44). The *osseous endplate* also known as the vertebral or bony endplate is the upper and lower shell of the vertebral body. The endplate consists of the epiphysial rim and the central endplate. The epiphysial rim also known as the epiphysial ring (19) is the rounded smooth elevated bone at the circumference of the endplate. The epiphysial rim is derived from the annular epiphysis, a place where the annulus fibrosis anchors to the vertebra. Within the epiphysial ring is the thinner central

endplate. The central endplate is characterized by rich marrow contact channels or blood vessel openings through which capillary buds emerge (45,46). The capillary buds' function to provide a nutritional supply to the disc. The capillary buds are important structures that are impaired in endplate sclerosis secondary to the accumulation of calcium plaques on the endplate.

1.2.3.1 Embryology and histology of the endplate

At the sixth embryonic week, the vertebrae begin as a cartilage anlagen from chondrification centers of the sclerotome (47). The anlagen begins ossification at its centrum around invading blood vessels (48), which is separated from the developing disc by an epiphyseal plate made up of columnar cartilage. The ring apophysis at the periphery of the epiphyseal plate forms the insertion of the annular fibres and does not participate in the longitudinal growth of the vertebrae. A complete endplate is formed by the age of 18 through the thinning of the epiphyseal cartilage and the formation of a subchondral plate and the fusion of the ring apophysis to the vertebral body (49).

The endplate is made up of cartilage, consisting of chondrocytes evenly spread within the extracellular matrix of proteoglycans, collagen (type I and II), and water. The endplate has its collagen fibres aligned horizontally, parallel to the vertebral endplate. In a healthy disc, the endplate is constituted of 300 µg/mg of cartilage proteoglycan, 78% water and 0.9 ng/mg Type I collagen (50). Although the thickness of the cartilaginous endplate varies across its surface, it is typically between 0.1 and 2.0 mm thick (40,51). The bony endplate is a thickened porous layer of trabecular bone consisting of osteocytes within saucer-shaped lamellar packets (52). The bony endplate is typically between 0.2 and 0.8 mm thick depending on the spinal level and location (53–56).

1.2.3.2 Innervation of the endplate

Unlike the intervertebral disc, the endplate has a plentiful nerve and blood supply as shown in Figure 1-2. The vertebral capillaries and nerves enter the vertebral body from the posterior vascular foramen, accompanying the basivertebral vessels (57), and by penetrating the anterior cortex into the vertebral marrow (57,58). The vertebral marrow adjacent to the bony endplate consists of hematopoietic and fat cells, small capillaries, and

nerves. The innervation system accompanies the vertebral vascular distribution, branches from these nerves extend to form an arterial grid at the vertebral centrum, then branch and end at the peripheral regions of the vertebral body, including the vertebral endplate (59,60). The central endplate is responsible for the nutrition exchange at the bone-disc interface, which contains a highly concentrated bed of capillaries and nerves (58). However, with the presence of disc degeneration or EPSD, the density of blood and neural supply has been found to be higher at all parts of the endplate (11).

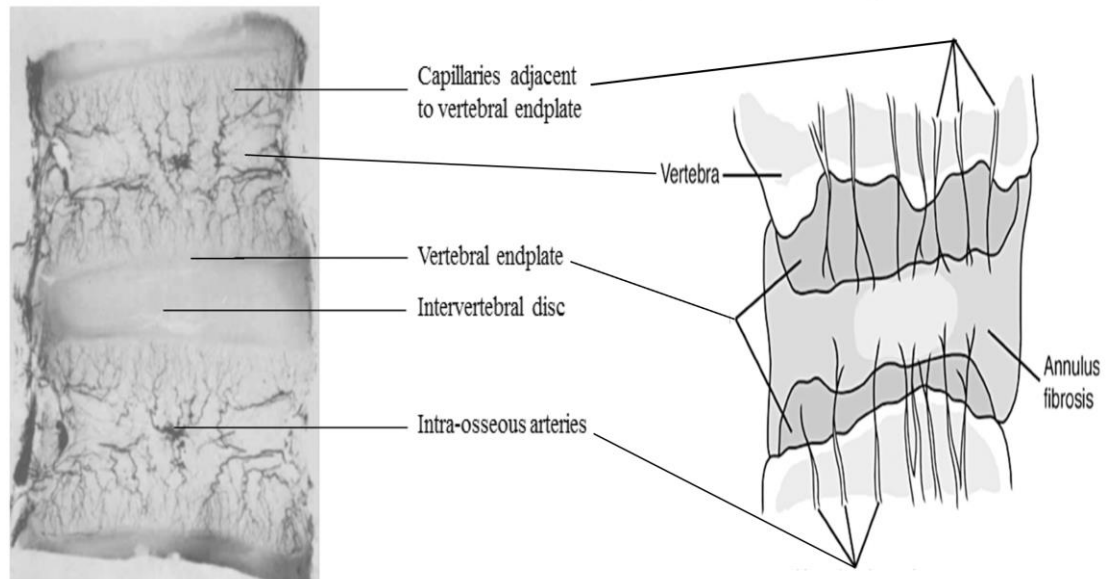


Figure 1-2: A cadaveric Functional Spinal Unit with a corresponding schematic diagram showing vascular and neural supply to the endplate and intervertebral disc.

Adapted from Crock et al (61) and Moore et al (37)

1.2.3.3 Functions of the endplate

The endplate serves the important functions of a biomechanical shield and nutritional gateway to the intervertebral disc. First, the endplate functions as a physical shield separating the disc from the vertebral bone, thereby preventing the highly hydrated nucleus pulposus from bulging or penetrating the adjacent vertebral bodies (62). As a mechanical interface, the endplate serves to absorb and evenly distribute the hydrostatic disc pressure from the mechanical loading of the spine from body weight, external weights and from the forces generated by trunk muscle contractions needed to stabilize posture during activities

(63,64). The trunk may generate a force ranging from 800N in standing to 3,000N during activities involving lifting (65). Consequently, the generated forces increase disc pressure to approximately 1.5MPa in standing to 2.3MPa lifting (66,67). As noted previously, the endplate is the nutritional gateway for the transport of nutrients between the vertebral marrow and the intervertebral disc. The endplate serves as the main diffusion channel via the marrow contact channels to the avascular intervertebral disc (45,68). Once nutrients reach the endplate, movement of solute particles takes place by diffusion (69,70). However, larger particles move by convective fluid flow created by mechanical disc compression and recovery. Concentration gradient between the blood plasma and tissue matrix represented by supply (i.e., capillary density) and demand (i.e., disc cell density and metabolic rate) determines the diffusion rate of the disc.

1.3 Imaging modalities and applications to the endplate

For this study, multiple imaging modalities were employed, specifically, CT scans, μ CT and MRI (Figure 1-3).

1.3.1 Computed Tomography

Advances in X-ray and technology brought the use of computers into the imaging field. In the early 1970s CT was introduced, which allows multiple tomographic images (slices) to be acquired through computer-processed X-rays for specific body parts. CT scans work on the principles of an X-ray machine, except that it spins around the axis of the object, while the radiation sensor (detector) moves in the same direction to receive the incident radiation. The multiple X-ray projection images at many angles of view around the object axis are processed for tomographic reconstruction by a high-speed computer to produce three-dimensional (3D) X-ray imaging consisting of a stack of thin tomographic images. The first-generation CT units produced crude images on a 64x64 matrix, which took a computer all night to process. However, modern CT uses a multidetector that acquired multiple submillimeter spatial resolution slices with processing speeds measured in milliseconds and allows the use of iodinated contrast agents. In the 1970s, G.N. Hounsfield and A.M. Cormack were given the Nobel Prize in medicine for the development of CT (71,72). CT scan has a high diagnostic accuracy for detecting bony defects, lung and chest imaging, and

cancer detection. However, high ionizing radiation has been one of its major disadvantages, although advances have been made in reducing the exposure to radiation while maintaining image quality.

1.3.2 Microscopic Computed Tomography

Microscopic Computed Tomography is referred to as micro-CT (μ CT), was first developed in the early 1980s (73,74). A cone beam is used to magnify the X-ray beam in the bench-top μ CT, which uses the same technology as X-rays and CT (75). However, technologies used in μ CT scanners differ from CT based on image quality and resolution, as well as the size of the 3D volume that can be imaged. As increased magnification generally results in a smaller volume for a given detector size, the imaging of larger volumes at high magnification requires increased array sizes, making μ CT suitable for smaller objects (76). μ CT radiation exposure increases with the fourth power of the voxel side dimension if the image noise is to remain unchanged. Consequently, higher spatial resolution corresponds with higher radiation exposure. μ CT can provide image data at resolutions much higher than achievable with clinical scanners such that deeper insights into pathoanatomy and physiological processes can be expected.

1.3.3 Magnetic Resonance Imaging

Magnetic Resonance Imaging (MRI) was invented by Paul Christian Lauterbur in 1971. MRI works on the principles of magnetic field to cause the alignment of hydrogen nuclei (protons) that are normally random in the body. The alignment is then disturbed by the sudden introduction of Radio Frequency (RF) energy. The proton returns to its resting alignment through various relaxation processes while emitting RF energy. The emitted signals are transmitted to the computer for reconstruction and displayed as shades of gray representing an image (77). By varying the order for the introduction and collection of the RF, different types of images are created. **Repetition Time (TR)** is the amount of time between successive pulse sequences applied to the same slice. **Time to Echo (TE)** is the time between the delivery of the RF pulse and the receipt of the echo signal. Relaxation times termed as sequence are used to characterize and differentiate tissues. T1-weighted and T2-weighted scans are the most common MRI sequences. **T1-weighted**

images (longitudinal relaxation time) are produced by using short TE and TR times. Conversely, *T2-weighted images* (transverse relaxation time) are produced by using longer TE and TR times. T1- and T2-weighted images can be easily differentiated on Cerebrospinal Fluid (CSF). CSF is dark on T1-weighted imaging and bright on T2-weighted imaging. In the 1970s weak magnetic fields were used to produce low spatial-resolution images. By 1980s and 1990s superconducting magnets became available at 1.5 Tesla and more recently 7 Tesla. One unit of Tesla, a measure of magnetic field strength, is 20,000 times stronger than the earth's magnetic field. In 2003, Paul Christian Lauterbur and Peter Mansfield shared the Nobel Prize in Physiology or Medicine for the development of MRI. MRI is generally better than CT for soft tissue evaluation, e.g., the intervertebral disc, ligament and tendon injury, spinal cord injury, and brain tumors, and has the advantage of no ionizing radiation.



Figure 1-3: The lumbar vertebrae on CT, MRI (T1) and μ CT. Adapted from Fournier et al (78) and Carter (79)

1.4 Theoretical Framework for EPSP in vertebrogenic pain

The theoretical requirement for vertebrogenic pain is injury or other pathology of an innervated structure, in this case the vertebra (80,81), however, scientists and clinicians have varying views of the etiology and management of back pain. The bony endplate and periosteum are the most densely innervated components of the vertebrae. Sensory and sympathetic fibres are frequently associated with blood vessels and consist of both fast myelinated fibres (group III or A-delta fibres with diameters ranging from 1 to 5 μm) that transmit sharp pain and slow unmyelinated fibres (group IV or C-fibers with diameters ranging from 0.5 to 2 μm) that transmit dull or aching pain (82). The best evidence for the role of endplates in chronic back pain is in provocation discography confirmed discogenic pain (12). Discography causes an increase intra-discal pressure stretching and mechanically stimulating the sensitized nociceptors within the outer annulus (83). Similarly, in presence of endplate microdamage, evidences indicated that at a pressure of 75 to 100 psi, the endplate deflect by 0.3mm when the annulus pulposus deflect by 0.5 mm due to intra-discal pressure during discography (84,85), resulting in increased interosseous pressure which further exacerbate the pain (86,87). There are two dominant theoretical frameworks to explain back pain, the biomedical and biopsychosocial model. The biomedical model was first proposed and later challenged by other views including the pain gate theory and the hospice movement, which later lead to the development of the biopsychosocial model of back pain/disability. These changes revolutionized and contributed to the 1978 and 2019 International Association for the Study of Pain definition of pain.

1.4.1 Biomedical model

The IASP subcommittee on taxonomy in 1978 defined pain as "An unpleasant sensory and emotional experience associated with actual or potential tissue damage, or described in terms of such damage" (88). The committee recommended that the definition serve as an operational framework and may be modified as other evidences unfolds (88,89). The IASP 1978 pain definition supports the biomedical view of nociception, as a protective mechanism from further injury involving noxious stimuli (90). However, in many clinical syndromes, pain is no longer protective. The pain in these situations arises spontaneously, can be elicited by normal stimuli (allodynia) or exaggerate a noxious stimulus

(hyperalgesia), and goes beyond the injury site (secondary hyperalgesia). This protective function occurring after a series of repeated or intense noxious stimuli causing the activation threshold to fall and amplified responses to subsequent stimuli is termed sensitization (91,92). Sensitization can occur at the peripheral or central level of the nervous system.

Peripheral sensitization is activated by nociceptors, to the increased peripheral transduction sensitivity and mostly requires the presence of peripheral pathology. While central sensitization corresponds to an enhancement in the functional status of neurons and circuits in nociceptive pathways throughout the neuraxis causing an increase membrane excitability, synaptic efficacy, or reduced inhibition (93). Thus, neurons in the dorsal horn of the spinal cord develop or increase in spontaneous activity, reduce activation threshold of peripheral stimuli, increase suprathreshold stimulation response, and receptive fields (91,92,94). Central sensitization involves the recruitment of novel inputs to nociceptive pathways such as large low threshold mechanoreceptor myelinated fibres to produce A β fibre-mediated pain (92), and hypersensitivity in noninflamed tissue by changing the sensory response elicited by normal inputs and increases pain sensitivity long after the initiating cause may have disappeared. The biomedical model links test-confirmed physical disorders and expressions of pain, however, this is not the case with many back problems. Critiques of the limitations of the biomedical mode have emerged, such as from Melzack and Wall (95,96), and Bonica (97). Developments, such as the widespread acceptance of Melzack and Walls's pain gate control theory and the hospice movement, shifted the pain paradigm, emphasizing the emotional and psychological components of pain.

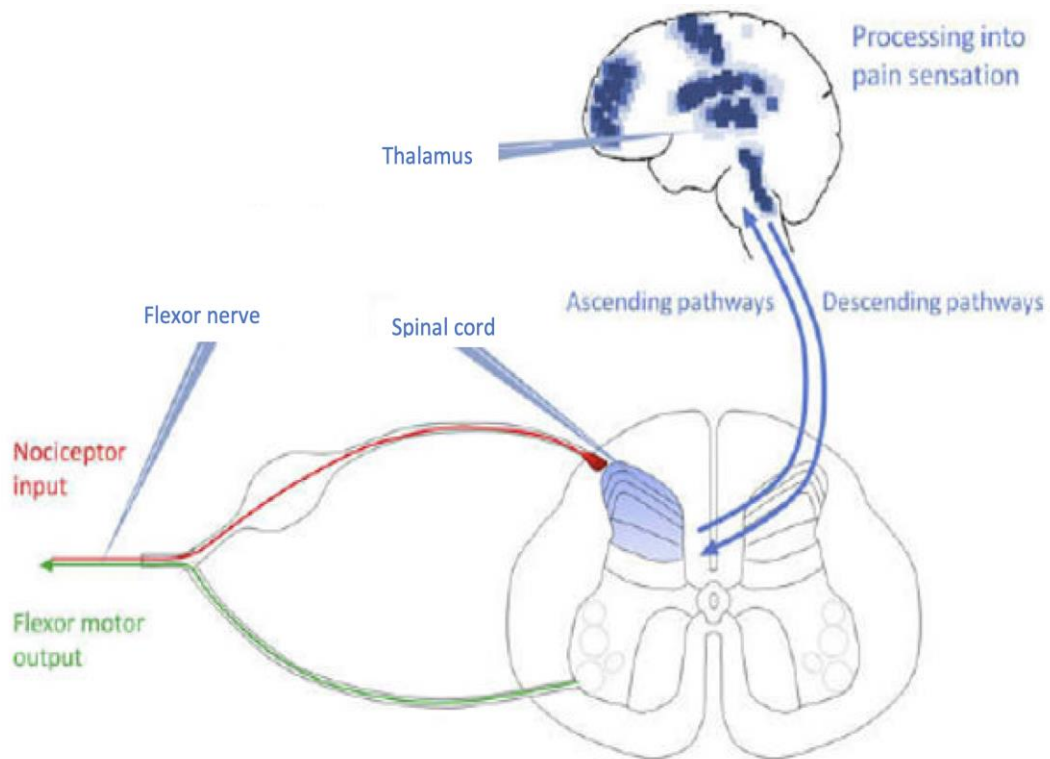


Figure 1-4: Schematic representation of peripheral and central sensitization.
Extracted from Latremoliere and Woolf (98)

1.4.2 The Pain Gate Control Theory

The gate control theory by Melzack and Wall in 1965 was a landmark toward understanding chronic and neuropathic pain. The gate control theory suggested that pain perception is modulated by endogenous modulatory mechanisms instead of depending solely on the transmission of noxious stimulus from the peripheral nervous system to the central nervous system. Nociceptive transmission is modulated by a gating mechanism in the dorsal horn composed of large-diameter and small-diameter fibres that inhibit and facilitate the pain gate. The pain gate control theory explains the scientific rationale for the efficacy of transcutaneous electric nerve stimulation in reducing pain and the effect of soothing the skin surface of an injured area to reduce pain by stimulating A-beta fibres thereby blocking nociceptive transmission. Furthermore, in 1999, Melzack proposed the neuromatrix theory. The neuromatrix model proposed that pain modulation involves the

cerebral pain processing and transmission mechanism, and cognitive and affective inputs. Thus, beliefs, knowledge, and fear of pain and other psychological factors such as anger, depression, and anxiety, influence the pain experience.

1.4.3 Biopsychosocial model

A vast majority of cases of chronic back pain are idiopathic, without any identified pathoanatomy. Chronic back pain goes beyond the anatomic aberration. It involves a substantial emotional component according to Plato and Aristotle (99). Increasing evidence suggests a significant impact of chronic back pain on both the affected individual, family and social environment (100). Consequently, chronic back pain can be considered a “biopsychosocial issue” (101). The biopsychosocial model is another paramount pain theory, explaining the uniqueness and peculiarity of the chronic back pain experience of each patient. In this line, the IASP in 2019 at the International Classification of Diseases 11th revision (ICD-11) revised the classification of chronic pain used for the diagnosis and the individualized management of chronic pain (102). In the ICD-11, the severity of chronic pain is rated according to three distinct dimensions including the intensity of pain, pain-related distress, and interference with daily living. The patient rates each dimension according to a 0–10 scale (0: absent; 1-3: mild; 4–6: moderate; 7–10: severe). Thus, a 3-digit code is used to denote the pain severity and indicate contribution of each dimension (101,103,104).

Waddell advocated the use of the biopsychosocial model in 1987 (105), and it has become the dominant framework for the study of low back pain and disability (106). The biopsychosocial model provides an important framework to conceptualize how biological, psychological, and social factors can influence patients’ outcomes. The model is based on a holistic philosophical view that illness is multidimensional and that how an individual experiences and interprets pain must consider the influence of biological, psychological, and social variables (107). The biopsychosocial model challenged the prevailing biomedical model of disease. In contrast to the biomedical model focusing solely on lumbar spinal anomalies, biochemical defects, and neurophysiological abnormalities (i.e., biological factors), the biopsychosocial model further explores a variety of factors, ranging from depression and anxiety (i.e., psychological factors) to educational level and

employment status (i.e., social factors). In describing how the biopsychosocial model should be applied to low back complaints, Waddell (105) differentiated low back pain from low back disability. According Waddell (105), low back pain is a benign, self-limited disease that results from a physical abnormality, and produces signs and symptoms proportionate to the abnormality. In contrast, low back disability as an illness that results from the dynamic interplay of biological, psychological, and social factors, and is characterized by distress and illness behaviors disproportionate to any identifiable abnormality (108). Although distinguishing back pain from back disability is difficult, back pain can be conceived to be explained by a biomedical model and back disability by a biopsychosocial model according to Waddell (106). However, the wide range of interpretations and applications of the biopsychosocial model, including the fragmentation of the model against the Engel's original concept, has resulted in limited understanding and suboptimal patient care for back pain and disability (109).

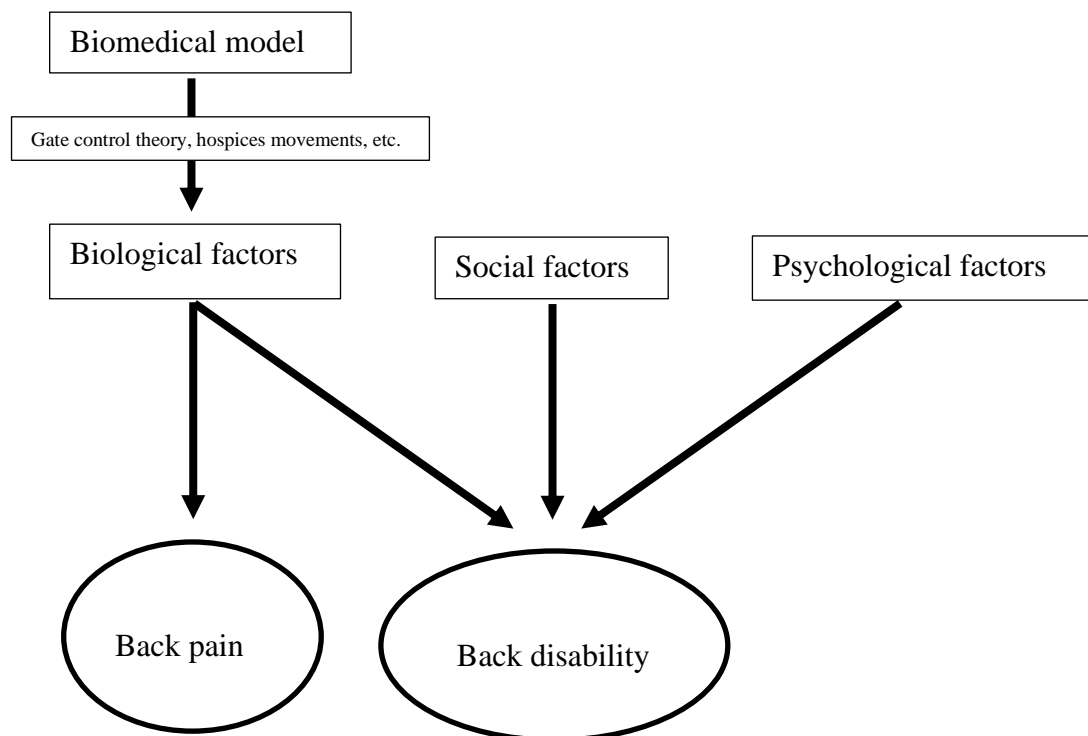


Figure 1-5: Theoretical Model for Chronic Back Problems. Showing the interaction between various models (biomedical) and (biopsychosocial comprising biological, social and psychological factors) and theories (gate control theory and hospice movement)

1.5 The Cadaveric and Twin Spine Study Samples

1.5.1 The Cadaveric Sample

The cadaveric sample was gathered from the Department of Anatomy and Cell Biology, Schulich School of Medicine and Dentistry, through the bequeathal program of the whole-body donation program. Twenty-two cadavers comprising both males and females used for medical training purposes, along with their postmortem CTs, were used for our study. The cadavers were from individuals that died in the hospital. The CTs were acquired prior to the study conception as part of teaching materials in the Department of Anatomy and Cell Biology of Western University. The clinical CT scans were determined by a panel of radiologists to be comparable to a typical clinical CT. While the μ CTs were acquired in collaboration with Robarts Research Institute to study EPSD. From the 22 cadavers, the spines of the three cadavers were not able to be harvested for μ CT. Therefore, complete data were available for 19 cadavers.

The 19 ethanol-phenol-formalin embalmed cadaveric spines comprised of 9 men and 10 women with a median age of 82 years (range 62-91) at the time of death. The sample age (median age 82, range 62-91) is higher than previous clinical imaging studies (median age 52-58.9) (15,32) (110,111) and, therefore, the prevalence of age-related findings may be greater than in younger samples. Recognizing the limitations of our sample size and age distribution, it is important to note that findings are applicable to older adults from a high-income country and may not generalize to the entire elderly population. Despite, the limitations associated with the sample, use of cadaveric spines is required to study the macroscopic structure of delicate spinal osseous structures, such as the endplate, with μ CTs used in the diagnostic test study.

1.5.2 The Twin Spine Study Sample

The TSS sample consists of 600 subjects drawn from the Finnish Twin Cohort and comprises 147 monozygotic (MZ) and 153 dizygotic (DZ) male twin pairs. The Finnish Twin Cohort contains all Finish sex-matched twin pairs born before 1958 and still alive in 1975. Among the Twin Spine Study sample is a subgroup of 117 pairs of MZ twins selected based on discordance between twin siblings for specific common behavioural or

environmental factors (e.g., sedentary or heavy occupational physical demands, routine exercise participation, or occupational driving). Those factors were important suspects in the etiology of spinal degeneration and back pain, and exposure information was available from the Finnish Twin Cohort database. The Twin Spine Study sample was found to be highly representative of the Finnish Twin Cohort, which is generally representative of the Finnish population, in terms of level of education, social class, smoking, level of leisure-time physical activity, and history of work-incapacitating neck, shoulder, or back pain, or sciatica (112). For this study, the subsample of 152 MZ and 51 DZ male twins that's participated in a follow-up study 10-15 years following their baseline measurements were included, yielding a total of 203 males. The group of 203 from the most recent wave of data collected in the Twin Spine Study has the advantage of better magnetic resonance imaging (MRI) quality, which allows a clearer view of the endplate, as compared to the images acquired at baseline.

The most recent wave of data collection of the Twin Spine Study (2008-2009) included lumbar MRI (1.5 Tesla, Siemens Zebra scanner, "Avanto" with software MR B15, Siemens AG Erlangen, Germany, using specific protocols for sagittal and axial images. T2-weighted images were obtained with repetition and echo times of 2450 and 90, respectively. The field of view was 320 mm (in axial, 348×384 mm) and the pixel size was 0.8125 mm. The slice thickness and interslice gap were 4 mm and 0.4 mm, respectively, for the sagittal images and 3 mm and 0.3 mm for axial slices (113,114) and associated assessments, including age and anthropometrics, among other measurements, using a structured interview and physical examination administered by trained research assistants who were blinded to the selection criteria and the study hypotheses.

Chapter 2

2 The association between vertebral endplate defects and back pain: A systematic review and meta-analysis

Summary

Background: Despite physiological evidence suggesting a role for the endplate in pain generation, the association between endplate structural defects (EPSD) and back pain remains unclear with conflicting results. *Objective:* To clarify the current state of knowledge on the association of EPSD and back pain. *Methods:* Five databases were searched for studies reporting on the association between EPSD and back pain. Covidence and Comprehensive Meta-analysis software were used for article screening and selection and pooling of extracted data. Overall quality of evidence was assessed using GRADE. *Results:* 26 studies comprised of 11,027 subjects met inclusion criteria. The presence of moderate heterogeneity ($I^2=73\%$; $p=0.001$) prevented the pooling of estimates across all studies. However, it was possible to pool studies of specific EPSD phenotypes, such as erosion (OR: 2.69; 95%CI: 1.35–5.50) and sclerosis (OR: 1.97; 95%CI: 1.50–2.58), which yielded significant associations with back pain. Schmorl's nodes were also associated with most individual back pain phenotypes (OR: 1.53-1326, $I^2=0\%-7.5\%$) and back pain overall (OR: 1.63, 95%CI: 1.37-1.94, $I^2=26\%$) in general population samples. The pooling of data from all studies of specific back pain phenotypes, such as frequent back pain (OR: 2.83; 95%CI:1.77–4.52) and back pain incidence (OR: 1.65; 95%CI:1.30–2.10), each yielded significant association with EPSD and was supported by low heterogeneity ($I^2 = <7.5\%$). *Conclusion:* Overall, there is moderate quality evidence of an association between back pain and EPSD, which is most evident for erosion, sclerosis and Schmorl's nodes. Going forward, research on specific EPSD phenotypes and back pain case definitions using strong study designs will be important in clarifying the extent of associations and underlying mechanisms.

The study was prospectively registered in Prospero (CRD42020170835) on 02/24/2020

Introduction

Pain generation and transmission require innervated tissues, and the vertebral endplate with its rich blood and nerve supply may be chemically or mechanically sensitized to serve as a source of back pain (115,116). Endplate structural defects (EPSD) have been associated with back pain (32), as well as disc degeneration (117) and Modic changes (118), and defects in the underlying bone (17). However, there are inconsistent findings across studies, with some studies supporting an association between EPSD and back pain (32,119–121), and other studies not supporting such an association (122–125).

These inconsistencies may have several explanations. Back pain is likely to have multifactorial etiologies that may differ between study populations, obfuscating associations between EPSD and back pain. Associations may be further clouded by uncontrolled confounding factors. Furthermore, the large variation in measurement methods and nomenclature of EPSD creates confusion, as do variations in case definitions of back pain, and may lead to faulty comparisons (13). Furthermore, while some studies examine specific types of EPSD, others aggregate all observed EPSD into one general phenotype when examining the association with back pain. There is also variation in study populations and sampling that not only contribute to inconsistencies in associations, but also a wide range of prevalence rates (9% to 76%) of EPSD across study samples (26,28,126).

Given the current interest in EPSD phenotypes and their clinical significance, the objective of the study was to systematically review the available scientific literature on the association between EPSD and back pain, using meta-analysis, when possible, to summarize the current state of knowledge. We were also interested in whether reported differences in associations are due to variations in EPSD phenotype, back pain definition, and population studied.

2.1 Materials and Methods

2.1.1 Search strategy and Databases

An initial search was conducted with assistance from a health sciences librarian using prespecified eligibility criteria based on the research question: are EPSD associated with back pain? The search strategy was further refined based on the recommendations of spine imaging and endplate research experts. Using the Medical Subject Headings (MeSH) for all key terms and Boolean operators, the databases of PubMed, Scopus, Cumulative Index of Nursing and Allied Health Literature (CINAHL), Google Scholar and EMBASE were searched without time and language restriction. The search terms were adapted for use with database-specific filters (Appendix 1: search strategy specific to each database). Broad search strategies were aimed to maximize the number of retrieved articles. An updated search was conducted before data analyses and the retrieved studies were screened for inclusion using the same screening and selection process as the initial search. The systematic review was designed according to the standard recommendations of the Preferred Reporting Items for Systematic reviews and Meta-Analyses (PRISMA) (Appendix 2: PRISMA checklist).

2.1.2 Selection criteria

Studies that assessed EPSD of the thoracic and lumbar regions of subjects with and without back pain, and with more or less back pain (e.g., frequency, intensity or related disability) from cohort, case-control, or cross-sectional study designs were included. Also, randomized and non-randomized clinical trials were included if an additional study question was to determine if EPSD are associated with back pain without considering the effect of an intervention. Reviews, case reports, case series, conference proceedings, abstracts, and editorial letters were excluded, as were studies where the etiology of back pain was from a specific known pathology, such as infection, cancer or fracture.

2.1.3 Data extraction

Using Covidence (RRID: SCR_016484) software for the management of systematic reviews, titles and abstracts of retrieved studies were screened independently by two reviewers to identify studies that potentially met the inclusion criteria. Full texts of

potentially eligible studies were then retrieved and independently assessed for eligibility by two reviewers. All disagreements in the screening and selection process between the reviewers over the eligibility of studies were resolved by a third reviewer. Finally, a standardized, piloted form was used to extract data from the included studies for assessment of study quality and evidence synthesis. One author extracted citation, design, subject characteristics, assessment or definition of EPSD and back pain, frequency counts, odds ratios (adjusted and unadjusted), and 95% confidence intervals (95% CI). If the adjusted or unadjusted OR was not reported, the unadjusted OR, 95% CI, and two-sided p-value were calculated for each outcome from the reported counts and proportions. Extracted data were then verified by a second reviewer. If relevant data were not reported, attempts were made to contact the study's corresponding author via e-mail and counts and proportions were requested so that an unadjusted OR could be calculated.

2.1.4 Risk of Bias (Quality) assessment

The Item Bank for Assessment of Risk of Bias and Precision for Observational Studies of Interventions or Exposures (IBARBPOSIE) was used to assess the methodological quality of each included full-text article and has been validated to assess the risk of bias and precision in observational studies (127). The IBARBPOSIE contains 29 items Relevant items on the original IBARBPOSIE were assessed for each study design and answered as “yes” or “no” or “partial” or “unclear,” similar to Raastad et al (128). Quality assessment results were categorized into selection and confounding, performance, attrition, detection, reporting and information bias. The overall study believability was determined based on the responses from the questions relating to internal validity (selection and confounding, performance, attrition and detection bias) of the study. We did not assess precision within the quality appraisal of each study (129), but it was considered in GRADE when assessing overall quality of evidence.

2.1.5 Analysis

Extracted data were summarised using means, frequencies, and percentages. Meta-analysis was conducted using Comprehensive Meta-analysis software (CMA version 3.0, Biostat Inc., Englewood, New Jersey, USA). As previously suggested (13), phenotypes of EPSD

were merged into the same construct. For example, sclerosis and calcification were merged into one group. Also, endplate damage, endplate defects and endplate destruction were merged into ‘endplate defects.’ All estimates were pooled using a random-effects meta-analysis. Heterogeneity was assessed using both the Chi-squared test (p-value) and the I-squared statistic. I-squared <40% was deemed as low heterogeneity, 30-60% as moderate, 50-90% as substantial, and 75-100% as considerable heterogeneity (130). Significant heterogeneity using the Chi-squared test was indicated with a $p < 0.05$. We hypothesized differences in associations between EPSPD and back pain are due to variations in the EPSPD phenotype, back pain definition, and population studied. The Grading of Recommendations Assessment, Development, and Evaluation (GRADE) system for rating quality of evidence in systematic reviews was used to summarize the strength of the evidence. GRADE assesses the level of evidence by considering study limitations, imprecision, indirectness, inconsistencies, and publication bias to classify the quality of evidence on which conclusions of the review are based as high, moderate, low or very low (131). The systematic review was prospectively registered in Prospero (CRD42020170835).

2.2 Results

2.2.1 Search and selection

Our search yielded 2,767 articles. After removing duplicates, 2,372 abstracts were screened against the eligibility criteria for inclusion, resulting in 192 full-text reviews. Furthermore, a follow-up search of the reference lists of articles that met the inclusion criteria and a final updated search each resulted in the identification of an additional article for full-text review. Overall, 26 studies met the inclusion criteria, including a total of 11,027 subjects (with individual study samples ranging from 49 to 1,276) from 11 countries, representing 3 continents: Asia (N=10), Europe (N=8), and North America (N=8).

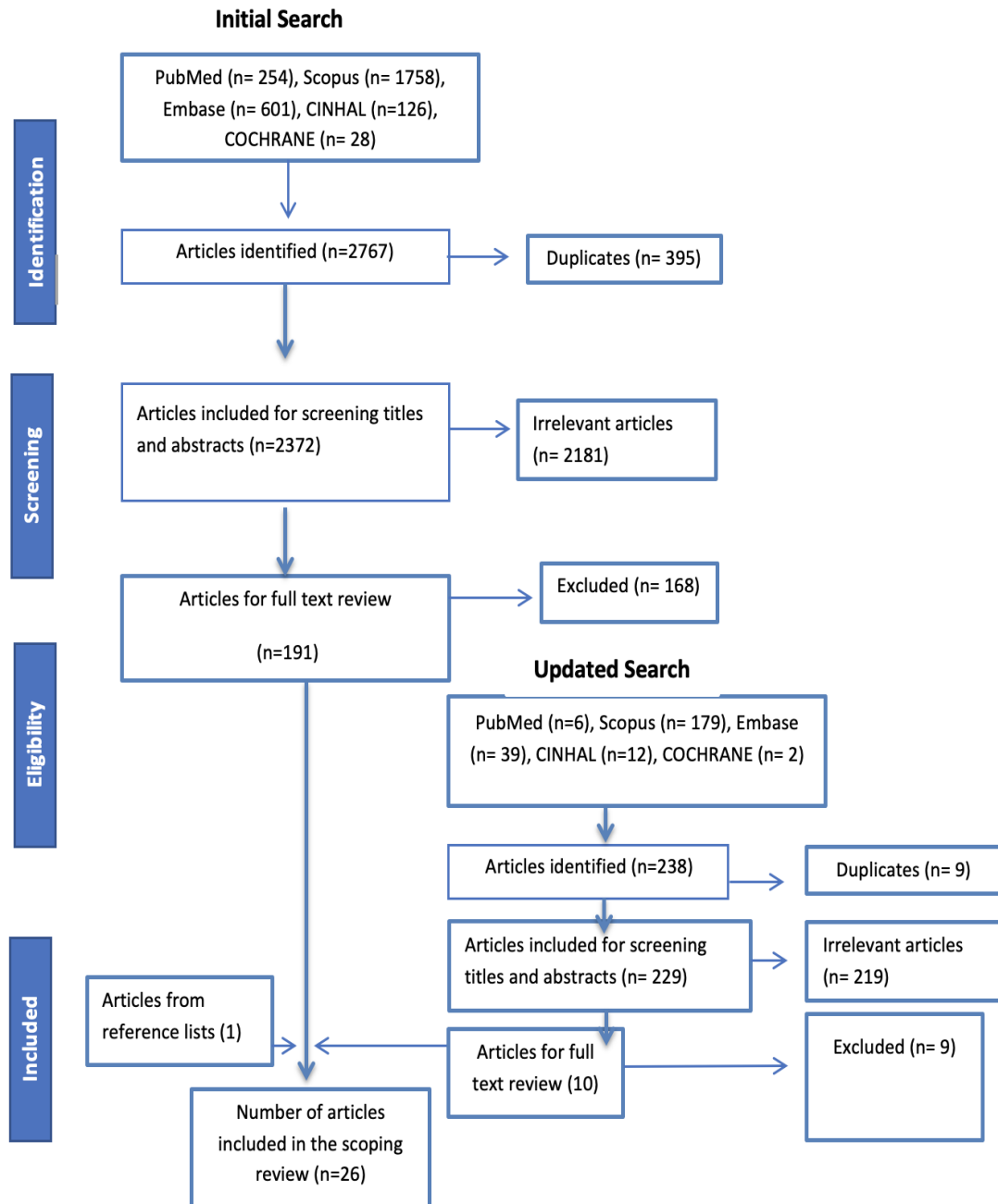


Figure 2-1: Flowchart of study selection and inclusion

2.2.2 Study characteristics

Table 2-1 provides information on the study design and sample, imaging modality used, definition/assessment of the EPSD and back pain, and the quality appraisal score of the included studies. Of the 26 studies included, cross-sectional studies were most common (n=15), followed by cohort studies (n=7) and case-control studies (n=4). The publications spanned 1990 to 2020, with half (n=13) published within the last decade (2011-2020) and only four published from 1990 to 2000. The most common imaging modalities used were MRI, which was used in 16 studies, and radiographs, used in 8 studies. CT scans and autopsy were used in one study each.

The frequency of EPSD and their association with back pain (odds ratios and 95% confidence intervals) are reported in Table 2-2. Of the 17 different definitions or terms used to describe EPSD among the 26 included studies, Schmorl's node (n= 15) was the most commonly studied phenotype, followed by general terms, such as endplate defects (n=3), endplate changes (n=2), endplate lesions (n=2) and endplate abnormalities (n=1). In addition, two studies reported endplate defects using cumulative scores, including "endplate defect score" (123) and "total endplate (TEPs) score" (132). There was also great variability in the assessment and definitions of back pain related to pain intensity (120,123,133–135), location (26,136,137), duration and disability (26,132,138,139) (Table 2-2).

The majority (59%) of the included studies did not adjust/control for any potential confounding in the study design or analysis. When confounding was considered, age (n=9) was most commonly adjusted, followed by BMI (n=6), sex (n=5), disc degeneration (n=5) and Modic changes (n=2). Other confounders, such as heavy manual labor, height, history of bending/twisting and spinal surgery, were controlled for in one study each.

Table 2-1: Sample characteristics of included studies, with endplate structural defect phenotype and back pain case definitions

| Study | Study Sample | Imaging Modality | Definition/Assessment of Endplate Defects | Definition/Assessment of Back Pain |
|-----------------------------------|---|------------------|---|---|
| Case-control studies | | | | |
| Abbas et al. 2017 (119) Israel | N= 345; 165 individuals with degenerative LSS (age range: 40–88, 52% females) and 180 without spinal stenosis related symptoms (age range: 40–99: 50% females) | CT | Presence or absence of Schmorl’s nodes on cranial or caudal endplates | Back pain accompanying degenerative LSS |
| Bailey et al. 2019 (120) USA | N = 52; CLBP patients=38, mean age 47.9 ± 12.6 years; Healthy controls=14, mean age 45.7±12.3 years. | MRI | Presence or absence of “cartilage” endplate damage in superior or inferior endplates | More than three continuous months of low back pain (VAS ≥4 or ODI ≥30) |
| Buttermann et al. 2008 (133) USA | N= 292; 60 pediatric and adult idiopathic scoliosis surgical patients, 60 age- and sex-matched asymptomatic controls, and 172 non-deformity symptomatic “DDD” surgical patients | MRI | Presence or absence of Schmorl’s nodes | Pain VAS score (0 = no Pain, 10 = severe excruciating pain) and pain diagram |
| Kanna et al. 2014 (140) India | N= 224; 91 patients with Disc Prolapse aged of 39±6 years, and 133 with DDD and BP aged 40±7 years | MRI | Presence or absence of Schmorl’s nodes | LBP related to activities, present for >6 months and lumbar DD, and no history of trauma, infection, tumor, previous spinal surgery and no sciatica |
| Cross-sectional studies | | | | |
| Teraguchi et al. 2015 (141) Japan | N= 975 adults (general population sample), mean age 66.4 years, range 21–97 years, 67% females | MRI | Schmorl’s node defined as a localized defect in an endplate, with a well-defined herniation pit in the vertebral body with or without a surrounding sclerotic rim | Questionnaire response to: “Have you experienced LBP on most days during the past month, in addition to now?” |

| | | | | |
|------------------------------------|---|------------|--|---|
| Chen et al. 2020 (121) China | N= 478 adults (general population sample), mean age 53.3 years, range 20–88 years, 57.1% females | MRI | A loss or disruption of the endplate surface on at least two consecutive sagittal images, further classified into focal, corner or erosive defects | Back pain or soreness in the area between the lower ribs and buttock crease, excluding pain related to fever or menstruation |
| Cheung et al. 2009 (122) China | N= 1043 lumbar spine MRIs of volunteers (general population sample) between 18 to 55 years of age | MRI | Schmorl's nodes were defined as areas of endplate irregularities, in which the darkened rim of the vertebral endplate was indented into the vertebral body | Pain in the lower back >2 weeks duration, sufficiently severe to require physician consultation or treatment |
| Inaoka et al. 2000 (142) Japan | N= 838 adults receiving a routine health examination, mean age 52 years, range 23–83 years, 35% females | MRI | An irregular ossification of the vertebral endplate, considered present when the bony endplate thickness was greater than 2 mm on lateral view | LBP reported through questionnaire |
| Kjaer et al. 2005 (136) Denmark | N= 413 40-year-old adults (general population sample), 52% females | MRI | Endplate defects categorized as 0= Normal; 1= defects, 2= Large defects and Schmorl's nodes | Have you had trouble with the lowest part of your back (diagram provided)? a. during the past 7 days b. during the past month c. during the past 12 months |
| Miura et al. 2019 (139) Japan | N= 1276 RA outpatients, mean age 64.6 years, 81% females | Radiograph | Presence or absence of Endplate erosion | Roland–Morris Disability Questionnaire score >5 |
| Rose et al. 2001 (143) USA | N= 53 patients with Stickler syndrome, mean age 31, range 1-70 years, 57% females | Radiograph | Endplate abnormalities, Schmorl's nodes | Pain in the upper or lower back (but not neck) occurring at least daily for a minimum of 6 months |
| Takatalo et al. 2012 (137) Finland | N= 554 subjects (general population sample), mean age 21.2, range 20–23 years, 58% females | MRI | Schmorl's node was defined as a vertical intervertebral disc protrusion through the endplate | A pain drawing with a shaded area between the lower ribs and gluteal folds indicating low back pain |
| Videman et al. 2003 (144) Canada | 230 male monozygotic twins (general population sample), mean age 49.4 years, range 35 to 69 years | MRI | 0: normal 1: slight defect (1–5 mm) 2: moderate defect (5–10 mm) 3: severe defect (>10 mm) | Detailed, structured interview, including frequency and intensity of BP during previous 12 months, disability and lifetime back pain |
| Videman et al. 1990 (138) Finland | N= 86 adult male cadavers, <64 years of age when deceased | Radiograph | Using discography with barium sulphate, endplate defects scored as 0= none; 1= dye penetrated only cartilage; 2= dye seen also in subchondral bone, | Immediate family member (typically spouse) was asked about back pain history of deceased, including frequency of back pain |

| | | | | |
|--------------------------------------|--|------------|---|--|
| | | | spreading ≤ 3 mm in diameter; 3= as in 2 but spreading >3 mm. Endplate defect $<II$ as absent and $\geq II$ as present. | and sciatica and related disability |
| Wang et al. 2012 (32) Canada | N= 136 lumbar spines of men <64 years of age when deceased (mean age 52 years) | Autopsy | Endplate lesions were evaluated as present or absent. If present, endplate lesions were further classified into Schmorl's nodes, fracture, erosion, or calcification. | Immediate family member (typically spouse) was asked about back pain history of deceased, including frequency of back pain (none, occasional or frequent) and "back injury" (sudden onset associated with a specific accident or unusual activity) |
| Williams 2007 (26) UK | N= 516 healthy female twins (150 monozygotic and 366 dizygotic) | MRI | Schmorl's nodes defined as localized defects in a vertebral endplate with a well-defined herniation pit in the vertebral body with or without a sclerotic rim | Pain between the twelfth ribs and the gluteal folds of a total duration ≥ 1 month and that was associated with disability in activities of daily living. |
| Zehra et al. 2019 (123) USA | N= 108 Southern Chinese (general population sample) | MRI | Cumulative EP Score [6]: Endplate defect width score 1-3 and depth score 1-3 based on extent. | Pain VAS (100 mm) was used to measure today's LBP/sciatica severity. |
| Sharma et al. 2011 (124) USA | N= 63 lumbar MRIs of patients, mean age of 30.0 ± 6.7 years, 63% females | MRI | Schmorl's nodes defined as focal depressions along the endplate | Presence or absence of low back pain |
| Sward et al. 1990 (145) Sweden | 142 student athletes aged 14 to 25 years | Radiograph | Schmorl's nodes as localized radiolucent defects, with bony or sclerotic margins in the vertebral endplate. | Any previous or present pain located in the thoracic or lumbar spine >1 week or recent pain irrespective of the duration |
| Cohort studies | | | | |
| Iwamoto et al. 2005 (125) Japan | N= 327 incoming high school rugby players, 15–16 years of age | Radiograph | Schmorl's nodes: sharply marginated, sclerotic indentation in the vertebral endplate | Non-traumatic low back pain that resulted in stopping playing rugby completely for at least 1 day |
| Iwamoto et al. (146) 2004 [29] Japan | N= 913; comprising of 171 high school and 742 freshmen college football players | Radiograph | Schmorl's node Sharply marginated, sclerotic indentation in the vertebral endplate | Non-traumatic low back pain that resulted in stopping playing football for at least 1 day |
| Kaupilla et al. 1997 (147) USA | N= 606 subject from the Framingham population-based cohort; 65% females | Radiograph | Presence or absence of Endplate sclerosis | Response to question: Have you ever had back pain (and at what age)? |

| | | | | |
|-----------------------------------|--|------------|--|---|
| Luoma et al. 2016 (135) Finland | 49 patients, mean age 43.7 years, range 18–65 years, 86% females | MRI | Bony endplate lesions subclassified as: focal subchondral hypointensity, small defect or larger Schmorl's like bony defect, multifocal lesions, diffuse irregularity, or combined. | LBP lasting >3 months, intensity during the preceding week using a 0–10 numerical rating scale (NRS): 0 = no pain, 10 = worst possible pain |
| Munir et al. 2018 (132) UK | N= 996 twins at baseline and 414 at follow-up Baselines mean age 53.6 years, range 19–74, 96% females | MRI | Total endplate defects score (TEPS) | Lifetime history of severe disabling LBP of more than 1 month, evaluated with modified version of the MRC Back and Neck Pain Questionnaire |
| Nagashima et al. 2013 (134) Japan | N= 192 high school football players, age 15 at baseline and 17 years at follow-up | MRI | Schmorl's node defined as sharply marginated indentation of the vertebral endplate | An 11-point VAS score of >5 at rest defined positive cases of LBP over prior 2 years. |
| Ogon et al. 2001 (148) Austria | N= 120 children who were skillful skiers, mean age 17 years, range 14–20 years, 35% females | Radiograph | Endplate abnormalities were divided into three groups according to their location: anterior lesions (involving the anterior vertebral edge), posterior lesions and Schmorl's nodes (not involving the vertebral edge). | Low back pain incidence assessed prospectively over 2 years |

Abbreviations defined: LSS=lumbar spinal stenosis, CLBP=chronic low back pain, DDD=degenerative disc disease, DD= disc degeneration, RA=rheumatoid arthritis, TEPS=total endplate score

Table 2-2: The frequency of endplate defects, proportions, and unadjusted and adjusted odds ratios (95% confidence intervals) as reported in each included study.

| Study | Population Type | Back pain Type | EPD phenotype | Back pain | | No Back pain | | Crude OR (95% CI) | Adjusted OR (95% CI) | Adjusted variables |
|--------------------------------|---------------------------------------|--|--------------------|-------------|------------|--------------|------------|-------------------------|-----------------------------|--|
| | | | | EPD Present | EPD Absent | EPD Present | EPD Absent | | | |
| Case control studies | | | | | | | | | | |
| Abbas et al. (119) 2017 | General | LBP | Schmorl's nodes | 122 | 43 | 80 | 100 | | | Age, height, weight, BMI, number of deliveries, heavy manual labor, smoking, hypertension and/or diabetes mellitus |
| | Male (L4/5) | LBP | Schmorl's nodes | | | | | | 2.624 (1.154–5.968) p=0.021 | |
| | Female (L4/5) | LBP | Schmorl's nodes | | | | | | 3.292 (1.162–9.330) p=0.023 | |
| Bailey et al. (120) 2019 | Adult subject | LBP | Endplate pathology | | | | | 14.1 (2.3–85.2); p<0.05 | 26.1 (1.1–639.1); p<0.05 | Modic changes and mean disc degeneration |
| Buttermann et al. (133) 2008 | Pediatric scoliosis | BP | Schmorl's nodes | | | | | r = 0.53 | | |
| | Adult Scoliosis | | | | | | | | | |
| Kanna et al. (140) 2014 | Patients with “DDD” and disc prolapse | LBP | Schmorl's nodes | 27 | 106 | 20 | 71 | | | |
| Cross-sectional studies | | | | | | | | | | |
| Teraguchi et al. (141) 2015 | General population sample of adults | Pain on most days during the past month, in addition | Schmorl's nodes | 5 | 388 | 10 | 582 | | 1.14 (0.3–3.6); p>0.05 | Age, body mass index (BMI); sex |

| | | | | | | | | | | |
|------------------------|------------------------------|--|----------------|-----|----|-----|-----|--------------------------|---------------------------------|---|
| | | on to now | | | | | | | | |
| Chen et al. (121) 2020 | General population of adults | Back pain ≥ 1 day over the past 12 months | EPD | 143 | 63 | 158 | 114 | 1.64(1.12-2.4); p=0.011 | 1.56(1.0-2.43); p=0.049 | Age, BMI; Modic changes; disc degeneration |
| | | | Focal defect | | | | | | 2.1(1.2-3.67); p=0.009 | Age, sex, BMI, and bending/twisting history |
| | | | Corner defect | | | | | | 1.63(0.89-2.99); p=0.113 | |
| | | | Erosive defect | | | | | | 1.64(1.0-2.7); p=0.51 | |
| | | Intensity of worst back pain over the past 12 months | EPDs | | | | | | 184.93(1.65-207443.74); p=0.03 | Age, BMI; Modic changes; disc degeneration |
| | | | Focal defect | | | | | | 1326.1(3.03-573779.24); p=0.02 | Age, sex, BMI, and bending/twisting history |
| | | | Corner defect | | | | | | 854.06(1.16-621567.63); p=0.045 | |
| | | | Erosive defect | | | | | | 343.78(1.57-74607.78); p=0.034 | |
| | | Back pain ≥ 1 day in lifetime | EPDs | | | | | 1.96(1.34-2.86); p=0.001 | 1.64(1.06-2.53); p=0.026 | Age, BMI; Modic changes (MCs); disc degeneration (DD) |
| | | | Focal defect | | | | | | 2.23(1.28- | Age, sex, BMI, and |

| | | | | | | | | | | |
|--------------------------|---|---|------------------------------|-----|-----|-----|-----|--|---------------------------------------|--|
| | | | | | | | | | 3.9); p=0.005 | bending/t wisting history |
| | | | Corner defect | | | | | | 1.77 (0.97- 3.23); p=0.62 | Age, sex, BMI, and bending/t wisting history |
| | | | Erosive defect | | | | | | 1.74 (1.06- 2.84); p=0.027 | Age, sex, BMI, and bending/t wisting history |
| Cheung et al. (122) 2009 | General population | LBP | Schmorl's nodes | | | | | 1.312 (0.681- 2.529), p=0.417 | | |
| Inaoka et al. (142) 2000 | General population | LBP | Irregular ossification of EP | 85 | 302 | 58 | 393 | $\chi^2=12.1963$, p<0.01 | Beta: 0.1323 Standard beta: 0.0998 | |
| Kjaer et al. (136) 2005 | General population (40-year-old adults) | LBP month | Endplate changes | 51 | 124 | 72 | 165 | | 0.9 (0.6– 1.4) | |
| | | LBP year | Endplate changes | 83 | 201 | 40 | 88 | | 0.9 (0.6– 1.4) | |
| | | LBP care | Endplate changes | 38 | 76 | 85 | 213 | | 1.3 (0.8– 2.0) | |
| Miura et al. (139) 2019 | RA patients | LBP related to dysfunction (disability) | Endplate erosion | 210 | 209 | 253 | 604 | | 1.41(1.01, 1.97) p=0.043 | |
| Rose et al. (143) 2001 | Patients with Stickler syndrome | Back pain | Endplate Abnormality | 30 | 4 | 9 | 8 | P=0.01 | | |
| | | | Schmorl's nodes | 26 | 8 | 8 | 9 | P=0.04 | | |
| Takata et al. (137) 2012 | Young adults (20-23 years) | Back pain | Schmorl's nodes | 79 | 308 | 17 | 150 | | | Sum score of DD, sex, and socioeconomic status |
| | | Always | Schmorl's nodes | 18 | 47 | 17 | 150 | | | |

| | | | | | | | | | | |
|---------------------------|---|--|--|----|-----|----|-----|-------------------------|--------------------------|-------------|
| | | painful | | | | | | | | |
| | | Recent Onset | Schmorl's nodes | 10 | 46 | 17 | 150 | | | |
| | | Moderate pain | Schmorl's nodes | 16 | 57 | 17 | 150 | | | |
| | | Minor pain | Schmorl's nodes | 35 | 158 | 17 | 150 | | | |
| Videman et al. (144) 2003 | General population sample of monozygotic adult male twins | Frequency of LBP in past 12 months (0-3 scale) | Worst endplate changes present (0-3 ordinal scale) | | | | | | 1.5 (1.1-2.1) | Age |
| | | No. of episodes (lifetime) (0-2 scale) | Worst endplate changes (0-3) | | | | | | 1.3 (1.0-1.7) | Age |
| | | Pain intensity of worst episode (0-2 scale) | Worst endplate changes (0-3) | | | | | | 1.4 (1.1-1.9) | Age |
| Videman (138) 1990 | Male cadavers | Hx of disabling back pain and sciatica | Endplate defect | | | | | 0.5 (0.1 – 2.8); p>0.05 | | |
| Wang et al. (32) 2012 | Male cadavers | Occasional BP | Schmorl's nodes | | | | | | 1.04 (0.45-2.36); p>0.05 | Age and BMI |
| | | | Fracture | | | | | | 1.54 (0.47-5.12); p>0.05 | |
| | | | Erosion | | | | | | 2.36 (0.93- | |

| | | | | | | | | | | |
|--------------------------|-------------------------------------|-----------------------------------|--------------------------|--|--|--|--|--|--|---|
| | | | | | | | | | 5.97); p>0.05 | |
| | | | Calcification | | | | | | 0.53 (0.05- 5.55); p>0.05 | |
| | | | Small defect | | | | | | | |
| | | | Moderate defect | | | | | | | |
| | | | Large defect | | | | | | 8.87 (1.17- 67.36); p=0.03 5 | Age, BMI and DD (no reports for other sizes) |
| | | Frequent BP | Schmorl's nodes | | | | | | 2.67 (1.34- 5.31); p<0.05 | |
| | | | Fracture | | | | | | 1.48 (0.45- 4.82); p>0.05 | |
| | | | Erosion | | | | | | 2.72 (1.05- 7.06); p<0.05 | |
| | | | Calcification | | | | | | 5.50 (1.15- 26.23); <0.05 | |
| | | | Small defect | | | | | | | |
| | | | Moderate defect | | | | | | | |
| | | | Large defects | | | | | | 13.08 (1.65- 103.45) ; p=0.01 5 | Age, BMI and DD |
| Williams (26) 2007 | Healthy adult female twins | BP disability (≥1 month) | 1 Schmorl's node | | | | | | 1.04 (0.52- 2.07) | Age, BMI and DD |
| | | | | | | | | | 1.41 (0.75- 2.65); p>0.05 | Age and BMI |
| | | | ≥2 Schmorl's nodes | | | | | | 1.97 (0.78, 5.0) | Age, BMI, DD |
| | | | | | | | | | 2.68 (1.11- | Age and BMI |

| | | | | | | | | | | |
|---------------------------|--|-----------------------------|--|-----------|-----------|----|-----|----------------------------|------------------|--|
| | | | | | | | | | 6.47); p<0.05 | |
| Zehra et al. (123) 2019 | Adult volunteers | BP today (VAS) | EPD score | 12.4±17.0 | 17.0±22.4 | | | p>0.05 | | |
| Sharma et al. (124) 2011 | Patients | LBP | Endplate defect | 13 | 40 | 2 | 8 | p>0.05 | | |
| Sward et al. (145) 1990 | Young athletes | Back pain | Schmorl's nodes | 28 | 64 | 7 | 43 | P=0.05 | | |
| | | Moderate back pain | Schmorl's nodes | 14 | 36 | 7 | 43 | | | |
| | | Severe back pain | Schmorl's node | 14 | 28 | 7 | 43 | | | |
| Cohort studies | | | | | | | | | | |
| Iwamoto et al. (125) 2005 | High school rugby players | History of pain | Schmorl's node | 18 | 78 | 28 | 203 | 1.66 (1.09, 2.28); p>0.05 | | |
| | | Incidence of pain (1 year) | Schmorl's node | | | | | 0.82 (0.21, 3.15); p>0.05 | | |
| Iwamoto et al. (146) 2004 | High school football players, 85/171 with BP | Incidence of LBP | Schmorl's node | | | | | χ ² = 1.047 NS | | |
| | College football players, 390/742 with BP | Incidence of LBP | Schmorl's node | | | | | χ ² = 10.895 NS | | |
| Kauppi et al. (147) 1997 | General population | Back pain during adult life | Endplate sclerosis | | | | | 1.9 (1.24, 2.90), p<0.003 | | Age and sex |
| Luoma et al. (135) 2016 | Chronic LBP patient | Chronic LBP | EPL bony endplate lesion (new irregular) | 9 | 119 | 12 | 189 | P=0.001 | P=0.001 | Age, sex, interval between the MRIs studies, and |

| | | | ty or focal defect) | | | | | | history of a previous spine surgery (yes/no) |
|-----------------------------|-----------------------------------|--|---------------------------|----|----|----|---------------------------|---------------------------------------|--|
| Munir et al. (132) 2018 | Twins (general population sample) | Back pain disability (≥ 1 month) | TEP score L1/L2 | | | | | Estimates (SE) 0.359 (0.113); p=0.001 | age, sex and BMI |
| | | | L2/L3 | | | | | 0.280 (0.112); p=0.013 | |
| | | | L3/L4 | | | | | 0.351 (0.114); p=0.002 | |
| | | | L4/L5 | | | | | 0.617 (0.131); p=0.001 | |
| | | | L5/S1 | | | | | 0.671 (0.127); p=0.001 | |
| Nagashima et al. (134) 2013 | Football players | 2-year history of LBP, | Schmorl's nodes | | | | 2.79 (0.89, 8.72) p=0.078 | | |
| Ogon et al. (148) 2001 | Young Skiers | Incidence of LBP | Endplate lesion | 10 | 5 | 47 | 58 | | |
| | | | Severe Anterior lesion | 8 | 7 | 17 | 88 | $\chi^2 = 11.56$, p<0.004 | |
| | | | Schmorl's node | 4 | 11 | 15 | 90 | 1.8, p=0.44 | |
| | | | Moderate Posterior lesion | 1 | 24 | 6 | 89 | 1.7, p=0.67 | |

Abbreviations defined: LSS=lumbar spinal stenosis, CLBP=chronic low back pain, DDD=degenerative disc disease, DD= disc degeneration, RA=rheumatoid arthritis, TEPS=total endplate score

2.2.3 Meta-analysis

Of the 26 studies included in the review, some studies analyzed more than one EPSD or back pain phenotype, resulting in 39 study units (estimating different associations) included in the meta-analysis. Despite no evidence of publication bias from Egger's Test ($p = 0.82$), the presence of moderate heterogeneity ($I^2 = 67\%$; $p = 0.001$) did not allow for the pooling of the data across all 39 units from the studies. As per the a priori hypothesis, results were pooled according to the EPSD phenotype (e.g., Schmorl's nodes, sclerosis, etc.); type of back pain assessed (e.g., incidents of back pain, back pain intensity, etc.), study population (e.g., general population, patients), and adjusted versus unadjusted odds ratios. Various EPSD phenotypes, such as calcification, ossification, and sclerosis, that may represent the same construct were merged into a single category as suggested by a previous study (13).

Figure 2-2 illustrates the pooled estimates for the association of each EPSD phenotype with back pain, including the number of studies in each analysis and heterogeneity statistics (I^2 and Chi-square p -value). Specific phenotypes of EPSD, such as erosion (OR: 2.69; 95% CI: 1.37–5.30 and sclerosis (OR: 1.97; 95% CI: 1.50–2.58), were pooled without significant heterogeneity ($I^2 = 39.6\%$, $p = 0.19$ and $I^2 = 0.0\%$, $p = 0.42$ respectively) and were significantly associated with low back pain.

The data for the outcomes of all back pain phenotypes could not be pooled due to high heterogeneity ($I^2 = 73\%$, $p = 0.01$), as was also the case for studies specifically of disabling back pain ($I^2 = 68.0\%$, $p = 0.01$). Whereas studies of frequent back pain (OR: 2.83; 95% CI: 1.77–4.52) and back pain incidence (OR: 1.65; 95% CI: 1.30–2.11) were each pooled, as supported by low I^2 values of 0% and 7.5% respectively, with each demonstrating a statistically significant association with EPSD (Figure 2-3). Also, the heterogeneity of the pooled estimate of the association between EPSD and back pain phenotypes ($I^2 > 75\%$) could not be explained by differences between adjusted vs unadjusted odds ratios.

Pooled estimates of studies of the association of Schmorl's nodes and back pain phenotypes in general population samples (OR: 1.63; 95% CI: 1.37–1.94, $I^2 = 26\%$), and in patients seeking care for conditions other than back pain, such as scoliosis, Stickler syndrome or disc prolapse (OR: 2.35; 95% CI: 1.88–2.93, $I^2 = 10.1\%$), demonstrated statistically

significant associations. However, data on associations of EPSD and back pain phenotypes in mixed population samples of patients vs. controls could not be pooled due to considerable heterogeneity ($I^2 > 75\%$). Figure 2-4 shows the forest plot of the pooled estimates specifically for the association of Schmorl’s nodes and back pain phenotypes in general population samples. Schmorl’s nodes were associated with unspecified back pain (OR= 1.77; 95%CI: 1.29–2.45; $I^2 = 7.5\%$, $p = 0.37$) and back pain incidence (OR= 1.53; 95%CI: 1.21–1.93; $I^2 = 0\%$, $p = 0.75$), and back pain overall irrespective of definition (OR= 1.63; 95%CI: 1.37–1.94; $I^2 = 26\%$, $p = 0.19$).

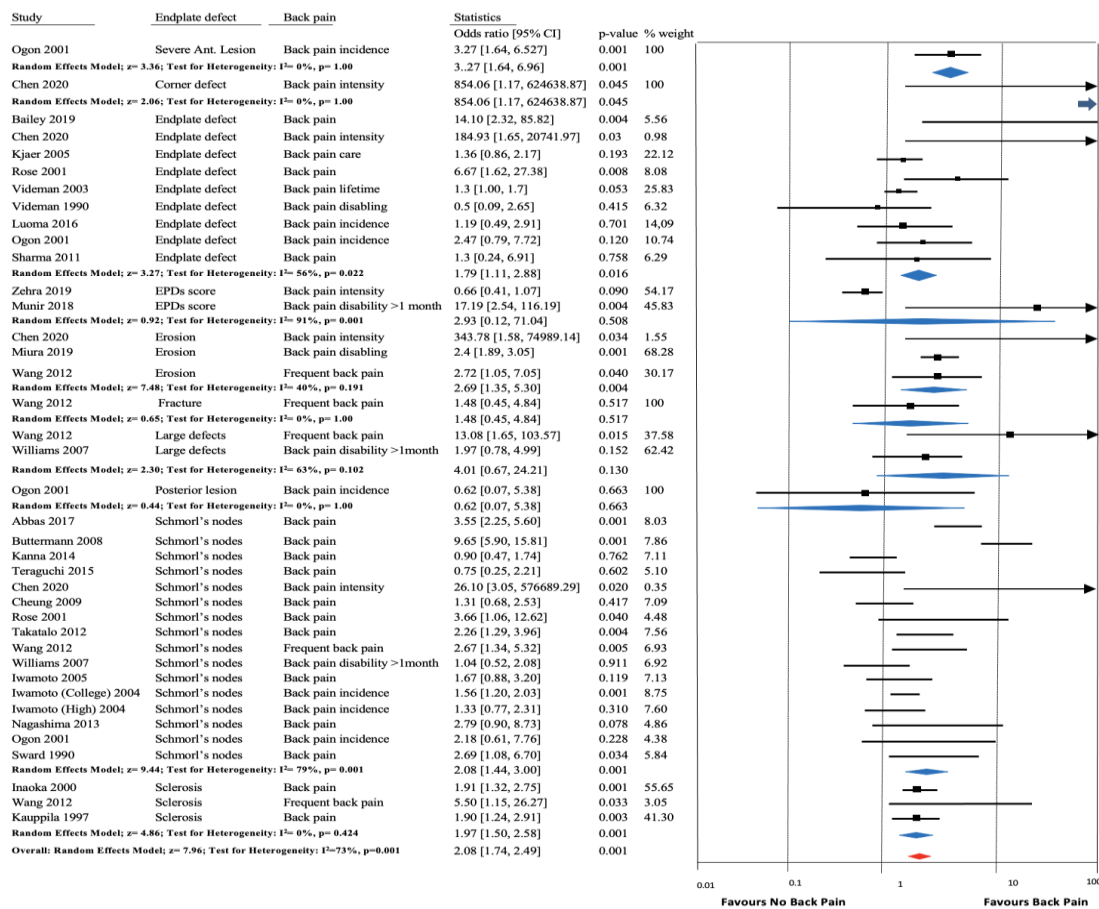


Figure 2-2: Forest plot for associations of each endplate defect type with various back pain definitions, with individual study and pooled estimates, and 95% confidence intervals. As can be seen from the high I^2 values, there was unacceptably high heterogeneity among all studies and those of particular endplate phenotypes to rely on the pooled estimates, with the exception of studies of *sclerosis* and *erosion*.

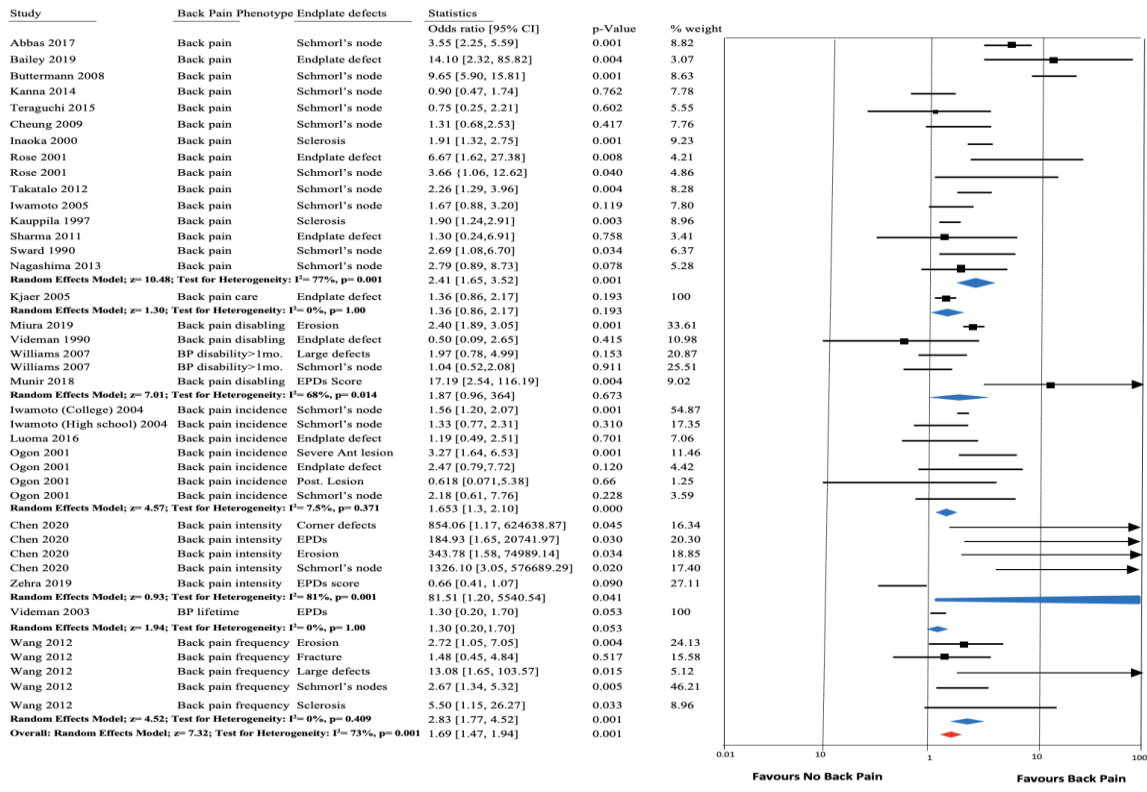


Figure 2-3: Forest plot of the association of various back pain phenotypes with endplate defects with pooled estimates and 95% confidence intervals. As can be seen from the high I^2 values, there was unacceptably high heterogeneity among all studies and those of particular back pain phenotypes to rely on the pooled estimates, with the exception of studies of *back pain incidence* and *back pain frequency*. It should be noted, however, that the estimates for the latter came from one study.

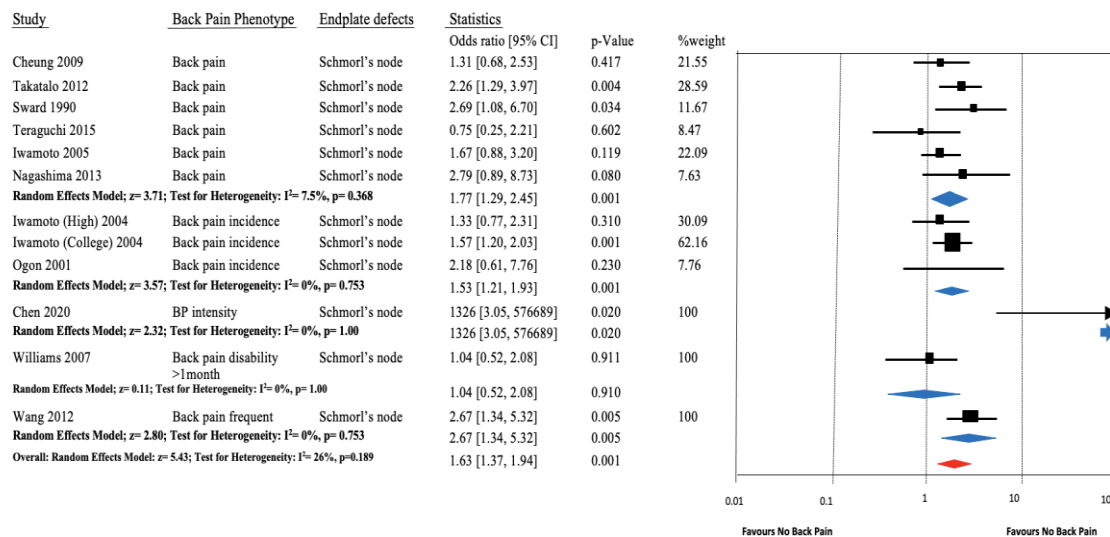


Figure 2-4: Forest plot of the association of Schmorl's nodes and various back pain phenotypes among general population samples with pooled estimates and 95% CIs.

2.2.4 Quality assessment and GRADE of evidence

Figure 2-5 shows the summary of each study's quality appraisal score and the percentage distribution of the types of bias that were insufficiently addressed specifically related to the study design used. The total scores of the case-control studies ranged from 11/16 to 15/16 (119,120,133,140), the cohort studies ranged from 11/19 to 19/19 (125,134,135,146–148), and the cross-sectional studies from 5/11 to 11/11 (26,32,121–124,136–139,141–145).

Selection and confounding bias were least commonly addressed, with no considerations of confounding in 12 studies, followed by failure to address information bias (using valid and reliable measures consistently across all participants to assess exposure, outcomes and confounders or effect modifiers) in 10 studies. Performance bias (e.g., a consistent strategy for recruiting participants across study groups or arms, an adequate description of the exposure) was most often addressed and adequately reported. The majority of the studies sufficiently addressed most of the questions or concerns relating to bias within the constraints of the study design used, with sufficiency of addressing bias ranging from 53%

to 100%. The extent to which various forms of bias were neglected in each study relative to the study design is presented in Figure 2-5.

Considering the various aspects of GRADE (study limitations, imprecision, indirectness, inconsistencies and publication bias), the evidence for the association between EPSD and back pain was of moderate quality due mostly the inconsistencies and imprecision of the estimates. However, the association between Schmorl’s nodes and back pain phenotypes in the general population was supported by high quality evidence.

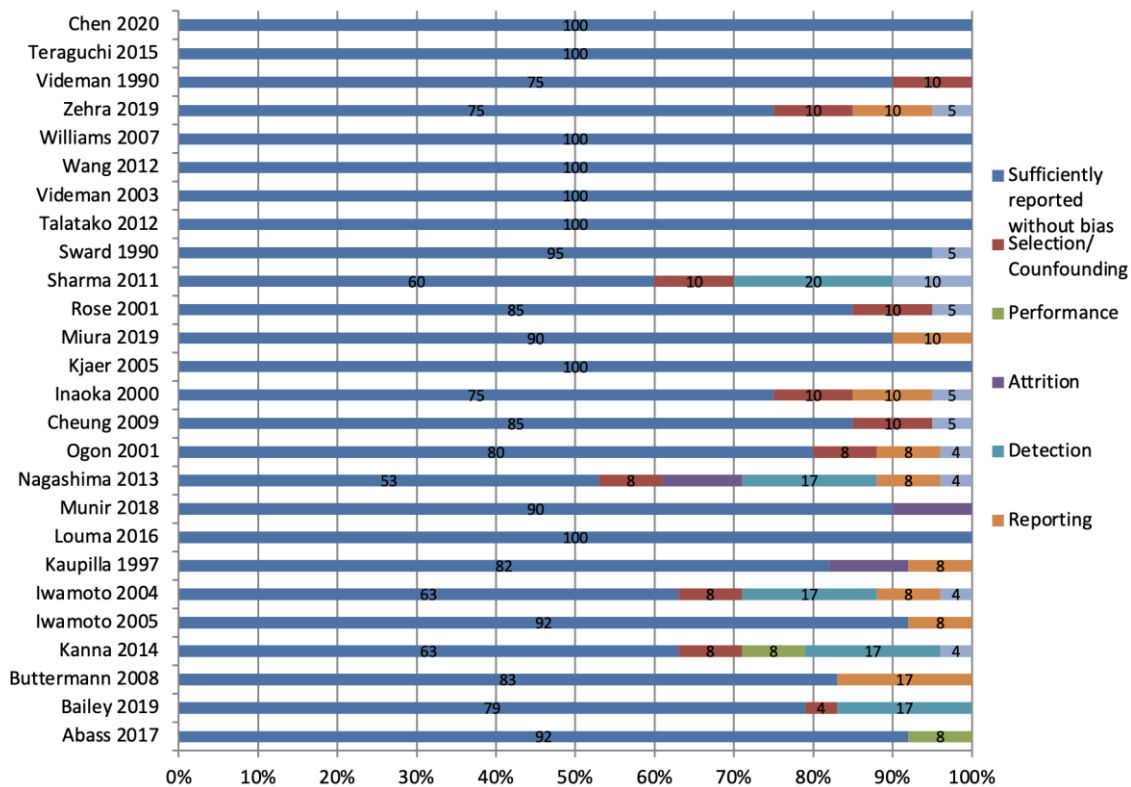


Figure 2-5: Percentage distribution of the types of bias sufficiently and insufficiently assessed in the quality appraisal criteria of the included studies, specific to the study design used.

2.3 Discussion

We aimed to systematically review the health sciences literature on the association between EPSD and back pain, and where applicable pooled the data in a meta-analysis. Findings revealed that despite the inconsistencies among the included studies' findings, the overall pooled data provide moderate quality evidence of an association between EPSD and back pain. The variation in the associations between EPSD and back pain was explained by the EPSD and back pain phenotypes, and the population studied. However, the heterogeneity of the pooled data was not explained by the difference between adjusted and unadjusted odds ratios.

There was consistent evidence for an association between the specific EPSD phenotypes of erosion and sclerosis, and back pain. Also, there was more consistency of associations of specific definitions of back pain, such as incidence of back pain and frequent back pain, with EPSD of various types, than for back pain overall. This indicates that clear, more precise case definitions for both EPSD and back pain are essential to decreasing inconsistent findings and heterogeneity and determining associations. Furthermore, there was high quality evidence supporting an association between Schmorl's nodes and back pain among the general population, again supporting the need for clear EPSD phenotypes and attention to study population.

Data from the two studies (123,132) that assessed EPSD using a cumulative score could not be pooled due to high heterogeneity, which may be explained by variation in the constructs assessed by each scale. Zehra et al (123) used the cumulative endplate score which is based on the width and depth of each EPSD. While Munir et al (132) used the Total Endplate (TEP) score that is based on a 6-point scale, ranging from 1=no defect and 2=focal endplate thinning to 6=extensive or complete endplate damage with gross irregularities or sclerosis.

It is important to acknowledge that different imaging modalities were used (e.g., MRI, CT scans and radiographs) to assess various phenotypes of EPSD among varied population samples related to different definitions of back pain, which make it difficult to draw firm conclusions on particular associations. Also, the multifactorial nature of the etiology of

back pain may have contributed to the heterogeneity of findings among the included studies. With this in mind, consideration of confounding is important. EPSD have been associated with other spinal imaging findings, such as Modic changes and disc degeneration, that have also been associated with back pain. Yet, only a few of the included studies considered possible confounding from such factors.

The results of this systematic review suggest several recommendations for future research on the association of EPSD and back pain. First, there is a need for better standardization and reporting of the nomenclature and measurement methods of EPSD phenotypes and back pain case definitions to allow study comparisons and pooling of data. Second, more attention needs to be given to potentially confounding factors. In particular, more studies need to examine possible confounding from other associated imaging findings (e.g., disc degeneration, Modic changes), as well as possible interactions between such findings associated with back pain. However, within the limitations of wide variations in the confounding factors considered in the literature reviewed, adjustment for confounding factors did not clearly contribute to the heterogeneity observed among the study results. Finally, robust longitudinal studies are needed to provide more insight into the role of EPSD in the causation of specific back pain phenotypes using well-defined population samples.

In conclusion, there is moderate quality evidence supporting an association between back pain and EPSD, and high-quality evidence of an association between Schmorl's nodes and back pain in the general population. Going forward, research on specific EPSD phenotypes (e.g., erosion and sclerosis) and back pain case definitions (e.g., incidence and frequency of back pain) using strong study designs will be important in clarifying the extent of associations and underlying mechanisms.

Chapter 3

3 Detection and characterization of Vertebral Endplate Structural Defects on CT: A Diagnostic Test Study

Summary

Background: Studies of EPSD may further the understanding of pathoanatomical mechanisms underlying back pain. However, with CT, as with MRI, the common methods used to document EPSD have not been validated, leaving uncertainty about what the observations represent or how accurately they capture the presence or absence of EPSDs.

Objective: To determine the reliability and validity of two common endplate structural defects (EPSD) assessment methods. *Methods:* Using an evaluation manual, 418 endplates on clinical-CT sagittal slices obtained from 19 embalmed cadavers (9 men and 10 women, aged 62-91 years) were independently assessed by two experienced radiologists and a novice for EPSD using the two methods. The corresponding μ CT from the harvested T7-S1 spines were assessed by another independent rater with excellent intra-rater reliability (Kappa=0.96, 95%CI:0.91–0.99). The study was approved by Western’s Research Ethics Board for Use of Cadaveric Materials (01202020), and prospectively registered at ClinicalTrial.gov: NCT04808960. *Results:* The inter-rater reliability was good for the presence (Kappa=0.60-0.69) and fair for specific phenotypes (Kappa=0.43-0.58) of EPSD. Erosion, for which Brayda-Bruno lacked a category, was mainly (82.8%) classified as wavy/irregular. While the majority of notched defects (n=15, 46.9%) and Schmorl’s nodes (n=45, 79%) using Brada-Bruno’s classification were recorded as focal defects using Feng’s. *When compared to μ CT*, endplate fractures (n=53) and corner defects (n=28) were routinely missed on clinical CT. Endplates classified as wavy/irregular on clinical-CT corresponded to erosion (n=29, 21.2%), jagged defects (n=21, 15.3%) and calcification (n=19, 13.9%) on μ CT. While some focal defects on clinical CT represented endplate fractures (n=21, 27.6%) on μ CT. Overall, with respect to the presence of an EPSD, there was a sensitivity of 70.9% and specificity of 79.1% for Feng’s method, and 79.5% and 57.5%, respectively, using Brayda-Bruno’s. All EPSD clinical-CT and μ CT dimensions significantly correlated ($p<0.001$), except with defect depth. *Conclusion:* There is good

reliability and support for the validity of assessing the presence of EPSD using the two methods. However, neither method contained all the needed EPSD phenotypes to provide optimal sensitivity (due to the high false negative result/ miss rate).

Introduction

Back pain is a common health problem and a substantial burden on affected individuals, their families and society (149). In fact, it is the single leading cause of disability worldwide (150). Unfortunately, the pathological mechanisms behind back pain are not well understood, hindering the development of well-targeted, effective prevention and treatment approaches. The anatomical structures referred to as the functional spinal units, each composed of an intervertebral disc, its two adjacent vertebrae, and other associated osteoligamentous structures, have been studied for decades with limited success in identifying the source of the pain. The intervertebral disc has received the most attention, and while disc degeneration or pathology is associated with other clinical syndromes of disc herniation with radiculopathy, and spinal stenosis, the role of the disc in common back pain is uncertain. More recently, the vertebral endplate has attracted attention as a possible contributor to back pain.

The vertebral endplate is a thin mechanical interface between the intervertebral disc and the cancellous bone of the adjacent vertebral body. Unlike the disc, the bony vertebral endplate is highly vascularized and has a plentiful neural supply, and endplate structural defects (EPSD) are relatively common in cadaveric, patient and general population samples (15,33,151). However, prevalence rates for EPSD vary widely across studies from 9% to 75% (26,28,126) and there are conflicting findings on their association with back pain (32,123,152). A lack of consistency in the use of terms and definitions for EPSD contributes to these inconsistencies and limits the ability to effectively communicate findings, interpret and compare study results, and build a coherent body of knowledge on the causes and consequences of EPSD (13).

Furthermore, the absence of clear definitions or descriptions of EPSD represented by various terms is problematic for measurement reliability, which is seldom reported in studies of EPSD. A morphologic description has been found to be more important in

establishing the reliability of a standardized MRI nomenclature than the experience of the reader (153). However, a recent review (13) identified few measurement methods with detailed classification and definition of structural endplate phenotypes. Among them were methods presented by Feng et al (15) and Brayda-Bruno et al (154). Both measurement methods stem from a previous study on EPSD phenotypes observed in a cadaveric sample (35). Good to excellent intra- and inter-rater reliability was reported for each classification system in a single MRI study, but neither has been validated.

Clinical CT is one of the most ideal and common imaging modality used to examine the osseous components of the spine and its use is expected to increase with advancements in clinical CT technology, such as low tube potential and iterative reconstruction that decreases scan time and radiation dose while optimizing image quality (155). Yet, with CT, as with MRI, the varied measurement methods used to document the appearance of EPSD on clinical imaging in the scientific literature, and the absence of validation of such methods, leaves uncertainty about what the observations on imaging actually represent. It is also unclear how sensitive clinical imaging is in picking up the different types and sizes of EPSD (e.g., diagnostic accuracy). μ CT has been used as a reference standard in human studies (156), including for the characterization of morphological features of EPSD in cadaveric samples (157–159). μ CT measurement is accurate, consistent and reproducible, and has the advantage of providing shape and texture information for an object within a single measurement due to its high spatial resolution (156).

This study aimed to address the reliability and diagnostic test validity of assessments of EPSD on clinical CT using μ CT as a reference standard. Such information is critical for establishing meaningful standards for evaluating and interpreting EPSD on imaging, as well as for studies of their etiology and clinical consequences.

3.1 Materials and Methods

3.1.1 Materials

The study sample comprised 19 embalmed (fixed) cadavers (9 males and 10 females) with a median age at the time of death of 82 years (range 62-91) from Western University's whole-

body donation program maintained by the Department of Anatomy and Cell Biology, Schulich School of Medicine and Dentistry. Embalming consisted of arterial distribution of embalming fluid, containing a mixture of ethanol, phenol, and formalin (Wessel & Associates: Troy, MI, USA), 24- to 48- hours post-mortem). All cadavers available for the harvesting of the spinal region T7-S1 with endplates and vertebral bodies intact and undamaged by prior use from the Anatomy Lab were used. There were no other exclusion criteria.

3.1.2 Image acquisition

Clinical CT was acquired (scanned at 1.25mm x 1.25mm on a standard bone algorithm and then reformatted into an axial, coronal and sagittal series at 3mm x 2mm) on all fully intact cadavers prior to the onset of this study. μ CT of all cadaveric spines was performed at a peak voltage of 80 kVp and a tube current of 50 mA. The X-ray projections were reconstructed into a single three-dimensional volume with isotropic voxel spacing of 154 μ m. In preparation for μ CT, the lower thoracic and lumbar spine (T7 through S1) was harvested from each cadaver. The ribs were dissected 1-2 cm lateral to the costovertebral joints and the soft tissues associated with the spine were preserved and remained intact during μ CT.

3.1.3 Assessment of EPSD on clinical CT scans

Three raters independently assessed the sagittal images of the clinical CT for EPSD presence, phenotype classification, and defect size and location, blinded to all prior assessments. EPSD measurement methods by Brayda-Bruno et al (154) and Feng et al (15) were strictly used. First, measurement according to Brayda-Bruno et al (154) was used to assess the 19 clinical CTs of the spines. Two weeks after the Brayda-Bruno assessment, evaluations according to Feng et al (15) as well as measure the location of defects, and anteroposterior and transverse diameter of the defects and endplates. Across all measurements, endplates were labelled with reference to the disc. All EPSD measurements were observed from the immediate normal slice before the defect to the first normal slice after the defect.

Feng et al's (15) initial measurement protocol used sagittal MR images to estimate the transverse diameter by dividing the number of images with EPSD by the total number of sagittal images containing the endplate. However, due to the large number of sagittal images in CT compared to MRI, the transitional distance covered by the defects was used to estimate the transverse diameter. Osteophytes were excluded from measurements. Each rater assessed the images in the same order (Brayda-Bruno et al (154) followed by Feng et al (15)). All measurements were taken in millimetres and rounded up to the nearest two decimal places. All assessments were entered into a pilot-tested excel data entry form. For discordant ratings by all three raters, a Nominal Group Technique was employed to reassess each endplate and a consensus vote for the presence and phenotype determination was used. Then, all the raters in collaboration measured the defect dimensions (anteroposterior and transverse diameter, and axial area) using Feng et al's method.

3.1.3.1 Raters, training, and consensus

The clinical-CT scans were assessed independently by two radiologists with experience in musculoskeletal imaging and a physical therapist, Ph.D. student studying EPSD. A master's student in Clinical Anatomy assessed and documented EPSD on μ CT, the reference standard. To ensure a consistent understanding of the nomenclature in each classification system, an evaluation manual (Appendix 3: EPSD assessment manual) consisting of measurement descriptions and figures was prepared based on the published articles introducing each classification system (15,154). For the purpose of training and to identify practical issues in the evaluation process, four joint training sessions were organized for the raters to evaluate training sets of clinical CT images and discuss practical issues. Each rater independently rated three clinical CT images (66 endplates). Results were collected and analyzed, conflicting domains were noted, discussed and clarified. All the raters indicated satisfaction with the understanding and ability to use each measurement method before the commencement of the study.

3.1.4 Assessment of EPSD on μ CT (reference standard)

Each bony vertebral endplate was studied by visually inspecting the entire vertebral endplate as seen on three-dimensional reconstructed images by a senior graduate student in

clinical anatomy. Three-dimensional reconstructed images were created using segmentation and thresholding tools in MicroView (Version 2.6.0-3, GE Healthcare: London, CAN) to visualize endplate architecture. EPSD were identified and characterized based on their morphological characteristics and were confirmed on at least two views (sagittal, coronal, or axial). The type, size, and location of each defect was recorded. EPSD were categorized as Schmorl's Nodes (with an osseous encasement), corner fractures or limbus vertebrae, other endplate fractures, erosion (with exposed trabecular bone), endplates with a jagged appearance (bumpy or irregular appearance without significant calcium deposition or exposed trabecular bone), calcification, and large contour depressions. Only EPSD with a surface area greater than 5mm^2 were recorded. Repeated assessments of a random sample of 100 vertebral endplates yielded an almost perfect agreement, with a kappa value of 0.90 (95% CI 0.83-0.97) for EPSD presence. The intra-rater reliability of the presence or absence of EPSD for a random sample of 112 defects from 100 spinal levels assessed on μCT was excellent (Kappa: 0.96, 95%CI: 0.91–0.10).

3.1.5 Statistical Analysis

Data were imported into Statistical Packages for Social Sciences (SPSS), version 22 (IBM Corporation, Armonk, NY, USA). All data were descriptively analyzed using frequencies and percentages for categorical data and means and standard deviations for continuous variables. Inter-rater reliability among the three raters was determined using Cohen's kappa statistic for categorical variables (presence or absence and type of defect), Intraclass Correlation Coefficients (ICC) for continuous variables (e.g., anteroposterior and transverse diameters) and weighted kappa for ordinal variable (axial area). ICC and Kappa values were interpreted as poor (< 0.40), fair (0.41–0.60), good (0.61–0.80), or excellent (0.81–1.00). Two-way Intraclass Correlations (ICC) for absolute agreement using a mixed-effect model for average-measures ICC were calculated. With respect to measurement validity, a 2x2 table was used to calculate sensitivity and specificity in detecting the presence and phenotype of EPSD for individual raters and the consensus assessments. Correlation between endplate defect size measurements (qualitatively and quantitatively) on clinical CT and μCT was assessed using Spearman rank moment

correlation, which is best for discrimination when variables are estimated on a continuous scale (160). The study was prospectively registered at ClinicalTrial.gov (NCT04808960).

3.2 Results

Among the 418 endplates assessed by the three raters according to Feng et al (15), there was agreement between the three raters in rating 261 endplates, and 143 endplates between any two of the raters, while 14 endplates were inconsistently rated by all the three raters. Similarly, using the Brayda-Bruno et al (154) method, 187 endplates were consistently rated by the three raters, 202 endplates by two raters, and 29 endplates were inconsistently rated by all three raters. With respect to validity analyses, endplate defects' presence and type were determined according to agreement by at least two of the raters. Size measurements were averaged from the measurements of the raters that agreed on the presence of the same endplate defect phenotype. In cases of discrepancies between the three raters on the type of defect, consensus was achieved by agreement of a simple majority vote, and defect measurements were taken in collaboration with all the raters during the Nominal Group Technique meeting.

Table 3-1 shows the inter-rater reliability for clinical-CT endplate defect assessments between pairs of raters, as well as the average correlation coefficients. There was good reliability for the assessment of the presence of endplate defects with both assessment methods for each pair of raters for the Brayda-Bruno et al (154) ($k=0.61 - 0.69$) and Feng et al (15) ($k=0.68 - 0.69$) methods. While reliability for detecting specific endplate defect phenotypes was poor to fair for the Brayda-Bruno et al (154) ($k=0.38 - 0.4$) and fair to good for the Feng et al (15) ($k=0.54 - 0.61$) methods. The reliability of the measurements of endplate defect sizes varied widely among the raters ($k=0.08 - 0.64$). Overall, on average, there was good inter-rater reliability for the Brayda-Bruno et al (154) ($k=0.63$, 95%CI: 0.56, 0.71) and Feng et al (15) ($k=0.68$, 95%CI: 0.61, 0.75) methods for the presence of endplate defects and fair reliability for endplate defect phenotype ($k=0.43$, 95%CI: 0.36, 0.49 and $k=0.58$, 95%CI: 0.51, 0.65). Poor reliability ($k=0.26$ and 0.37) was observed for the average defect dimensions, except for the axial area measurements ($k=0.47$, 95%CI: 0.31, 0.63).

Table 3-1: Inter-rater reliability of endplate defect assessments by raters using Brayda-Bruno (B-B) et al and Feng et al methods. (Values are kappa coefficients (95% CI) for categorical variables and ICCs (95% CI) for continuous measurements.)

| | Assessor 1 and 2 | Assessor 1 and 3 | Assessor 2 and 3 | Average score |
|---------------------------|--------------------|---------------------|--------------------|--------------------|
| Brayda-Bruno et al | | | | |
| Defect presence | 0.62 (0.54, 0.70) | 0.61 (0.53, 0.67) | 0.69 (0.62, 0.76) | 0.63 (0.56, 0.71) |
| Defect phenotype | 0.44 (0.37, 0.50) | 0.38 (0.32, 0.45) | 0.46 (0.40, 0.52) | 0.43 (0.36, 0.49) |
| Feng et al | | | | |
| Defect presence | 0.69 (0.61, 0.76) | 0.68 (0.60, 0.75) | 0.68 (0.61, 0.75) | 0.68 (0.61, 0.75) |
| Defect phenotype | 0.60 (0.53, 0.66) | 0.536 (0.47, 0.60) | 0.61 (0.54, 0.67) | 0.58 (0.51, 0.65) |
| Ant-post diameter | 0.59 (0.43, 0.70) | 0.181 (-0.13, 0.41) | 0.34 (0.08, 0.53) | 0.37 (0.12, 0.55) |
| Transverse diameter | 0.06 (-0.30, 0.32) | 0.637 (0.50, 0.74) | 0.08 (-0.30, 0.35) | 0.26 (-0.03, 0.47) |
| Axial area | 0.53 (0.37, 0.68) | 0.370 (0.21, 0.53) | 0.52 (0.36, 0.69) | 0.47 (0.31, 0.63) |

Details of the comparison of EPSD detected using the two methods are shown in Table 3-2. All normal endplates according to Brayda-Bruno et al (154) (n=151) were also classified as normal with the Feng et al (15) method. However, only 67.7% of normal endplates according to Feng et al (15) were rated as normal using the Brayda-Bruno et al (154) method. Of normal endplates using Feng et al's system(15), 26% (n=58) corresponded to wavy/irregular endplates using Brayda-Bruno et al's (154), a category that does not exist in the Feng et al system.(15) Similarly, erosion, for which Brayda-Bruno et al (154) lacked a category, was mainly (82.8%) classified as wavy/irregular. While most notched defects (n=15, 46.9%) and Schmorl's nodes (n=45, 79%) using Brayda-Bruno et al's classification (154) were recorded as focal defects using Feng et al's (15). No cases of fracture according to Brayda-Bruno et al (154) or corner fracture according to Feng et al (15) were detected.

Table 3-2: Frequencies of endplate structural defects detected by Brayda-Bruno et al and Feng et al methods

| B-B et al / Feng et al | Normal | Wavy/irregular | Notched | Schmorl's node | Fracture | Total |
|------------------------|----------------------|-----------------------|-----------------------|----------------------|----------|-------------|
| Normal | 151(67.7%) (100%) | 58 (26.0%) (38.2%) | 11 (4.9%) (34.4%) | 3 (1.3%) (5.3%) | 0 | 223 (56.9%) |
| Focal | 0 | 22 (26.8%) (14.5%) | 15 (18.2%) (46.9%) | 45 (54.9%) (79%) | 0 | 82 (20.9%) |
| Corner defect | 0 | 0 | 0 | 0 | 0 | 0 |
| Erosion | 0 | 72 (82.8%) (47.4%) | 6 (6.9%) (18.8%) | 9 (10.3%) (15.8%) | 0 | 87 (22.2%) |
| Total | 151(38.5%) | 152 (38.8%) | 32 (8.2%) | 57 (14.5 %) | 0 | 392 |

Table 3-3 shows the comparison of EPSD phenotypes assessed using each of the clinical-CT assessment methods to what they represent on the μ CT reference standard. There was a higher number of normal endplates according to the Brayda-Bruno et al (154) (n=148, 40.6%) and Feng et al (15) methods (n=210, 58.2%) assessed on clinical-CT, as compared to μ CT (36%). Notably, 53 fractures and 28 corner defects detected on μ CT were missed on the clinical-CT consensus assessments. However, 22 fractures and 6 corner defects were identified by a single rater during assessments. Endplates classified as wavy/irregular on clinical CT corresponded to erosion (n=29, 21.2%), normal (n=26, 19.0%), jagged defects (n=21, 15.3%) or calcification (n=19, 13.9%) on μ CT. While erosion assessed on clinical CT mainly represented erosion (n=29, 38.7%), fracture (n=16, 21.3%), or calcification (n=13, 17.3%). Schmorl's nodes assessed on clinical CT often represented erosion (n=16, 32%) on μ CT while 27.6% of focal defects represented endplate fractures. The complexity in detecting specific EPSD phenotypes, such as fracture, corner defect, calcification, and jagged can be seen in the images in figure 3-2.

Table 3-3: Frequencies of endplate structural defects categorized according to Brayda-Bruno et al and Feng et al methods and corresponding μ CT.

| μ CT Findings | Normal | Schmorl's nodes | Fracture | Compression | Erosion | Calcification | Corner defect | Jagged appearance | Total |
|---------------------|----------------|-----------------|---------------|--------------|---------------|---------------|---------------|-------------------|-------|
| Brayda-Bruno | | | | | | | | | |
| Normal | 104 (70.3%) | 0 | 5 (3.5%) | 1 (0.7%) | 9 (6.1%) | 5 (3.4%) | 13 (8.8%) | 11 (7.4%) | 148 |
| Wavy/irregular | 26 (19.0%) | 3 (2.2%) | 25 (18.2%) | 6 (4.4%) | 29 (21.2%) | 19 (13.9%) | 8 (5.8%) | 21 (15.3%) | 137 |
| Notched | 1 (3.3%) | 3 (10.0%) | 12 (40.0%) | 1 (3.3%) | 3 (10.0%) | 1 (3.3%) | 1 (3.3%) | 8 (26.7%) | 30 |
| Schmorl's node | 1 (2.0%) | 9 (18.0%) | 10 (20.0%) | 2 (4.0%) | 16 (32.0%) | 4 (8.0%) | 4 (8.0%) | 4 (8.0%) | 50 |
| Fracture | 0 | 0 | 0 | 0 | 0 | 0 | 0 | 0 | 0 |
| Total | 132 (36.2%) | 15 (4.1%) | 52 (14.2%) | 10 (2.7%) | 57 (15.6%) | 29 (7.9%) | 26 (7.1%) | 44 (12.1%) | 365 |
| Feng | | | | | | | | | |
| Normal | 124 (59.0%) | 0 | 15 (7.1%) | 2 (1.0%) | 13 (6.2%) | 10 (4.8%) | 17 (8.1%) | 29 (13.8%) | 210 |
| Focal | 2 (2.6%) | 14 (18.4%) | 21 (27.6%) | 4 (5.3%) | 17 (22.4%) | 6 (7.9%) | 4 (5.3%) | 8 (10.5%) | 76 |
| Corner fracture | 0 | 0 | 0 | 0 | 0 | 0 | 0 | 0 | 0 |
| Erosion | 2 (2.7%) | 2 (2.7%) | 16 (21.3%) | 3 (4.0%) | 29 (38.7%) | 13 (17.3%) | 3 (4.0%) | 7 (9.3%) | 75 |
| Total | 128 (35.5%) | 16 (4.4%) | 52 (14.4%) | 9 (2.5%) | 59 (16.3%) | 29 (8.0%) | 24 (6.6%) | 44 (12.2%) | 361 |

Table 3-4 shows the sensitivity and specificity for detecting the presence of EPSD assessed by each rater for the clinical-CT assessment methods using μ CT as the reference standard. There was a higher specificity for EPSD across all raters for Feng (66.6% - 79.2%) compared to Brayda-Bruno (46.5% - 58.9%). While a higher sensitivity among the raters was observed for Brayda-Bruno (72.9% - 82.4%) compared to Feng (62.8% - 72.7%). Overall, for the consensus rating, there was a sensitivity of 70.9% and specificity of 79.1% for Feng's method, and 79.5% and 57.5%, respectively, using Brayda-Bruno's.

Table 3-4: Sensitivity for the assessment of endplate structural defects for Brayda-Bruno et al and Feng et al compared to the reference standard (μ CT) for individual rater and the consensus rating.

| | Assessor 1 | | Assessor 2 | | Assessor 3 | | Consensus | |
|----------------------------|----------------|----------------|----------------|----------------|-----------------|----------------|----------------|----------------|
| | Normal | Defective | Normal | Defective | Normal | Defective | Normal | Defective |
| <i>Brayda-Bruno</i> | | | | | | | | |
| Normal | 92 (46.5%) | 30 (17.6%) | 119 (58.9%) | 46 (27.1%) | 106 (53.3%) | 41 (24.3%) | 115 (57.5%) | 34 (20.5%) |
| Defective | 106 (53.5%) | 140 (82.4%) | 83 (41.1%) | 124 (72.9%) | 93 (46.7.9%) | 128 (75.7%) | 85 (42.5%) | 132 (79.5%) |
| <i>Feng</i> | | | | | | | | |
| Normal | 139 (66.5%) | 41 (27.3%) | 171 (79.2%) | 58 (37.2%) | 164 (76.2%) | 56 (36.6%) | 167 (79.1%) | 44 (29.1%) |
| Defective | 70 (33.5%) | 109 (72.7%) | 45 (20.8%) | 98 (62.8%) | 51 (23.8%) | 97 (63.4%) | 44 (20.9%) | 107 (70.9%) |

Table 3-5: Correlation of clinical-CT endplate structural defects measurements with μ CT

| | Ant-Post diam | Trans diam | Axial area | Surface Area | X - sagit_AP | Y coron_Trans | Z-height | Axial area |
|---------------|---------------|------------|------------|--------------|--------------|---------------|----------|------------|
| Ant-Post diam | 1.00 | 0.80** | 0.80** | 0.37** | 0.49** | 0.29** | -0.17 | 0.34** |
| Trans diam | 0.80** | 1.00 | 0.76** | 0.39** | 0.45** | 0.37** | -0.01 | 0.37** |
| Axial area | 0.80** | 0.76** | 1.00 | 0.39** | 0.48** | 0.32** | -0.19 | 0.42** |
| Surface area | 0.37** | 0.39** | 0.39** | 1.00 | 0.83** | 0.88** | 0.09 | 0.63** |
| X-sagit-AP | 0.49** | 0.45** | 0.48** | 0.84** | 1.00 | 0.62** | 0.01 | 0.63** |
| Y-coron-Trans | 0.29** | 0.37** | 0.32** | 0.88** | 0.62** | 1.00 | 0.14 | 0.59** |
| Z-height | -0.17 | -0.01 | -0.19 | 0.09 | 0.01 | 0.14 | 1.00 | 0.05 |
| Axial area | 0.34** | 0.37** | 0.42** | 0.63** | 0.63** | 0.59** | 0.05 | 1.00 |

Figure 3-1 shows the sensitivity of EPSD phenotype consensus assessments for the two clinical-CT assessment methods. The designations of Schmorl's nodes (60%) and wavy/irregular (54.2%) had the highest sensitivity, followed by Focal defects (52%) and erosion (49.2%). EPSD dimensions were estimated according to Feng et al's assessment methods (Table 3-5). While all EPSD clinical-CT and μ CT dimensions were statistically significantly correlated ($p < 0.001$), except defect depth, the highest correlation was $r = 0.49$ for the anteroposterior diameter of the defect, followed by axial area ($r = 0.42$).

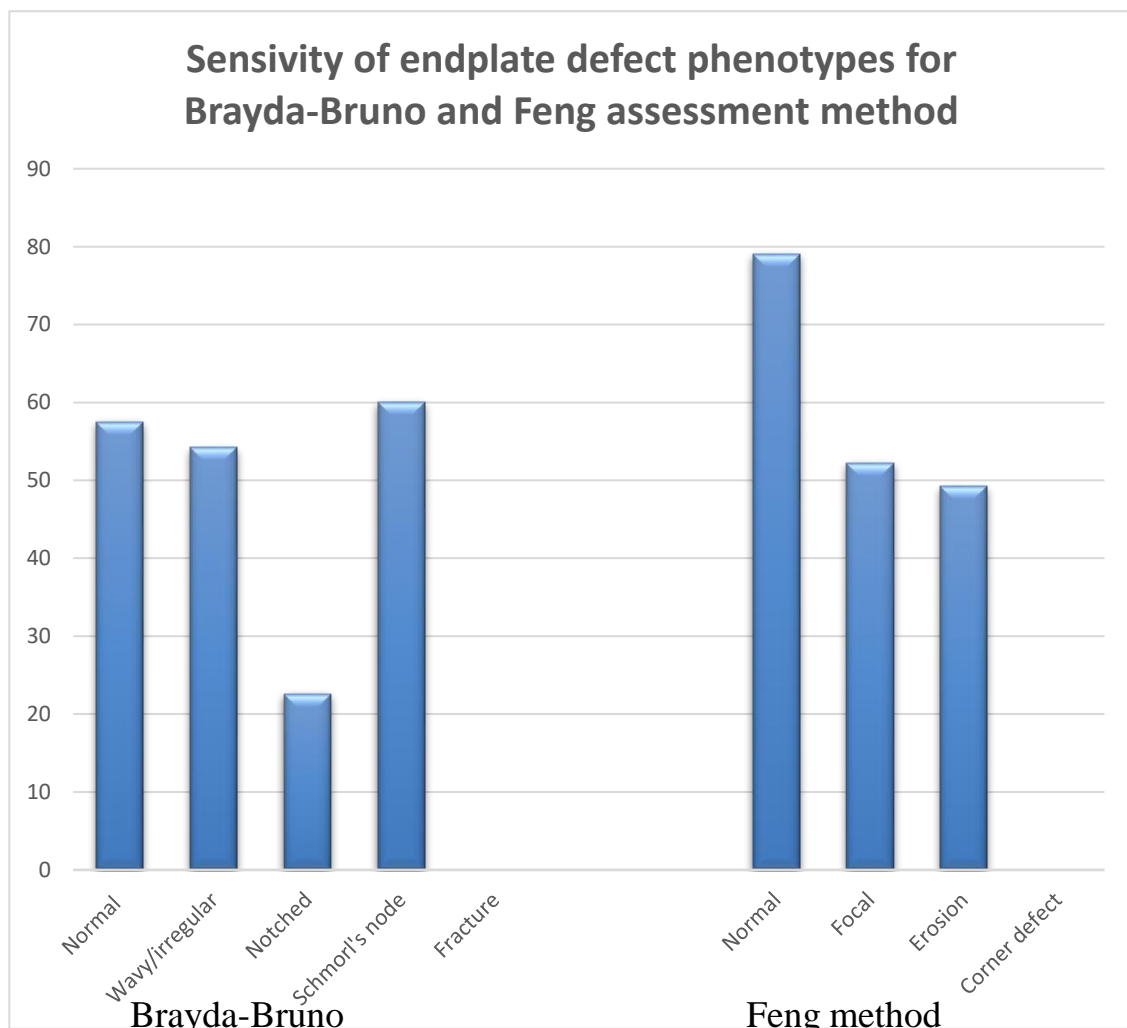
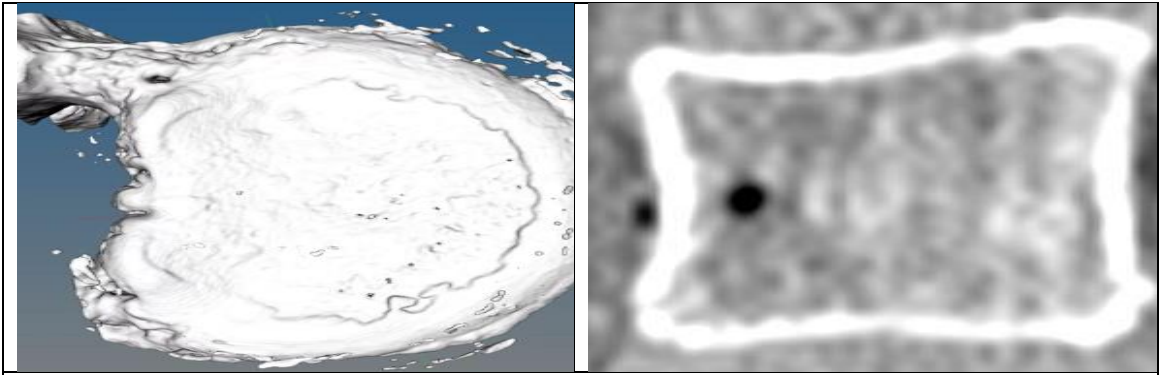
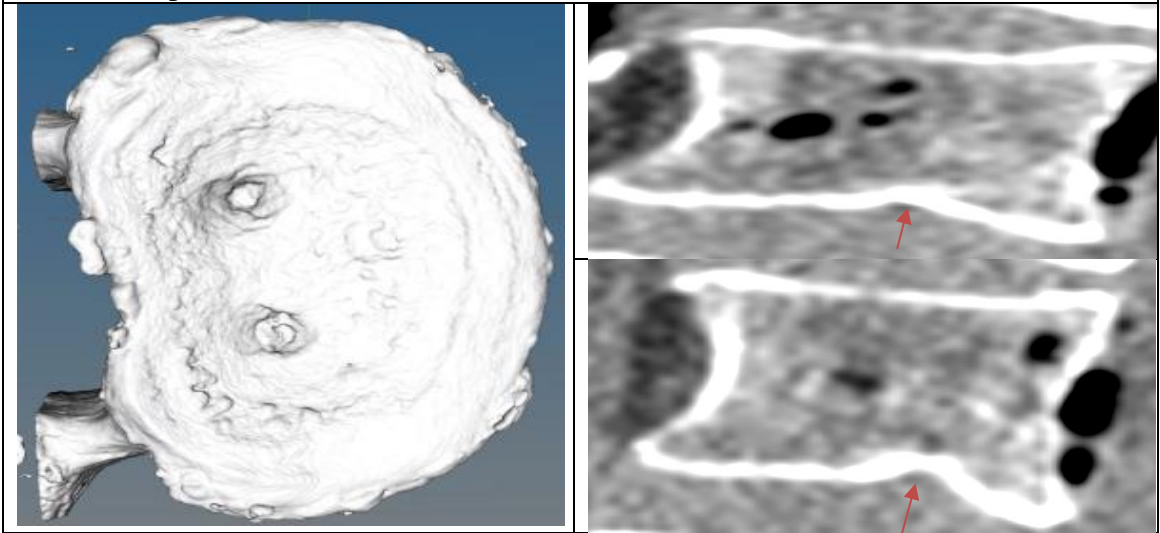


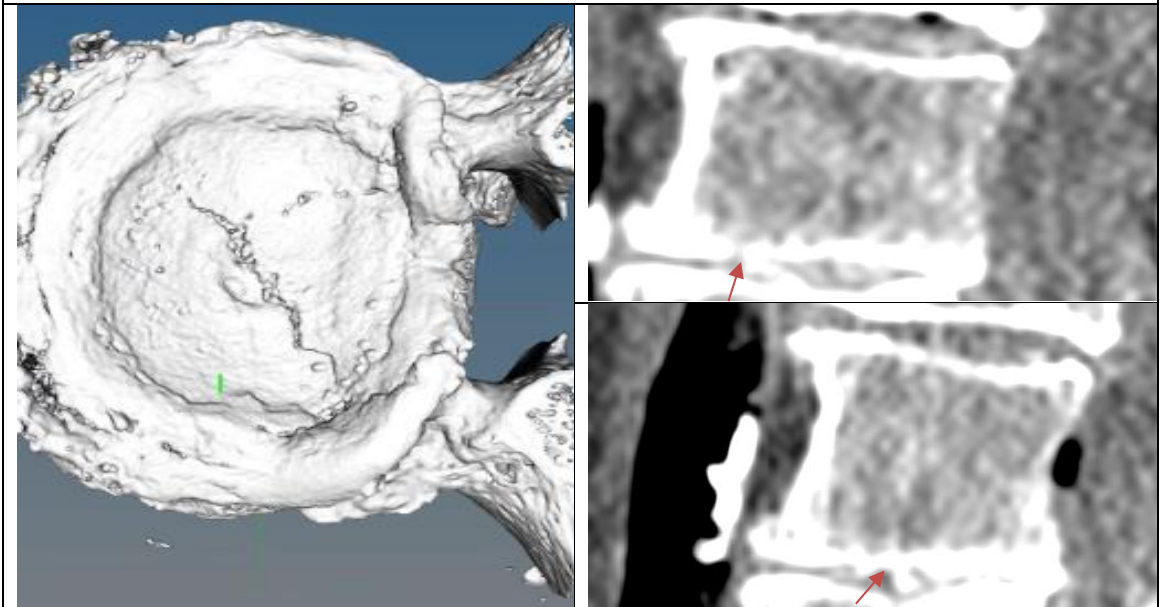
Figure 3-1: Sensitivity of endplate structural defect phenotypes assessments on Clinical CT (Brayda-Bruno and Feng) to the reference standard (μ CT)



Normal endplate



Schmorl's node or focal defect



Calcification (dominant) and Fracture (non-dominant)

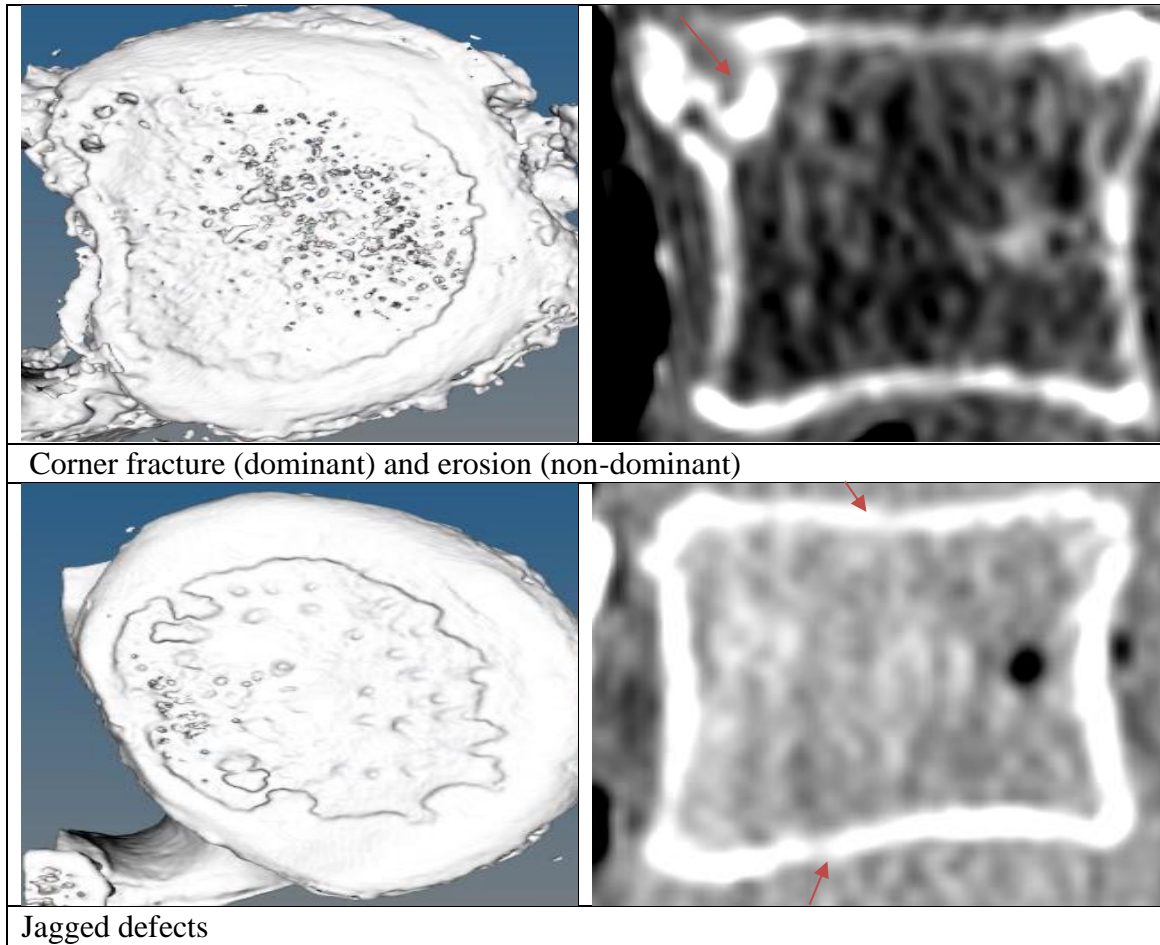


Figure 3-2: EPSP phenotypes observed on μ CT and corresponding CT

3.3 Discussion

Radiologic evidence of structural abnormalities is an important aspect of musculoskeletal diagnosis. However, valid methods are needed to ascertain with confidence what such observations on clinical imaging represent, particularly in the case of subtle findings in small structures, such as the thin, delicate vertebral endplate. Yet defects in vertebral endplates are of great interest with respect to common back pain. We assessed EPSP using two published measurement methods (15,154) to determine their inter-rater reliability and the diagnostic accuracy of EPSP classification when applied to clinical-CT (index test), as compared to μ CT as the reference standard.

In our study, we found good inter-rater reliability and support for the validity of the diagnostic accuracy of the two methods for detecting the presence of EPSD on clinical CT. The reported reliability and validity are similar between the expert radiologist and the novice. However, neither method contained sufficient content for the EPSD phenotypes present to provide the needed sensitivity. The Brayda-Bruno et al (154) system lacked a category for erosion, whereas Feng et al (15) lacked a category for wavy/irregular defects. There is also an overlap in what the phenotype terms represent, which influenced the classifying of certain phenotypes of EPSD. For example, the lack of a wavy/irregular category influences assigning an endplate as normal and, similarly, without a category for erosion, such defects were given other classifications, as wavy/irregular.

Our finding that the two clinical-CT EPSD assessment methods identify fewer defects with relatively low reliability on sagittal slices of clinical-CT as compared to μ CT on multiple planes with higher resolution is not surprising. It is expected that measurements from a single plane such as the sagittal view may not be highly reliable because of the non-parallel projections of the endplate at some levels and the posterior elements of the vertebrae may superimpose on the same area.(29) Also, the discrepancies in μ CT and clinical CT assessments of specific EPSD, such as jagged endplates, supports the view that higher resolution may be needed to depict certain type of EPSD, which would be missed with low-resolution clinical imaging. Also, detecting the presence of fracture and corner defects largely depends on the plane of view, which explains, in part, their misclassification and demonstrates the limitations of assessing EPSD in a single (sagittal) plane. Understanding specific problems associated with the detection of certain EPSD phenotypes is needed to improve accuracy. One step in this direction is the establishment of an evaluation guide. This recommendation conforms to the suggested use of not only a classification system but also an evaluation guide containing an atlas and descriptions to optimize the reliability of spinal image assessments irrespective of years of clinical experience of the assessor (161).

It is also important to note that fractures and corner defects that were absent on the clinical CT assessments may have been expected considering our sample of 19 subjects and a previously reported prevalence of 0.2% for fracture in 996 subjects (154) and 3.2% for corner defects in 133 subjects using clinical imaging (15). However, our findings of 28

corner defects (e.g. limbus vertebrae) and 53 other fractures identified on μ CT, suggest that many such EPSD may be routinely missed on clinical imaging.

As mentioned earlier, neither of the two systems contain both wavy/irregular and erosion phenotypes, which were common EPSD, and may contribute to the poor sensitivity for correctly classifying the type of EPSD. Wavy/irregular endplates on clinical imaging may represent an important phenomenon of calcification (sclerosis) which was shown to have clinical meaning in a recent meta-analysis for the association with back pain (162). The ability to detect endplate sclerosis/calcification is a limitation of routine clinical MRI, which was the modality for the method conceptualized by Brayda-Bruno et al (154), related to detecting endplate sclerosis (163), except with special advanced techniques such as T1 relaxation time (164). Ideally, endplate sclerosis/calcification would always be considered in endplate assessment, and further work is needed to validate whether wavy/irregular endplates may be an indicator of sclerosis or calcification on other imaging modalities, such as MRI.

The available EPSD phenotypes included in each method influence the rater's choice of EPSD phenotypes. As an example, irregularity and erosion are entirely different phenotypes in definition and morphology, but the absence of one influence the selection of the other. Similarly, on clinical imaging, notched and Schmorl's node may be indistinguishable as represented by focal defect. Yet, only a small portion of focal defects using Feng et al's method correspond to Schmorl's nodes (18.4%) as determined by μ CT, while a large portion represents fracture (27.6%) and erosion (22.4%). This may indicate the need to consider Schmorl's nodes as a separate entity from other focal defects, which is further supported by the evidence that typical and atypical Schmorl's nodes have different prevalence and etiology (165–167). The presence of a significant correlation between all the EPSD dimensions measured on clinical-CT and μ CT is promising. A standardized, combined method, with a publicly available measurement atlas, along with advances in imaging, will likely improve reliability and validity of assessments of EPSD presence and phenotype.

Among the strength of the study is the use of a pragmatic approach to assess endplate structures, assessors had no prior focus on EPSD assessment and with varying experience levels, which allows the generalizability of the findings to a typical clinical and research setting. Similarly, the study protocol was registered prospectively and adhered to the STARDs checklist (Appendix 4: STARDs checklist). However, among the limitations encountered is the relative low sample size of the study. The low sample size may have limited the prevalence of type of EPSD which consequently have affects the precision of our estimates of the reliability and validity of such phenotypes on the clinical CT even though detected on the reference standard. Furthermore, the quality of the clinical CTs is not the current best, which may have undermined the extend of the reliability and validity of the current study. Also, the sampled population represents an aged population with high degenerative spinal conditions and thus increase the likelihood of spectrum bias due to high prevalence of the condition compared to younger population group.

Chapter 4

4 Development and Validation of a novel Endplate Structural Defects Classification System

Summary

Background: Recent advances in imaging modalities have pointed to the vertebral endplate, rich in neural and blood supply, as a possible culprit in back pain. Endplate structural defects (EPSD) are common, but lack of standardized, valid assessment methods have impeded progress in understanding their etiology and clinical importance. *Objective:* To develop and validate an EPSD assessment method for clinical imaging. *Methods:* Boateng's three steps of scale development and validation were followed. In phase one, items were generated based on existing literature while content validity was assessed by a panel of experts. Scale development (phase 2) was conducted on a sample of 88 endplates from clinical CT by two end-users and feedback on the classification was received regarding ambiguity in the definitions and use of the atlases. Finally (phase 3) the classification was evaluated for its reliability and validity using repeated measurements from CT-scans (index-test) of 19 cadavers and corresponding μ CT (reference-standard) from their harvested spines (T7-S1) by three blinded assessors. The study was approved by Western's Research Ethics Board for Use of Cadaveric Materials (01202020), and prospectively registered at ClinicalTrial.gov (NCT04808960). *Results:* The final classification consisted of definitions and atlases of six EPSD phenotypes comprising Schmorl's node, focal defect, corner defect, erosion, wavy/irregular, and sclerosis/calcification. Inter-rater reliability was good for EPSD presence ($K= 0.65-0.72$), fair to good for the specific phenotype ($K= 0.52-0.63$) and good to excellent for anteroposterior diameter ($ICC= 0.69-0.87$) and axial area ($K_w= 0.58-0.88$). When assessments of the presence of EPSDs from the clinical CT were compared to the reference standard, μ CT, sensitivity (71%-79%) and specificity (77%-87%) were good, and measurements of dimensions for anteroposterior diameter and axial area were significantly correlated ($r= 0.30 - 0.62$). *Conclusions:* This system provides the basic classification of EPSD with a reasonable degree of reliability needed for understanding its etiology and clinical outcome. Although this valid classification is based on the consensus of

experienced researchers and clinicians using CT scans, further studies are needed to confirm its psychometric properties and applicability to other imaging modalities.

Introduction

The vertebral endplate is comprised of a thin osseous and cartilaginous layer located at the interface between the vertebral body and the intervertebral disc. It functions as a diffusion channel to provide the metabolically active part of the intervertebral disc with nutrients, while also functioning to maintain the stress-strain relation between the vertebral bodies and discs, and distribute the body's compressive forces along the spine (40,68). Thus, the vertebral endplate is susceptible to mechanical failure and defects, which are hypothesized to result in back pain. However, knowledge of endplate structural defects (EPSD) and their clinical consequences has been limited by variations in nomenclature affecting comparisons across studies, and questionable reliability and validity of measurement methods. The need to standardize EPSD assessment to pave the way for understanding the etiology and clinical importance of EPSD has been emphasized by spine researchers and clinicians (168).

A previous review on nomenclature of EPSD unveiled the magnitude of problems associated with EPSD nomenclature and assessment methods. EPSD were reported using 34 different terms, with the majority (65%) of terms never defined in the studies. Some terms appeared to represent the same phenomenon, while other terms were occasionally defined differently between studies (13). Furthermore, we found no studies validating EPSD assessment methods. Of the published endplate assessment methods, there is also evidence suggesting inadequate coverage of EPSD phenotypes when using the classification system of Brayda-Bruno et al (154), which lacks a category for erosion, or the classification of Feng et al (15), which lacks a category for endplates with wavy/irregular appearance (Chapter 3).

Furthermore, EPSD with different topographical appearances also vary in prevalence rates and patterns of distribution, suggesting they may also differ in their etiologies and clinical presentation (12,32). For example, Schmorl's nodes are found predominantly in the upper lumbar and thoracolumbar region (24) where the endplate may be more fragile due to lower

bone density compared to the lower lumbar region (169). In contrast, endplate erosion and calcification are more common in the lower lumbar vertebrae (17,33), where the endplate is susceptible to a greater range of motion in flexion and extension (34). As Schmorl's nodes were the first recognized EPSD (19), the term may have been used broadly in early imaging studies of the endplate to represent a range of EPSD phenotypes (19). Similarly, we found certain EPSD phenotypes, such as erosion and wavy/irregular endplates, were often misclassified (Chapter 3), which makes it difficult to differentiate the effects and associations of erosion from wavy/irregular endplates. Therefore, it would appear some refinement and merging of the Feng et al and Brayda-Bruno et al systems may be needed to create a more reliable and valid EPSD assessment system for the comprehensive identification of EPSD phenotypes. This study aims to develop and validate such an EPSD classification system, with adequate representation of common EPSD phenotypes.

4.1 Materials and Methods

Following our head-to-head comparison of the reliability and validity of the EPSD assessment methods developed by Feng et al (15) and Brayda-Bruno et al (154), we developed and assessed the validity of a novel EPSD classification system.

4.1.1 Materials

Clinically comparable CT images from 19 cadaveric spines and the corresponding μ CT were used for the study. Two experienced clinical radiologists (AL, SL), a senior researcher in degenerative spinal conditions (MCB), a specialist in clinical anatomy (JF) and a graduate student in rehabilitation science studying the endplate (AL) served as the expert judges. While two radiologist (DW and KT) and a radiology resident (VL) with an interest in spinal imaging evaluate the scale.

4.1.2 Image acquisition

Clinical CT was acquired (scanned at 1.25mm x 1.25mm on a standard and bone algorithm and then reformatted into an axial, coronal and sagittal series at 3mm x 2mm) on all fully intact cadavers prior to the onset of this study. μ CT of all cadaveric spines was performed at a peak voltage of 80 kVp and a tube current of 50 mA. The X-ray projections were

reconstructed into a single three-dimensional volume with isotropic voxel spacing of 154 μm . In preparation for μCT , the lower thoracic and lumbar spine (T7 through S1) was harvested from each cadaver. The ribs were dissected 1-2 cm lateral to the costovertebral joints and the soft tissues associated with the spine were preserved and remained intact during μCT .

4.1.3 Procedure

The development and validation of the new EPSD classification method followed the three phases of scale development recommended by Boateng et al (170).

Phase 1- Item development consisted of two steps, item development and generation, and content validity. Domain identification and item generation involved analyzing previous findings from the literature involving EPSD nomenclature and measurement methods (AL and MCB).

Content validity was established through experts' (AL and SL) evaluation and consensus via a Delphi process to determine content relevance, representativeness, and technical quality with respect to distinct EPSD phenotypes included in the classification system. The experts judged each item on three criteria, which included ensuring that each had a generally accepted meaning and definition; the phenotype for which the items are hypothesized to belong was unambiguously defined; and relevant to the concept of EPSD phenotypes. Clinicians with duties or research interest in EPSD were given the final drafted scale items, including definition and atlas, and asked to complete an anonymous survey. Responses from each judge were collected to ensure content construct coverage and unambiguous definitions.

Phase 2 - Scale development: In this phase, pre-testing was done to ensure the extent to which items of the classification reflect the domains of interest by the end-users. The draft of the classification method, including item definitions and images, was then used by two potential end-users (AL and SL) to assess EPSD on a sample of four clinical-CT images including 88 endplates, and feedback was received regarding the new classification. The process allowed items on the new classification system to be further modified, clarified or

augmented to fit the constructs of interest. The iterative process was continued until consensus was achieved by all the assessors.

Phase 3 – Scale evaluation: In this phase, two radiologists and a radiology resident with clinical and research interest in spine imaging were given the final drafted scale items and was used to assess EPSD on clinically comparable CT scans of a sample of 19 cadaveric spines (T7-S1). A thorough assessment of EPSD using μ CT was available to serve as the reference standard.


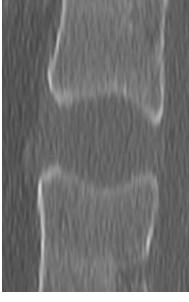
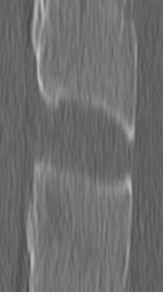
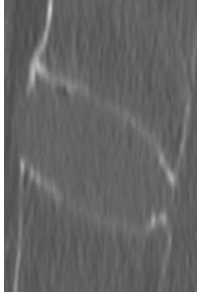

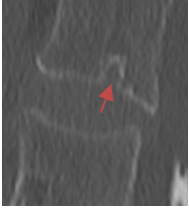

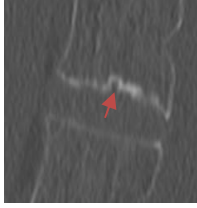



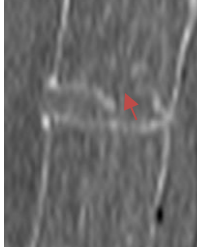

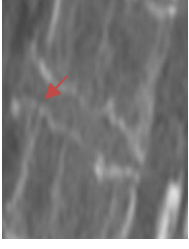

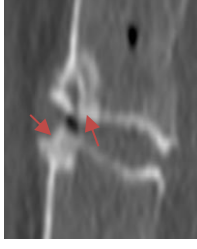

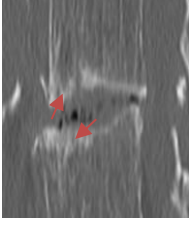
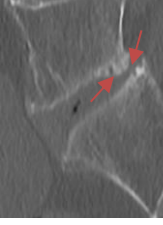
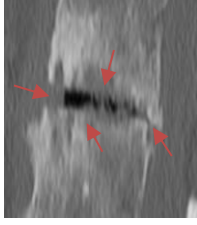
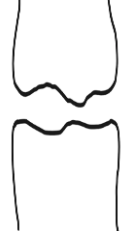
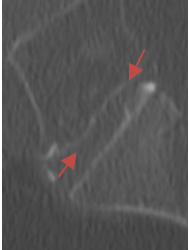
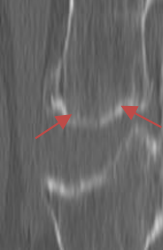
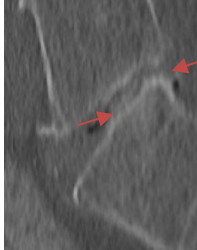
4.1.4 Statistical Analysis

Data were collected from individual assessors and combined on a single data entry form which was later imported into IBM Statistical Packages for Social Sciences (SPSS), version 22 (IBM Corporation, Armonk, NY, USA), for statistical analysis. Data were checked for missing values and outliers using counts and boxplots, respectively. All data were summarized using frequencies and percentages or means and standard deviations. All refinements and consensus on the final index test assessments of EPSD classifications were reached in agreement with a simple majority vote by the assessors. Inter-rater reliability for clinical CT measurements was determined using Cohen's kappa statistic for categorical variables (presence and type of defect), and weighted kappa for ordinal variables (axial area of the defect). ICC and Kappa values were interpreted as poor (< 0.40), fair (0.41–0.60), good (0.61–0.80), and excellent (0.81–1.0). Each pair was analyzed from the three raters to compute a single mean kappa. Using a two-way Intraclass Correlation (ICC) for absolute agreement using a mixed-effect model of the average measures, ICC were calculated. The dominant defect of each endplate on the clinical CT and μ CT was compared on a 2x2 table to determine the sensitivity and specificity of the presence and type of EPSD. Also, the correlation between the EPSD axial area measurements on clinical-CT and μ CT were assessed using Spearman rank moment correlation. The study was prospectively registered at ClinicalTrial.gov (NCT04808960).

4.2 Results

Item development

After an extensive review of the literature relating to measurement methods and classification of EPSD phenotypes, seven phenotypes (Schmorl's node, focal defect, corner defect, fracture, erosion, wavy/irregular, and sclerosis/calcification) were included for consideration in the new classification method. Consensus was reached among the five experts on the inclusion of six of the seven phenotypes (Schmorl's node, focal defect, corner defect, erosion, wavy/irregular, and sclerosis/calcification) after four iterations of the standardized rating form, including a Delphi meeting in each round. Five EPSD phenotypes were brought into the combined new classification system from the previously studied assessment methods (15,154), and sclerosis was added due to its reported high prevalence (163,171,172) and clinical significance (13). A manual containing the included EPSD phenotypes with their descriptions and atlases was created (Figure 4-1). The description of each phenotype went through several rounds of assessment to optimize clarity and reduce ambiguity. All assessors attested to the content relevance, representativeness, and technical quality with respect to the distinct EPSD phenotypes included in the classification system manual. The content validity was deemed adequate by the expert assessors.

| | | | | |
|--|---|--|---|---|
| <p>Normal: No defects are visually detected in any of the sagittal slices encompassing the intervertebral space. The curvature of the endplate is physiological as flat, or slightly concave, and the surface is smooth, and osteophytes may or may not be present.</p> |  |  |  |  |
| <p>Schmorl's node: A rounded indentation of the vertebral endplate with a smooth sclerotic margin.</p> |  |  |  |  |
| <p>Focal defects: A local discontinuity or indentation of the endplate (other than a Schmorl's node), with or without trabecular bone exposed. The indentation can be symmetrical or asymmetrical.</p> |  |  |  |  |
| <p>Corner defects: A lytic lesion with corticated bone fragment at the anterior or posterior corner of the vertebral body, with apparent disruptions of the subchondral trabeculae.</p> |  |  |  |  |
| <p>Erosion: Extensive disruptions or damage of the endplate. Typically, the trabecular bone is widely exposed with a permeative or worm-eaten appearance.</p> |  |  |  |  |
| <p>Wavy/ Irregular: No specific lesions but an alteration in the shape of physiological curvature of the endplate. Calcium deposition is not apparent and trabecular bone is not exposed.</p> |  |  |  |  |

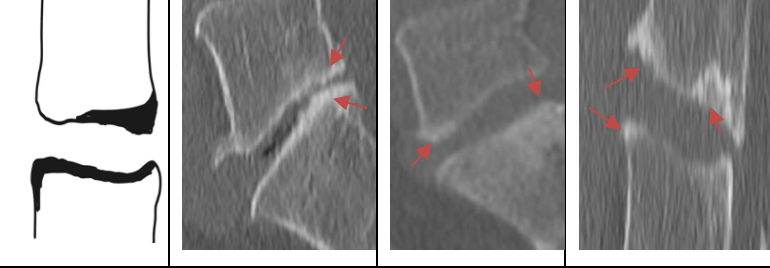
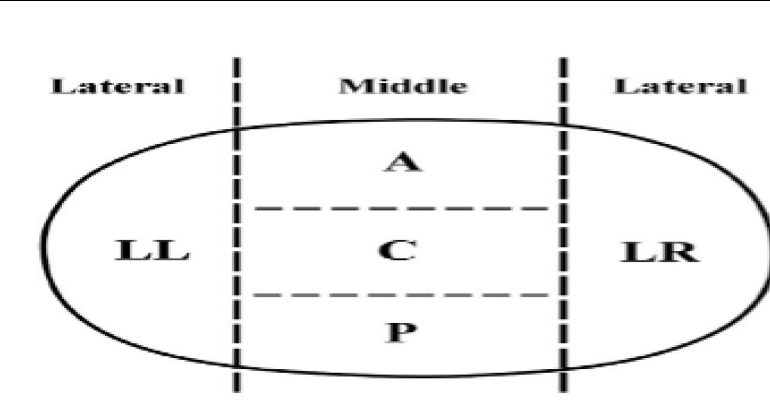
| | |
|---|--|
| <p>Sclerosis/Calcification: Intensive sclerosis or calcium deposition on the endplate with or without bony outgrowth, as evidenced by the presence of high-density material on the surface of the endplate.</p> |  |
| <p>The cross-sectional area of an endplate depicts the regions that should be noted when recording the endplate defect location for estimating the axial area affected. However, measurements are obtained by scrolling through the sagittal images. (Extracted from Feng et al 2018)</p> |  |

Figure 4-1: Assessment manual comprising of EPSPD phenotypes, definitions, and atlases

Scale development

In the scale development stage, an adapted cognitive interview method was used by two radiologists that served as end-users (170). Qualitative and quantitative data were collected from the three expert raters and analyzed. Results regarding the reliability, agreement and validity of the classification were presented during one of the Delphi meetings. Subsequently, the assessors identified reasons for these discrepancies, and decisions were made by majority vote to revise the definitions and illustrations with clearer, clinically relevant definitions and an atlas including an illustration and sample CT scans to minimize ambiguity and coding disagreement among users. The iterative process was undertaken during four Delphi sessions and, was finalized when all the assessors and expert judges attested to the face and content validity. Finally, the scale development was concluded with the assessment of four clinically comparable CT scans comprising 88 endplates using the new classification system. The assessors attested to the ease of usage, excellent agreement

in the presence or absence of EPSD, and good agreement in identifying phenotype and, good to excellent for dimensions (Table 4-2).

4.2.1 Instruction Manual: Endplate Structural Defects Classification Assessment

All assessments are carried out on the sagittal images and are recorded in relation to spinal level, i.e., cranial, or caudal to the disc. Osteophytes were excluded when taking measurements. All measurements were obtained in millimeters, rounded up to the nearest decimal point. All assessments were entered into a pilot-tested excel data entry form using the six EPSD phenotypes, as defined and depicted in the atlases (Figure 4-1).

Measurements include:

1. Endplate structural defect phenotype: record the type of defect as either normal, Schmorl's node, focal defect, corner defect, erosion, wavy/irregular, or sclerosis/calcification. In the case of multiple defects on an endplate, note the dominant and the non-dominant defects type. However, size measurements were recorded for only the dominant defect.
2. Axial area: record the number (1 to 5) of sections of the endplate affected, the cross-sectional area of the endplate is divided into five sections, lateral left, lateral right, anterior, central, and posterior. When scrolling through the sagittal slices, one-fourth of the endplate on the left and a corresponding one-fourth on the right are referred to as the left and right lateral, respectively. The middle half is further divided into anterior, central, and posterior sections. The area was rated as none if no defects are present, small if one or two sections are involved, moderate if three sections are involved or large if four or five sections are involved.
3. Anteroposterior diameter: Record the anteroposterior diameter of the dominant defect at the largest point on the sagittal slices. Also, record the anteroposterior diameter of the vertebral body at the endplate surface in the mid-sagittal image. The anteroposterior diameter was calculated as the ratio of the maximal anteroposterior diameter of EPSD to the anteroposterior diameter of the vertebral body measured on the midsagittal image.

4.2.2 Scale evaluation

Following the item generation, content validation and scale development, a pragmatic approach was employed to assess the spines of 19 embalmed cadavers by 3 radiologists using the developed classification system (instruction manual as above). As shown in table 4-1, there was good inter-rater reliability between the three assessors for identifying the presence or absence of an EPSD ($k= 0.65-0.72$) and fair to good reliability for identifying specific phenotypes ($k=0.52-0.63$). Size dimensions correlated between the anterior-posterior diameter ($ICC= 0.69-0.88$), affected endplate sections ($K= 0.61-0.82$), and axial area ($K_w= 0.58-0.88$). While near perfect validity was achieved for each assessor for clinical CT and μ CT assessment for the sensitivity (71% - 79%) and specificity (77% - 87%) of EPSD. Overall, specificity was higher than sensitivity for the three assessors' ratings. Schmorl's nodes (71%-75%) had the highest sensitivity, followed by erosion (25%-48%). While focal defects had the least sensitivity (1%-15%). The details of the sensitivity and specificity of the classification are reported in table 4-2.

Table 4-1: Inter-rater reliability of endplate structural defect assessments by raters. Values are kappa coefficients (95% CI) for categorical variables and ICCs (95% CI) for continuous measurements.

| | Cognitive assessment | Assessor 1 and 2 | Assessor 1 and 3 | Assessor 2 and 3 |
|-------------------|----------------------|-------------------|-------------------|-------------------|
| Defect Presence | 0.72 (0.59, 0.85) | 0.65 (0.57, 0.73) | 0.71 (0.62, 0.77) | 0.65 (0.56, 0.74) |
| Defect type | 0.62 (0.51, 0.69) | 0.63 (0.57, 0.69) | 0.55 (0.50, 0.60) | 0.52 (0.47, 0.57) |
| AP diameter | 0.87 (0.58, 0.89) | 0.79 (0.72-0.84) | 0.70 (0.59-0.78) | 0.69 (0.56-0.78) |
| Sections Affected | 0.82 (0.63, 0.92) | 0.70 (0.60-0.78) | 0.72 (0.61-0.80) | 0.61 (0.46-0.71) |
| Axial area | 0.88 (0.79, 0.97) | 0.69 (0.59, 0.77) | 0.68 (0.54, 0.77) | 0.58 (0.40, 0.70) |

Table 4-2: Specificity and sensitivity for the assessment of endplate structural defects to the reference standard (μ CT) for individual rater.

| CT μ CT | Assessor 1 n (%) | | Assessor 2 n (%) | | Assessor 3 n (%) | |
|----------------|------------------|-----------|------------------|-----------|------------------|-----------|
| | Normal | Defective | Normal | Defective | Normal | Defective |
| Normal | 114 (87%) | 49 (21%) | 96 (77%) | 65 (29%) | 106 (80%) | 67 (29%) |
| Defective | 18(14%) | 182 (79%) | 30 (24%) | 162 (71%) | 26 (20%) | 168 (72%) |
| Schmorl's node | 2 (1.5%) | 12 (75%) | 0 (0%) | 10 (67%) | 7 (5%) | 13 (81%) |
| Focal defect | 0 (0%) | 3 (5%) | 0 (0%) | 3 (5%) | 1 (1%) | 9 (15%) |
| Corner defect | 0 (0) | 7 (25%) | 1 (1%) | 6 (22%) | 1 (1%) | 5 (18%) |
| Erosion | 4 (3%) | 26 (48%) | 12 (10%) | 23 (42%) | 3 (2%) | 14 (25%) |
| Wavy/irregular | 11 (8%) | 8 (18%) | 9 (7%) | 6 (12%) | 3 (2%) | 2 (5%) |
| Sclerosis | 1 (1%) | 5 (17%) | 8 (6%) | 6 (21%) | 11 (8%) | 6 (21%) |

Non-dominant endplate structural defect detection and characterization

Non-dominant defects are EPSD identified on an endplate adjacent to another defect of larger dimensions termed as the dominant defect. The assessments of the non-dominant defects varied between the assessors. Wavy/irregular defects (n=22) and Schmorl's nodes (n=14) were the most assessed non-dominant defects, among which only 1 wavy/irregular defect and 5 Schmorl's nodes were accurately detected according to μ CT. Schmorl's nodes were the most detected non-dominant defect for rater 1 (n=5, 50%), rater 2 (n=4, 36%) and rater 3 (n=2, 14%). Details of the non-dominant defects assessed, and corresponding number accurately detected are reported in table 4-3.

Table 4-3: Sensitivity and specificity of non-dominant endplate structural defect assessments by raters. Values are kappa coefficients (95% CI) for categorical variables.

| | Assessor 1 n (%) | | Assessor 2 n (%) | | Assessor 3 n (%) | |
|----------------|------------------|-----------|------------------|-----------|------------------|-----------|
| | Assessed | Defective | Assessed | Defective | Assessed | Defective |
| Schmorl's node | 14 (50%) | 5 (50%) | 4 (18%) | 4 (36%) | 2 (7%) | 2 (14%) |
| Focal defect | 7 (25%) | 1 (9%) | 1 (5%) | 1 (13%) | 0 | 0 |
| Corner defect | 0 | 0 | 0 | 0 | 3 (10%) | 0 |
| Erosion | 0 | 0 | 9 (41%) | 1 (50%) | 2 (7%) | 0 |
| Wavy/irregular | 1 (7%) | 0 | 2 (9%) | 0 | 22 (76%) | 1 (100%) |
| Sclerosis | 6 (22) | 0 | 6 (27%) | 0 | 11 (8%) | 6 (21%) |

Dimensions of endplate defects on the clinical-CT and μ CT of the 418 endplates assessed, 10 defects of <3mm in AP diameter for rater 1; 13 defects for raters 2 and 1 defect for rater 3. Majority of the <3mm endplate defects were assessed as focal defects. As shown in table 4-4, the sizes of endplate defects on the clinical CT and reference standard, μ CT, were significantly correlated ($r=0.31-0.62$, $p<0.001$). The anteroposterior diameter of the defect was the most correlated measure of the dimensions (mean $r= 0.45$).

Table 4-4: Correlations between dimensions of clinical CT and corresponding μ CT

| AP diameter | Endplate sections | Axial Area |
|-------------|-------------------|------------|
| 0.62* | 0.47* | 0.59* |
| 0.30* | 0.32* | 0.32* |
| 0.42* | 0.44* | 0.32* |

Values are for Spearman's Rho correlation (r); * = significant at $p<0.001$

4.3 Discussion

A reliable and valid EPSD assessment method is needed to understand the etiology and outcome of EPSD phenotypes. However, our recent validation study of the two common EPSD assessment methods pointed to the inadequacies of each method (chapter 3), which led to the development and validation of the new combined EPSD classification system. The resulting assessment manual consists of a classification system, with definitions and atlases of EPSD phenotypes developed through a careful process of scale development. The new classification consists of six EPSD phenotypes including Schmorl's node, focal defect, corner defect, erosion, wavy/irregular, and sclerosis. The classification system has demonstrated good reliability ($K= 0.65-0.72$ for presence and $k=0.52-0.63$ for phenotype) and validity (sensitivity: 71%-79% and specificity: 77%-87%) for detecting the presence of EPSDs, providing the minimum domains or phenotypes to consider for EPSD assessment. While there is increased interest in the specific EPSD phenotypes to move the field forward, limitations in their assessment reliability and validity remained of concern. Identifying specific phenotypes remain challenging, especially the validity of identifying focal defects (5%-15%) and wavy/irregular (5%-18%), from Schmorl's node and erosion, respectively, making it difficult to determine associations despite presumed distinct etiology and clinical relevance (12,32,165–167).

The reported reliability for the presence or absence of the new classification (0.65 – 0.72) and phenotypes (0.52-0.63), was greater than the previous methods, which demonstrated reliability of $Kappa=0.60-0.69$ for the presence of EPSD and $Kappa=0.43-0.58$) of EPSD for specific phenotypes (chapter 3). Similarly, the validity (sensitivity: 71%-79% and specificity: 77%-87%) of the current combined classification was greater than each method. In chapter three, the validation shows that with respect to the presence of an EPSD, there was a sensitivity of 70.9% and specificity of 79.1% for Feng's method (15), and 79.5% and 57.5%, respectively, using Brayda-Bruno's method (154). Despite the relatively poor performance of the new scale concerning the validity of some specific phenotypes, there are no studies to compare the findings. Therefore, it is unknown how the new scale performance could be compared to the other existing measures in terms of such specific phenotypes. Otherwise, our findings could speculate that the newly developed

classification may be considered appropriate for use with enhanced capabilities than the previous methods.

Furthermore, it is arguable that certain EPSD phenotypes may be more reliably detected than others, and that others may be more clinically important, but further studies are required to confirm the clinical importance of the specific phenotypes. Despite several studies (12,32,165–167) pointing toward different aetiologies of each EPSD phenotype, previous study (chapter 3) pointed to the challenges in assessing specific EPSD phenotypes in relation to others, erosion vs wavy/irregular, and wavy/irregular vs normal endplate. Similarly, Schmorl's nodes and focal defects have a similar appearance, but previous studies have demonstrated etiological differences between Schmorl's nodes and a subtype or focal defect based on bone mineral density (165). Also, some EPSD phenotypes are rare, and their low prevalence made it difficult to evaluate their measurement reliability and validity, and associations with other factors. Yet, it may be important to report the absence or low prevalence of such phenotypes than to collapse phenotypes together. Furthermore, considering how often fracture defects were missed in our previous study (Chapter 3). It was recommended that the EPSD phenotype of fracture, other than corner fracture/defect, be dropped from the classification due to, in addition, the likelihood that fracture would be classified as a focal defect. The study also confirmed similar reliability between raters irrespective of assessors level of experience, as has been found in previous imaging study (153), suggesting that a detailed morphologic description was important in establishing reliability than the experience of the assessors. However, informal training to familiarize the raters with the classification may be required to improve consistency among assessors.

One of the study limitations is the use of low-resolution CT-scan which may have consequential effects on the image quality. However, the evaluation process indicated an acceptable reliability and validity for the presence or absences EPSD and identifying its phenotypes. It is expected that the psychometric properties (reliability and validity) of the system would improve with higher resolution imaging. Also, there are some EPSD phenotype, including focal and wavy/irregular defects assessments that did not reach good to excellent reliability and validity in their assessment on the new classification, but the participating panelist were unanimously convinced that this system represents the basic

clinically relevant phenotypes of EPSD that are worth implementing in EPSD assessment. The classification consists of harmonized categories from previous EPSD assessment methods (15,154,165,173) and some revised changes in definitions, such as distinguishing Schmorl's nodes from other focal defects, and the inclusion of sclerosis.

Among the strengths of the new classification was the use of a carefully developed, rigorous methodology that allowed the expert judges and assessors to overcome several problems associated with previous methods (15,154), such as the inclusion of the missing phenotypes. The resulting classification system based on CT-scan, provides a measurement method for assessing the osseous endplate, which we hope will be useful to further studies of the etiology, associated factors, and clinical outcomes of EPSD. With the continued interest in the role of EPSD in back pain, the importance of a comprehensive, reliable, and valid classification of EPSD cannot be underestimated. The reliability and validity of the classification was tested on CT scans, and further studies are needed to confirm its applicability and psychometric properties for use with other imaging modalities and by other investigators with various levels of experience.

Chapter 5

5 Endplate Structural Defects: Prevalence, Distribution and Association with Age and BMI in Adult Males

Summary

Background: Recent advances in imaging modalities have turned attention to the endplate, a thin mechanical interface rich in blood and neural supply, as a possible source of back pain. However, the limited use of standardized assessment methods has impeded progress and resulted in wide ranging prevalence rates of Endplate Structural Defects (EPSD) and conflicting findings. *Objective:* To determine the prevalence and distribution of EPSD, including specific phenotypes, and associations with age and body mass index (BMI) in an adult male population. *Methods:* Previously collected MRI and age and BMI data for 200 adult males from the population-based Twin Spine Study were used. The lumbar MRI were assessed twice using a novel standardized classification system for EPSD consisting of phenotypes of Schmorl's nodes, focal defects, corner defects, and erosion. The repeated assessments were blinded to earlier readings, and any conflicts between the two readings were reconciled after reviewing the MRI a third time. Descriptive statistics were calculated to determine prevalence and distribution patterns, and associations were investigated with chi-square and logic regression. *Results:* There was a high prevalence of EPSD (45.6%, n=1087) with erosion (17.6%, n=420) and focal defects (16.2%, n=386) being the most common EPSD phenotypes, while corner defects (1%, n=24) were the least often observed. When all EPSD phenotypes were aggregated, EPSD occurred more at the upper lumbar levels ($\chi^2= 41.68$, $p<0.01$) and on the caudal endplate ($\chi^2= 9.28$, $p<0.01$), and were associated with age (OR: 1.02, 95%CI: 1.01-1.03, $p=0.03$) but not BMI (OR: 1.00, 95%CI: 0.98-1.03, $p=0.72$). However, the trends differed by each phenotype. While focal defects and Schmorl's nodes were more prevalent at the upper lumbar levels, erosion and corner defects were more prevalent at the lower lumbar levels. Age was associated with focal defects (OR: 1.02, 95%CI: 1.00 - 1.03, $p=0.02$) but not Schmorl's nodes (OR: 1.01, 95%CI: 0.99 - 1.03, $p=0.21$). Erosion was associated with age (1.03, 95%CI: 1.014, 1.043, $p<0.01$) but not BMI (OR: 1.02, 95%CI: 0.98 - 1.05, $p=0.34$). Conversely, corner defects were associated with BMI (OR: 1.15, 95%CI: 1.03 - 1.30, $p=0.02$) but not age (OR: 1.01, 95%CI:

0.95, 1.08, $p=0.68$). All EPSD phenotypes more commonly occurred on the caudal than cranial endplate. *Discussion:* EPSD are common among older adult males, and the various EPSD phenotypes appear to have distinct etiologies based on different associated factors. Our findings support a developmental rather than degenerative origin of Schmorl's nodes, and the association of corner defects with BMI suggests biomechanical influences. Conversely, erosion and focal defects are associated with aging.

Introduction

While the intervertebral disc has garnered most attention as a possible culprit in back pain (32,144,174), with increased capabilities of imaging modalities over recent years, attention has turned to the endplate, the thin mechanical interface between the vertebral body and intervertebral disc (11,13,32). The endplate serves to transmit compressive forces along the vertebral body (175,176), which makes the delicate structure susceptible to mechanical forces that may result in endplate structural defects (EPSD). In addition to excessive loading or trauma, there are theories of congenital and developmental causes of EPSD (17,20,177).

Endplate structural defects are physical deformations in the typical appearance of an endplate presenting as Schmorl's nodes, fracture, erosion, and other defect phenotypes. EPSD may lead to enhanced communication between the disc and vertebral marrow, which may become sensitive to chemical stimulation, result in neoinnervation, or lead to stimulation of mechanoreceptors and pain (12). Unfortunately, most diagnostic tools do not depict small EPSD, resulting in misclassification, and the clinical significance of endplate defects may be underappreciated and remains unclear (12). The wide variation in prevalence rates (9% to 75%) of EPSD (26,28,126) may be related, in part, to such misclassifications and varied EPSD definitions used. The lack of agreement among expert spine clinicians and researchers on terminology and definitions of EPSD has been well documented (13,168). Consequently, EPSD are typically assessed without the benefit of standardized measurement methods with known reliability and validity (13).

As a result, there is uncertainty about the prevalence, nature, and etiology of EPSD observed on clinical imaging and their relation to other degenerative and pathological

changes in the lumbar spine, and back pain. Studies are needed to establish prevalence rates of EPSSD in the general population on clinical imaging to serve as a reference for clinical observations, and to gain insights into the nature and etiology of EPSSD, using a reliable and valid EPSSD assessment method.

We aimed to estimate the prevalence and distribution within the lumbar region of EPSSD phenotypes, and their association with constitutional factors, including age and body mass index, in adult males using a standardized, validated assessment method to provide insights into the development of EPSSD.

5.1 Sample and Methods

5.1.1 Sample

We conducted a secondary data analysis using data from the population-based Twin Spine Study (7). The entire Twin Spine Study sample includes 600 subjects comprising 147 monozygotic (MZ) and 153 dizygotic (DZ) male twin pairs recruited in 1991/1992 and 1996/1997 from the Finnish Twin Cohort, containing Finnish sex-matched twin pairs born before 1958 and still alive in 1975. Among the Twin Spine Study sample, a subgroup of 117 pairs of MZ twins was initially selected based on discordance between twin siblings for specific common behavioural or environmental factors (e.g., sedentary work, heavy occupational physical demands, routine exercise participation, or occupational driving). They were found to be highly representative of the Finnish Twin Cohort, which was representative of the corresponding Finnish population, in terms of the level of education, social class, smoking, level of leisure-time physical activity, and history of work-incapacitating neck, shoulder, or back pain, and sciatica (112). An additional 33 male MZ pairs were randomly selected from the Finnish Twin Cohort. Using identical selection criteria, 150 DZ pairs were recruited, making up the Twin Spine sample of 600 adult males (7).

For the current study, a subsample of 152 MZ twins, still living and available for follow-up imaging 15 years later, and 51 DZ male twins, imaged approximately 10 years following baseline, yielding a total of 203 male twin subjects were included. The group of 203 participated in the most recent wave of data collected in the Twin Spine Study, with the

advantage of better magnetic resonance imaging (MRI) quality that allowed a clearer view of the endplate, as compared to the images acquired at baseline. All subjects from the subgroup with follow-up images were included.

5.1.2 Data Acquisition

The most recent wave of data collection of the Twin Spine Study (2008-2009) was used for the current study, which included lumbar MRI, age and BMI. *Anthropometric measurements*, including weight and height, were used to calculate BMI. Weight was measured using a balance scale and was recorded to the nearest 0.1 kg and standing height was measured using a stadiometer. BMI was obtained by dividing weight by the square of standing height (Kg/m^2). *Age*, recorded in years, was used in analyses. The data were gathered by trained research assistants who were blinded to the selection criteria and the study hypotheses.

Magnetic Resonance Imaging of the lumbar spine was conducted at a central location in Finland using a 1.5-Tesla MRI Siemens Zebra scanner (“Avanto” with software MR B15). The field of view was 320 mm (in axial, 348 by 384 mm), and the slice thickness and interslice gap were 4mm and 0.4mm for the sagittal images, and 3 mm and 0.3 mm for axial slices. The pixel size was 0.8125 mm. For each lumbar spine image there were 11 sagittal slices of T2-weighted images. The T2-weighted images were obtained with repetition and echo times of 2450 and 90, respectively (113,114).

5.1.3 Endplate Structural Defect Evaluation Protocol

All MRIs were evaluated on a PC workstation using Horos (RRID: SCR_017340) for the presence of EPSD phenotypes and defect location and dimensions, including anteroposterior diameter and axial area of the defects. All assessments were blinded and read on two separate occasions with a two-week interval between the first and second readings. Discrepancies between the first and second readings were then identified, and all conflicts were resolved by reassessing the endplate using the evaluation protocol to produce the final data set for analysis.

Endplate structural defect classification System: The examination of EPSDs was performed using the novel EPSD classification system presented in Chapter Four. The new assessment method stems from the observed limitations of other EPSD assessment methods identified in our previous study (Chapter 3). The new classification comprises six EPSD phenotypes, including Schmorl's nodes, focal defects, corner defects, erosion, wavy/irregular appearance, and sclerosis/calcification, which we found demonstrated higher validity (relative to a reference standard of observations on μ CT) than the previous assessment methods examined. After the modification needed to suit its use with MRI, including omitting sclerosis/calcification and wavy/irregular from the classification due to their limited reliability on MRI, each spinal endplate from the superior T12/L1 endplate to the inferior L5/S1 endplate was inspected, including a total of 12 endplates per subject. When an EPSD was observed, its spinal level and cranial or caudal location relative to the disc were recorded. Using a standardized assessment manual with atlases, EPSDs were evaluated for their presence or absence. If present, the EPSD was classified as follows:

- i. *Normal endplate:* No defects are visually detected in any of the sagittal slices encompassing the intervertebral space. The curvature of the endplate is physiological as flat or slightly concave, the surface is smooth, and osteophytes may or may not be present.
- ii. *Schmorl's node:* A rounded indentation on the vertebral endplate with a smooth sclerotic margin.
- iii. *Focal defect:* A local discontinuity or indentation of the endplate (other than a Schmorl's node), with or without trabecular bone exposed. The indentation can be symmetrical or asymmetrical.
- iv. *Corner defect:* A lytic lesion with corticated bone fragment at the anterior or posterior corner of the vertebral body, with apparent disruptions of the subchondral trabeculae.
- v. *Erosive defect:* Extensive disruption or damage of the endplate. Typically, the trabecular bone is widely exposed with a permeative or worm-eaten appearance.

If two or more types of defects were present, the dominant defect based on size was noted and its measurements were taken, as follows:

- i. *Anteroposterior diameter:* the anteroposterior diameter of the dominant defect was recorded at the largest point on the sagittal slices, and the anteroposterior diameter of the

vertebral body was recorded at the endplate surface in the mid-sagittal image. Finally, the anteroposterior diameter was calculated as the ratio of the maximal anteroposterior diameter of an endplate defect to the anteroposterior diameter of the vertebral body measured on the midsagittal image.

ii. Transverse diameter: the percentage of sagittal images containing an endplate defect, calculated as the number of slices demonstrating EPSD divided by the total number of slices capturing the endplate in the sagittal plane (usually 11) and multiplied by 100.

iii. Axial area: was indicated by the number of sections of the endplate affected (1-5), with the cross-sectional area of the endplate divided into the five sections of lateral left, lateral right, anterior, central, and posterior. When scrolling through the sagittal slices, one-fourth of the endplate on the left and the corresponding one-fourth on the right were referred to as the left and right lateral, respectively. The middle half was further divided into anterior, central, and posterior sections. If an EPSD was present, the area was rated as small if one or two sections were involved, moderate if three sections were involved or large if four or five sections were involved.

Intra-rater reliability of the EPSD classification system was determined using repeated measurements obtained at a two-week interval of the MRI of 20 randomly selected subjects, with measurements blinded to all previous measurements. Cohen's Kappa and ICC (two-way ICC for absolute agreement and a mixed-effect model of the average-measures ICC) were used to determine intra-rater reliability for categorical and continuous variables. ICC and Kappa values were interpreted as poor (< 0.40), fair (0.41–0.60), good (0.61–0.80), and excellent (0.81–1.0) (178).

5.1.4 Data Analysis

Data were imported into STATA (Version 16.1, Stata Corp, USA) for statistical analysis. All coded data were checked for outliers and missing values. Descriptive statistics of mean and standard deviation or frequency and percentage were used to summarize the data. Prevalence of EPSD phenotypes by upper vs. lower lumbar region and cranial vs caudal endplates were analyzed using chi-square test. First, all aggregated EPSD phenotypes were aggregated for hypothesis testing and then dummy variables of each EPSD phenotype were

created. Logistic regression was used to explore the associations of EPSD phenotypes with age and BMI. Then the individual EPSD phenotypes were analyzed separately using nominal logistic regressions with each independent variable. Considering that EPSD data pertaining to the 12 distinct endplates were acquired for each subject's spine, the dependency of the data for multiple endplates was accounted for within the regression analyses by including each endplate type as a cluster (n= 12, representing endplates from upper-T12/L1 to lower-L5/S1) to adjust for their standard error using 'cluster' command in STATA. For all statistical tests, the level of significance was set at an alpha value of <0.05.

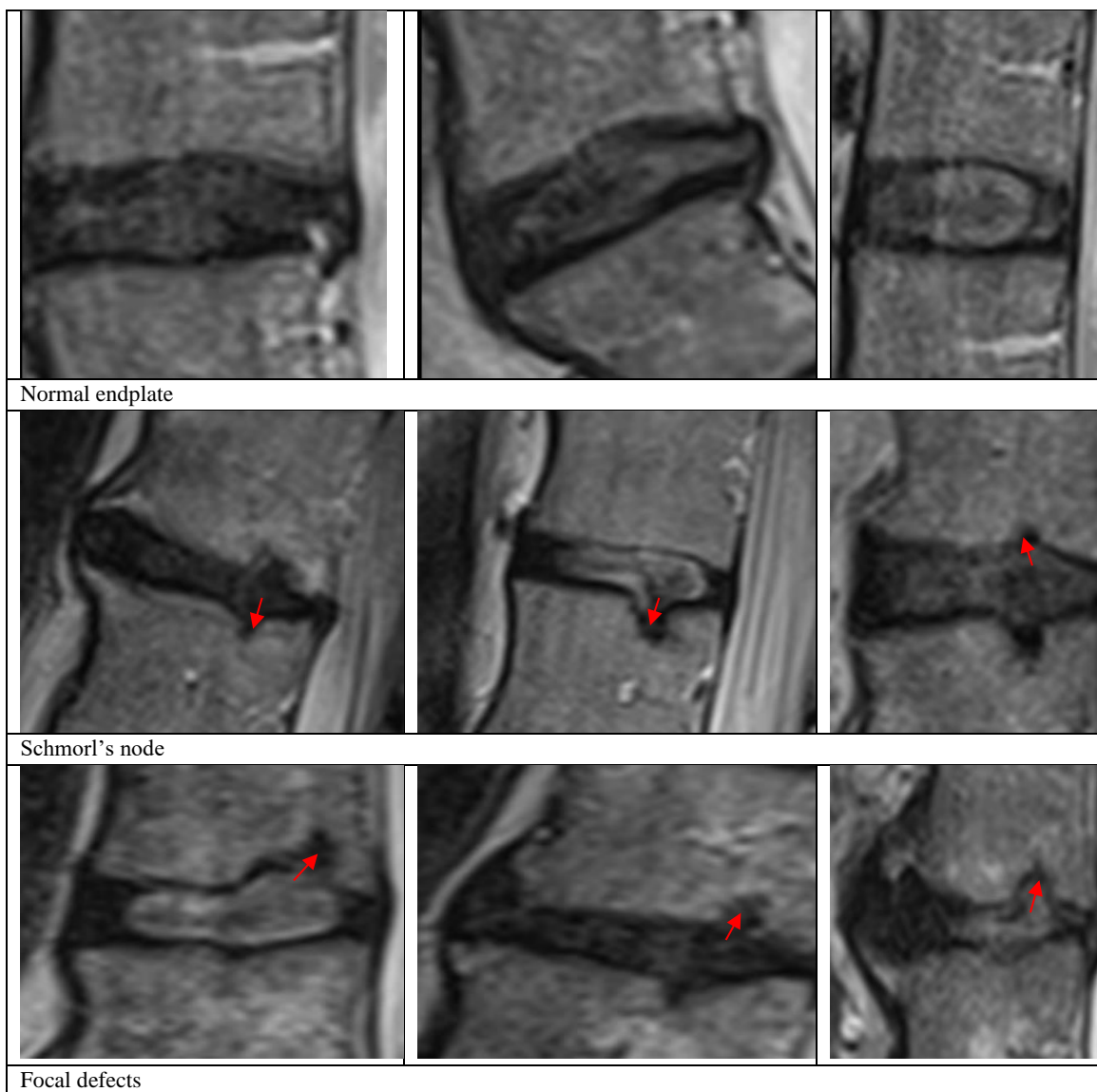
5.2 Results

5.2.1 Prevalence of Endplate Structural Defects

Of the 203 men who participated in the follow-up study and were eligible for inclusion in the current study sample, three were missing MRIs. Thus, the sample consisted of 200 male adults, with a mean age of 61 ± 7.5 years (range: 50 to 79 years) and BMI of 26.5 ± 3.4 kg/m². Of the subjects 2400 endplates assessed, including two endplates at each of six-disc levels (T12/L1 to L5/S1), 16 endplates were excluded from the analysis because the upper T12/L1 spinal level was cut from the image (n=4), and other exclusions were due to vertebral collapse (n=2), fusion of the intervertebral space (n=4), and poor image quality (n=6). Thus, the final data set consisted of 2384 endplates. As judged by the blinded repeated measurements of 240 randomly selected endplates, intra-rater reliability for the EPSD classification system was excellent for the presence of EPSD (Kappa= 0.83), good for specific phenotypes (K=0.62), and excellent for dimensions (ICC: 0.77 to 0.85), as shown in Table 5-1. Overall, EPSD were present in 45.6% (n=1087) of the endplates. Erosion was the most common EPSD (n=420, 17.6%), followed by focal defects (n=386, 16.2%) and Schmorl's nodes (n=257, 10.8%), while corner defect was the least prevalent EPSD phenotype (n=24, 1.0%).

Table 5-1: Intra-rater reliability the EPSD classification

| Measurements | Kappa/ICC | 95% CI |
|--------------------------|-----------|------------|
| EPSD Presence/absence | 0.83 | 0.66, 0.95 |
| Type of EPSD | 0.62 | 0.47, 0.72 |
| Anteroposterior diameter | 0.85 | 0.71, 0.99 |
| Transverse diameter | 0.79 | 0.70, 0.88 |
| Axial area | 0.77 | 0.70, 0.86 |



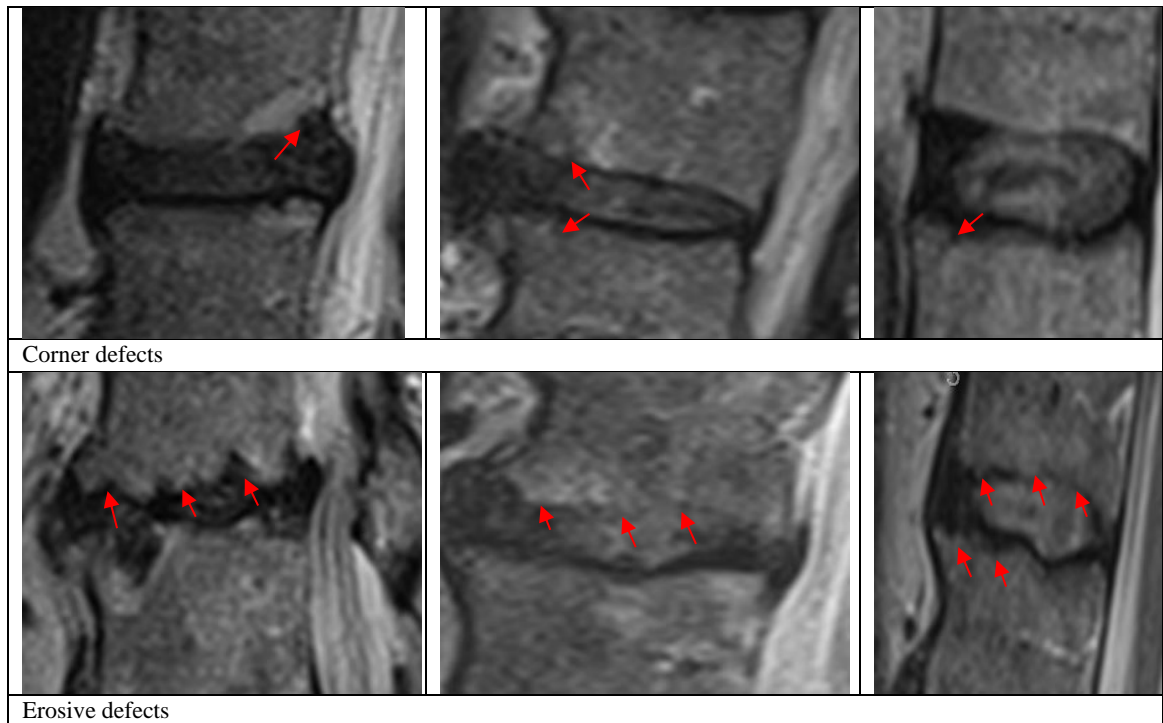


Figure 5-1: EPSPD phenotypes assessed using the new classification system

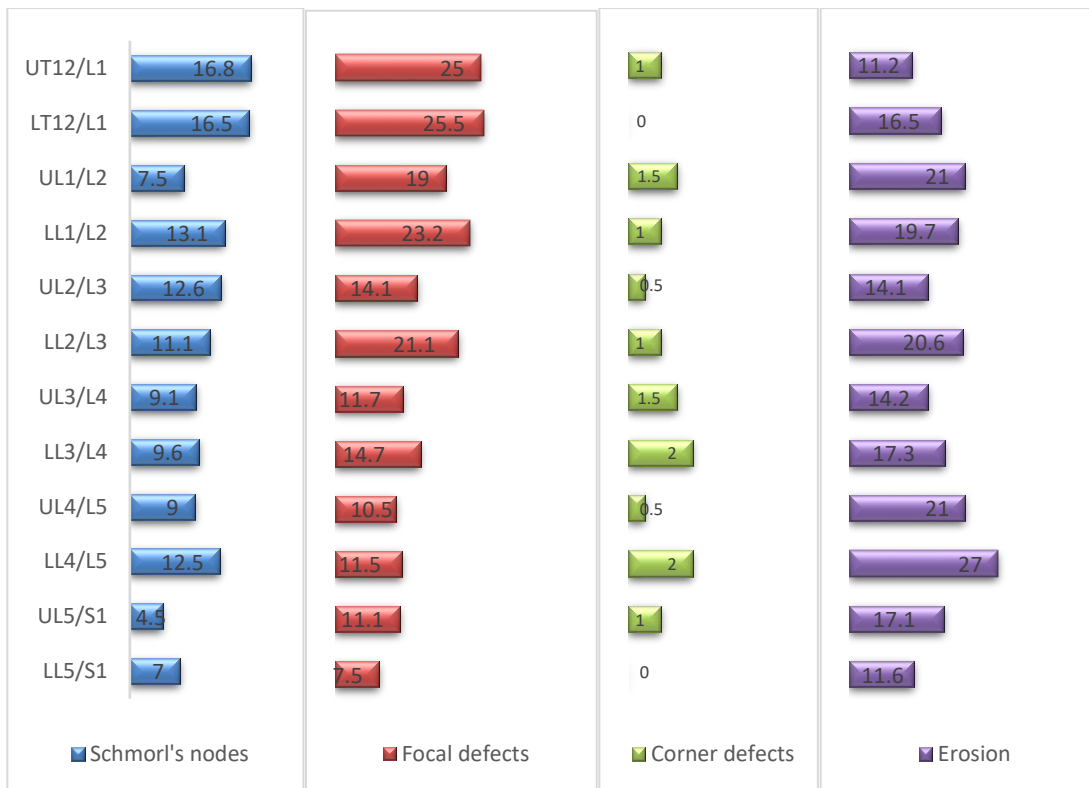


Figure 5-2: Distribution of endplate structural defect phenotypes by disc level. The numbers are percentages of all endplates assessed at each spinal level with the EPSD phenotype.

5.2.2 Size of Endplate Structural Defects

Table 5-2 shows the size of EPSD. The majority of Schmorl’s nodes (n=251, 97.7%) were rated as small while erosion was the most common large defect (n=150, 35.7%). Schmorl’s nodes had the smallest anteroposterior (7.13±4.08) and transverse diameter (2.45±1.45), followed by focal defects (8.58±4.65 and 2.94±1.99), with erosion having the largest anteroposterior (23.89±8.08) and transverse diameter (5.36±3.18). When all the 1087 EPSDs were aggregated, most EPSDs were small (n=801, 73.7%), with large defects a distant second (n=160, 14.7%).

Table 5-2: Size of endplate structural defect phenotypes (means and standard deviations or frequencies and percentages)

| Endplate defects | AP diameter (mm) | AP defect-Vert ratio | Transverse diameter (mm) | Transverse diameter ratio | Surface Area (mm ²) | Axial area | | | Total |
|------------------|------------------|----------------------|--------------------------|---------------------------|---------------------------------|---------------|---------------|---------------|---------------|
| | | | | | | Small | Moderate | large | |
| Schmorl's nodes | 7.1±4.1 | 0.20±0.12 | 2.5 ±1.5 | 0.22±0.13 | 125.1±145.5 | 97.7%, 251 | 2.3%, 6 | 0 | 23.6%, 257 |
| Focal defects | 8.6±4.7 | 0.26±0.21 | 2.9±2.0 | 0.27±0.18 | 173.0±210.8 | 89.9%, 347 | 7.5%, 29 | 2.6%, 10 | 35.5%, 386 |
| Corner defects | 9.9±2.8 | 0.28±0.08 | 4.2±1.7 | 0.38±0.16 | 184.2±92.3 | 95.8%, 23 | 4.2%, 1 | 0 | 2.2%, 24 |
| Erosion | 23.9±8.1 | 0.67±0.22 | 5.4±3.2 | 0.49±0.29 | 628.1±492.8 | 42.9%, 180 | 21.4%, 90 | 35.7%, 150 | 38.6%, 420 |
| All defects | 14.2±9.8 | 0.40±0.29 | 3.8±2.7 | 0.34±0.25 | 337.5±409.8 | 73.7%, 801 | 11.6%, 126 | 14.7%, 160 | 1087 |

5.2.3 Distribution of Endplate Structural Defects

Of the 1087 EPSD identified, 581 (53.5%) occurred on the caudal endplate and 506 (46.5%) on the cranial endplate. There was a significant association for the occurrence of EPSDs at the caudal endplate compared cranial endplate ($\chi^2 = 9.28$, $p < 0.01$), except for corner defects which were evenly distributed between the cranial (12, 50%) and caudal endplates (12, 50%). The majority of EPSDs occurred on the endplate centrum, including 14.2% (296) on the centrum only, and 20.2% on the centrum, in part. On specific EPSD, Schmorl's nodes ($n=112$) and focal defects ($n=163$) were on the centrum only, while corner defects were predominantly at the anterior part of the endplate ($n=10$). Erosion defects predominantly spanned all locations, especially including the anterior ($n=247$) and central ($n=292$) endplate. There was a significantly ($\chi^2 = 41.68$, $p < 0.01$) greater number of EPSD at the upper lumbar levels (57.2%, 622) compared to the lower lumbar levels (42.8%, 465). However, there is variation in the trend of each EPSD, erosion and corner defects tend to occur more at lower lumbar levels (51.2% and 58.3%) compared to the upper lumbar levels (48.8% and 41.7%). While Schmorl's nodes and focal defects occur more at T12/L1 compared to all other levels which decrease caudally.

Table 5-3: Distribution of EPSD within the endplate (frequency (and percentage) of defects located solely or partially in part in the portion of the endplate noted)

| Endplate defects | Right lateral | | Anterior | | Central | | Posterior | | Left lateral | |
|------------------|---------------|-------------|------------|-------------|-------------|-------------|------------|-------------|--------------|-------------|
| | Only | In part | Only | In part | Only | In part | Only | In part | Only | In part |
| Schmorl's nodes | 18 (7.0%) | 15 (5.8%) | 34 (13.2%) | 3 (1.2%) | 112 (43.6%) | 34 (13.2%) | 31 (12.1%) | 27 (10.5%) | 22 (8.6%) | 6 (2.4%) |
| Focal defects | 18 (4.7%) | 36 (9.5%) | 38 (9.8%) | 23 (6.1%) | 168 (43.6%) | 94 (24.6%) | 31 (8.0%) | 78 (27.6%) | 25 (6.5%) | 20 (5.3%) |
| Corner defects | 1 (4.2%) | 7 (29.2%) | 10 (41.7%) | 6 (25.0%) | 0 | 0 | 2 (8.3%) | 6 (25.0%) | 0 | 0 |
| Erosion | 36 (8.6%) | 160 (38.2%) | 11 (2.6%) | 247 (58.5%) | 16 (3.8%) | 292 (69.7%) | 6 (1.4%) | 266 (63.5%) | 39 (9.3%) | 147 (35.1%) |
| All defects | 73 (3.5%) | 218 (10.5%) | 92 (4.4%) | 279 (13.4%) | 296 (14.2%) | 420 (20.2%) | 70 (3.4%) | 377 (18.1%) | 86 (4.1%) | 173 (8.3%) |

Table 5-4: Distribution of EPSDs by endplate location (cranial vs caudal) and spinal region (upper vs lower)

| Endplate defects | Prevalence | Cranial | Caudal | Upper Spinal level | Lower Spinal level |
|------------------|-------------|---------------------------|------------|----------------------------|--------------------|
| Normal | 54.4%, 1297 | 52.8%, 685 | 47.2%, 612 | 43.9%, 570 | 56.1%, 727 |
| Schmorl's nodes | 10.8%, 257 | 45.9%, 118 | 54.1%, 139 | 59.9%, 154 | 40.1%, 103 |
| Focal defects | 16.2%, 386 | 46.6%, 180 | 53.4%, 206 | 65.5%, 253 | 34.5%, 133 |
| Corner defects | 1.0%, 24 | 50.0%, 12 | 50.0%, 12 | 41.7%, 10 | 58.3%, 14 |
| Erosion | 17.6%, 420 | 46.7%, 196 | 53.3%, 224 | 48.8%, 205 | 51.2%, 215 |
| All defects | 45.6%, 1087 | 46.6%, 506 | | 57.2%, 622 | |
| | | $\chi^2 = 9.28, p < 0.01$ | | $\chi^2 = 41.68, p < 0.01$ | |

5.2.4 Association of Endplate Structural Defects with Age and BMI

The presence of any EPSD was statistically significantly associated with age (OR: 1.02, 95%CI: 1.01, 1.03, $p=0.03$) but not BMI (OR: 1.00, 95%CI: 0.98, 1.03, $p=0.72$). With respect to specific EPSD phenotypes, focal defects and erosion were significantly associated with age (OR: 1.02, 95%CI: 1.00, 1.03, $p=0.02$ and OR: 1.03, 95%CI: 1.01, 1.04, $p<0.01$, respectively) but not Schmorl's nodes and corner defects (OR: 1.01, 95%CI: 0.99, 1.03, $p=0.21$ and OR: 1.01, 95%CI: 0.95, 1.08, $p=0.621$, respectively). In other words,

for every additional year, the odds of having an EPSD or focal defect increased by 2%, while the odds increase by 3% for endplate erosion, or for every additional 10 years there is a 22% increase in the odds of having an EPSD or focal defect, and a 35% increase in the odds for erosion. Of the EPSD phenotypes, only corner defects were associated with BMI (OR: 1.15, 95%CI: 1.03, 1.30, p=0.02). For every unit increase in BMI, the odds of having a corner defect increased by 15%, while a complete transition from one BMI category to the next (5 unit increase in BMI) resulted in 101% increase in the odds of having a corner defect. However, defect size using any measure was not associated with age or BMI.

Table 5-5: Association between EPSDs with age and BMI

| Variables | Age | BMI |
|----------------------------------|------------------------------------|---------------------------------|
| | OR or Beta Coef. (95% CI) | OR or Beta Coef. (95% CI) |
| EPSD presence [†] | 1.02 (1.01, 1.03) p=0.03 | 1.00 (0.98, 1.03) p=0.72 |
| Schmorl's nodes [†] | 1.01 (0.99, 1.03) p=0.21 | 0.98 (0.94, 1.02) p=0.36 |
| Focal defects [†] | 1.02 (1.00, 1.03) p=0.02 | 1.00 (0.96, 1.04) p=0.97 |
| Corner defects [†] | 1.01 (0.95, 1.08) p=0.68 | 1.15 (1.03, 1.30) p=0.02 |
| Erosion [†] | 1.03 (1.01, 1.04) p<0.01 | 1.02 (0.98, 1.05) p=0.34 |
| Larger defects [†] | 1.00 (0.98, 1.03) p=0.87 | 0.98 (0.93, 1.03) p=0.98 |
| Anteroposterior [‡] | 0.04 (-0.04, 0.12) p=0.32 | -0.02 (-0.20, 0.15) p=0.80 |
| Transverse diameter [‡] | -0.01 (-0.03, 0.01) p=0.39 | -0.02 (-0.07, 0.03) p=0.51 |
| Axial area [‡] | -0.15 (-3.38, 3.08) p=0.93 | -5.82 (-12.99, 1.35) p=0.11 |

†: Odd ratio; ‡: Beta Coefficients

5.3 Discussion

The study's main findings were that nearly half of all endplates assessed had EPSDs, which were more prevalent in the upper lumbar levels than the lower levels and more commonly on caudal than cranial endplates. Also, EPSDs, when phenotypes were aggregated, were associated with age but not BMI. However, the distribution pattern and associated factors vary by EPSD phenotype, supporting the theory that EPSD phenotypes may have unique etiologies and clinical consequences (12,32).

The study affirms previous findings (15,154) of EPSD as a common MRI finding (45.8%) in general population samples. While the prevalence of each EPSD phenotype varied, erosion was the most common (17.6%) followed by focal defects (16.2%) and Schmorl's nodes (10.8%), with corner defects the least EPSD (1%). The prevalence of EPSD in this study is higher than previous MRI patients studies which reported a prevalence of 27.8% (focal: 13.5%, erosion: 11.1%, corner defect 3.2%) (15) and 14.1% (wavy/irregular: 1.5%, notched: 8.6%, Schmorl's node: 4%, and fracture: 0.2%) (154). However, our prevalence is comparable to a study of visual inspection with a prevalence of 45.6% (Schmorl's node: 22%, erosion: 14.1%, fracture: 6.3% and calcification: 3.3%) (35), and a study of μ CT with a prevalence of 44% (SN:18%, erosion: 16%, fracture 2.5%) (179). Conversely, previous cadaveric studies (17,24,28,180) without a standardized EPSD classification system reported a much higher and wider prevalence (48% to 75%). Perhaps our study achieved greater reliability and validity that is comparable to the reference standards (visual inspection and μ CT) because of the standardized classification system, double-blinded readings and setting no restriction on EPSD size for inclusion (35,179). Furthermore, the lack of available studies of the prevalence of Schmorl's nodes as a separate entity from focal defects limits comparison with our study. Previous studies have studied EPSD grouped as Schmorl's nodes (122,133,165,180–185), focal defects (15,186), Schmorl's nodes and notched (154), and Schmorl's node and other endplate abnormalities (143,187).

Distinguishing between focal defects and Schmorl's nodes is one of the novel features of the classification system we used, which may be responsible for Schmorl's nodes not being the most common EPSD phenotype in our sample. The approach views Schmorl's nodes as distinct from focal defects based on the presence or absence of a sclerotic or smooth margin, and the study findings suggest this may be an important distinction based on differences in association with age, suggesting different etiologies. Also, Schmorl's node and focal defects presented varying morphological characteristics of distribution and dimensions. Schmorl's nodes were smaller than all the EPSD phenotypes and common at the upper spinal levels. They occur most commonly in the central part of the endplate where the notochord regresses, which represents a developmental weak spot of the endplate (16). While, focal defects are mainly small, but seldomly occur as moderate to large and occur more in the upper spinal regions. The findings of the present study were consistent with

previous studies (26,35,154) that reported a high prevalence of Schmorl's nodes and focal defects at the thoracolumbar and upper lumbar region (24), where the endplate may be more fragile due to lower bone density compared to the lower lumbar regions (169).

Previous studies have often focused on Schmorl's nodes when studying EPSD and reported wide ranging prevalence rates of 7.6% (180,182), 9.4% (126), 30% (188), 50% (26), and 67% (165), which may have been influenced by varying assessment methods and nomenclature. For example, Williams et al (26) defined a Schmorl's node as a localized defect in a vertebral endplate with a well-defined herniation pit in the vertebral body with or without a surrounding sclerotic rim and reported a prevalence of 41% in the lumbar region and 59% in the thoracic. However, in other studies, when the definition was narrowed to include Schmorl's nodes containing a sclerotic margin with a round base, the prevalence of Schmorl's nodes was lower. Using the stricter definition, Dar et al (180,182) studying the Hamann–Todd Osteological Collection defining a Schmorl's node as a depression with sclerotic margins on the vertebral body surface reported a prevalence of 7.6%. Sward et al (145) described Schmorl's nodes as localized radiolucent defects, with bony or sclerotic margins, which exclude smooth shallow bulges of the endplate or minimal endplate irregularities reported a similar low prevalence of 24.7% of individuals. Previous studies have reported Schmorl's nodes (35), notched (154) and focal defects (15) as the most common types of EPSDs. However, the present study showed otherwise, with erosion as the most common EPSD phenotype. Our study differentiating the two Schmorl's-like phenomena led to lower prevalence for either Schmorl's node or focal defect compared to other studies that group all Schmorl's-like defects together, resulting in erosion being the most common phenotype.

In the present study, all EPSD phenotypes were more common on the caudal than cranial endplate. This finding supports previous findings (132,189) that the cranial endplate is thicker (53,158,172) and stronger (190) than the caudal endplate with less dense trabecular bone, making it susceptible to fracture when continuously compressed by the intervertebral disc (53). Although most EPSD occurred at the caudal endplate, larger defects were observed on both endplates adjacent to a disc. This mirroring pattern is similar to the observations of other degenerative changes, such as Modic changes (118), osteophytes and

sclerosis (191,192). Perhaps, the lack of significant difference between cranial and caudal endplate in the prevalence of EPSD in previous studies (35,148,193) may be due biased assessment, focusing on larger EPSD and negating the presence of smaller defects.

Although age was associated with EPSD in this study, as in prior studies, Khoury et al (194) noted that the effects of age are complex and largely unknown. Khoury et al (194) further state that advanced age is associated with an increased risk of disease due to cumulative personal, occupational and environmental exposures, leading to physiologic and psychological changes, which are in part under genetic control. This assertion is supported for other age related findings, such disc degeneration and pathology, by the Twins Spine Study (7) and a review by Ala-Kokko (195) which noted associations with several environmental and constitutional risk factors, as well as a large contribution from genetic factors. Furthermore, variability in the definition of EPSD and its phenotypes influenced the prevalence and association with other factors. Our study described Schmorl's node as a round indentation with a smooth sclerotic margin, the study confirmed that Schmorl's nodes are independent of age and BMI, and other studies (180,182) with similar Schmorl's node description corroborate with our findings. Dar et al (180,182) show that Schmorl's nodes as a depression with sclerotic margins on the vertebral body surface are independent of age, which are predominant at the upper lumbar region and the caudal endplate. Contrary to our study, Williams et al (26) show that Schmorl's nodes, defects with and without sclerotic margins are associated with age but not with BMI. Such a definition would have included both focal and Schmorl's nodes and therefore diluted the specific association with age.

The present study shows that both Schmorl's nodes and focal are independent of BMI, this may be the reason for the consistent lack of association in previous studies, irrespective of Schmorl's nodes' definition. Many studies that describe Schmorl's nodes with sclerotic margin are independent of age (122,165,180,182), while studies that defined Schmorl's nodes as a defect with or without a sclerotic margins (15,35,145,181) or studies that did not provide any definition (133,143,183,185,196) are associated with age. The lack of Schmorl's nodes definition makes it difficult to ascertain what they precisely represent, and therefore potentially could include other focal defects. The present study disagrees with the

traditional theory that supports traumatic, or disease causes of Schmorl's nodes (20,21,197). Schmorl's node occurrences are probably associated with the vertebra development process during early life (16), the disc pressing the notochord, the weakest part of the endplate (16). Therefore, the variations among specific EPSD phenotypes in their association with age and BMI, as well as differences in distribution patterns, supports the need to distinguish the phenotypes in studies of etiology and clinical consequences.

Also, the reported level of association between EPSD and age (OR: 1.02 95%CI: 1.01 - 1.03, $p < 0.01$) conforms with previous studies (35,181,198,199), indicating a similar weak association (OR: 1.02 to 1.06). Despite the weak association, a striking low prevalence of 15% (148) and 12% (200) of EPSD in studies of young children compared to our study of 45.6% from the aged population may confirm the role of age in the occurrence of EPSD.

Erosion and corner defects occur most at the caudal endplate and the lower lumbar levels (especially L4/L5). The susceptibility of the lower lumbar region to these EPSD phenotypes may be due to greater forces experienced in a wide range of flexion and extension, with the highest range of motion at L4/L5 (201,202). Furthermore, other imaging findings which are age and activity dependent, such as osteophytes (203–205), show a similar trend of dominance at L4/L5 disc level. Corner defects were associated with BMI and common at the anterior endplate indicating the role of axial loading of the spine causing anterior corner defects. These findings are consistent with Rachbauer et al (200) who reported a significant presence of anterior lesions in the group that performed competitive ski sport compared to the control group. We can therefore speculate that body weight loaded axially on the spine, especially anteriorly, may be responsible for corner defects. Also, this assertion is supported by Bruno et al (206) that found the highest compressive loads occurring at the anterior part of the vertebrae during activities involving the weight of the body or external weight during trunk flexion or weightlifting. Similarly, using telemeterized vertebral implants to investigate the spinal impact of 1000 different activities of daily living, Rohmann et al (207) reported the highest lumbar vertebral loads occurred in activities where the center of gravity is tilted anteriorly.

One of the study limitations is that all participants are men, and the prevalence and associations may differ in women. Secondly, the studied population is an aged sample and

posed the bias of higher degenerative spinal conditions which may heighten the prevalence and therefore findings may not be representative of the general population. Also, due to the cross-sectional nature of the study, causation cannot be established. A fourth limitation relates to the MRI quality. The study uses 1.5T scanner and use of scanner currently available with higher magnetic field strength (e.g. 3.0T) may have led to greater observed prevalence. Despite the unsatisfactory MRI quality, one of the study's strengths is the use of a well-developed EPSD assessment method for assessing the sample and the use of an explicit criterion of double-blinded assessment to ensure all EPSDs are accurately depicted to improve the reliability and validity of the assessments. Also, the use of the large Twin Spine Dataset which may allow generalizability of the results added to the study's strength.

In conclusion, our study found that 45.6% of endplates had an EPSD of some type, with erosion and focal defects most common. The EPSD phenotypes varied in their characteristics, including prevalence, distribution and association with age and BMI. Our results support differentiating focal defects from Schmorl's nodes, due to possible differences in their association with age, which may explain the conflicting results of earlier studies. The association of corner defects with BMI suggests they are likely the result of excessive axial loading on the anterior part of the endplate in flexion. With advancements in imaging resulting in better resolutions and tissue contrast, future large-scale longitudinal studies assessing specific EPSD phenotypes and their relation to environmental and constitutional factors (e.g., heritability and gene variants) will be needed to advance knowledge of the etiology of EPSD, as well as their association with other imaging findings and clinical outcomes.

Chapter 6

6 General Discussion and Conclusions

Despite decades of research focusing on the intervertebral disc as the culprit in back pain (32,144,174), the pathoanatomical cause of the vast majority of back pain cases remains unknown. However, recent advances in imaging modalities have targeted the vertebral endplate, a thin mechanical interface with better neural and blood supply than the disc (11,13,32). The endplate serves as a diffusion channel for disc nutrition and distributes compressive forces along the spine (175,176), and has received attention as a possible culprit in back pain. Furthermore, histological analysis indicated an increase in neural density in defective endplates and those adjacent to a degenerated disc (11,12). Research on endplate structural defects (ESPD) has been criticized, however, for lack of standard nomenclature and measurement methods making it difficult to compare findings between studies, resulting in a wide range of prevalence rates and conflicting findings. The lack of validity studies to ascertain what ESPD phenotypes on clinical imaging represent have added to the impediments in advancing knowledge of ESPD and their clinical consequences (13,168).

This doctoral thesis began with a systematic review and meta-analysis of the literature to examine the current state of knowledge on the association of ESPD with back pain. Recognizing the challenges in advancing such knowledge due to measurement issues, we then conducted a head-to-head comparison of the two common ESPD assessment methods in terms of reliability and validity. Observations of limitations in these common measurement methods led to a third study developing and validating a new ESPD classification and assessment method. Finally, using the new classification system on lumbar MRI, we explored ESPD prevalence, distribution patterns and associations with age and BMI in a sample of adult males.

6.1 Distinct ESPD phenotypes are associated with Back Pain

Pooling data from the 26 studies included in our review, representing 11,027 subjects, revealed moderate quality evidence of an association between ESPD and back pain, despite inconsistencies among studies' findings. The variations in the associations between ESPD

and back pain were explained by EPSD and back pain phenotypes, and the population studied. However, the heterogeneity of the pooled data was not explained by the difference between adjusted and unadjusted odds ratios. Our findings supported an association of specific EPSD phenotypes, including erosion and sclerosis, with back pain. On the other hand, Schmorl's nodes were only associated with back pain in general population samples, not patient samples, for a specific (frequent and incident) type of back pain and back pain overall.

Further confirming the problems associated with nomenclature and measurement methods, we were unable to pool Schmorl's nodes overall data except in general population. Also, the wide differences in effect magnitudes of the association between Schmorl's nodes and back pain further confirm variability in what EPSD categorized as Schmorl's nodes truly represent. Thus, further studies segregating definitions and nomenclature of Schmorl's nodes may supplement our findings in resolving the conflicting findings as evidence of high heterogeneity. Similarly, specific back pain phenotypes, such as frequent back pain and back pain incidence were each associated with EPSD and were supported by low heterogeneity ($I^2 = <7.5\%$). These findings collaborate previous studies suggesting that distinct back pain definitions may allow comparison between studies. Overall, there is moderate quality evidence of an association between back pain and EPSD, which is most evident for erosion, sclerosis and Schmorl's nodes.

Going forward, research on specific EPSD phenotypes using the best available standardized ESPD assessment methods that consider specific back pain case definitions, using strong study designs, will be important in clarifying the extent of associations and underlying mechanisms.

6.2 Common EPSD assessment methods are limited by phenotypes represented

The previous chapter of this thesis (Study 1) highlight the need for studies of EPSD, including specific phenotypes and use of standardized assessment methods outlining nomenclature and definitions to further the understanding of pathoanatomical mechanisms underlying back pain. However, with CT, as with MRI, common methods used to document

EPSD have not been validated, leaving uncertainty about what the observations represent or how accurately they capture the presence or absence of EPSD (13). This level 2 evidence of the two common EPSD (including phenotypes) assessment methods on sagittal slices of clinical CT and corresponding μ CT shows acceptable reliability for the presence of EPSD and its phenotypes using the two common assessment methods. However, the available EPSD phenotypes included in each method influence the rater's choice of EPSD phenotypes selection. For example, erosion, for which Brayda-Bruno et al (154) system lacked a category, was mainly (82.8%) classified as wavy/irregular. While the majority of notched defects (n=15, 476.9%) and Schmorl's nodes (n=45, 79%) using Brayda-Bruno's classification were recorded as focal defects using Feng's method (15). Irregularity and erosion are entirely different phenotypes in definition and morphology, but the absence of one influence the selection of the other. Similarly, on clinical imaging, notched and Schmorl's node may be indistinguishable as represented by focal defect. Yet only a small portion of focal defects using Feng et al's method corresponds to Schmorl's nodes, while a large portion represents fracture defects. Thus, there is the need to consider Schmorl's nodes as a separate entity from other focal defects, which is further supported by the evidence that typical and atypical Schmorl's nodes have different prevalence and etiology (165–167). *When compared to μ CT*, endplate fractures (n=53) and corner defects (n=28) were routinely missed on clinical CT. Endplates classified as wavy/irregular on clinical-CT corresponded to erosion (n=29, 21.2%), jagged defects (n=21, 15.3%) and calcification (n=19, 13.9%) on μ CT. While some focal defects on clinical CT represented endplate fractures (n=21, 27.6%) on μ CT.

Overall, for the presence of an EPSD, there was a sensitivity of 70.9% and specificity of 79.1% for Feng's method, and 79.5% and 57.5%, respectively, using Brayda-Bruno's. All EPSD clinical-CT and μ CT dimensions significantly correlated ($p < 0.01$), except with defect depth. It was concluded that there is good reliability and support for the validity of assessing the presence of EPSD using the two methods. However, neither method contained all the needed EPSD phenotypes to provide optimal specificity. Therefore, a standardized combined assessment may be needed to improve the assessment of EPSD and its phenotypes.

6.3 Introduction of a new EPSD classification and assessment method

The long-standing confusion on EPSD nomenclature among scientists and clinicians (168) was laid bare in a comprehensive review of EPSD terminology and definitions, which we previously conducted (13). In addition to the problem of widely varying EPSD measurement methods, there is the problem of limited content coverage of currently available EPSD assessment methods, leading us to recommend a standardized, combined EPSD assessment method (Chapter Three). The new EPSD classification system was based on available literature on morphology, etiology and clinical relevance of EPSD phenotypes (12,32,165–167). The result was a classification system with definitions and atlases of six EPSD phenotypes, including Schmorl's nodes, focal defects, corner defects, erosion, wavy/irregular endplates, and sclerosis/calcification, using a standard process (170). The description of each phenotype and content of the new classification went through several iterations to optimize clarity and reduce ambiguity, with all assessors attesting to the content relevance, representativeness, and technical quality of each EPSD included in the classification system manual. The content validity was deemed adequate by the expert assessors.

The novel EPSD classification had good interrater reliability for the presence of EPSD ($K=0.65-0.68$), fair for the specific phenotypes ($K=0.52-0.55$) and good to excellent for anteroposterior diameter ($ICC=0.69-0.87$) and axial area ($K_w=0.58-0.88$) of the defects. When assessments of the presence of EPSD using clinical CT were compared to the reference standard, μ CT, sensitivity (71%-79%) and specificity (77%-87%) were good, and measurements of dimensions for anteroposterior diameter and axial area were significantly correlated ($r= 0.30 - 0.62$).

Our study also confirmed similar reliability between raters irrespective of the assessors' level of experience, as has been found in previous imaging studies (153,208) , suggesting that a detailed morphologic description is more important in establishing reliability than the experience of the readers. However, informal training to familiarize the raters with the classification is needed to improve consistency among assessors. Overall, the system provides a basic classification of EPSD with a higher degree of reliability and validity than

the previously assessed methods. As the new classification is based on the consensus of experienced researchers and clinicians using CT scans, further studies are needed to confirm its psychometric properties and applicability to other imaging modalities.

6.4 EPSD phenotypes have distinct prevalence, distribution patterns and possible etiology

Using the novel standardized EPSD assessment method (chapter 4), our study revealed that nearly half (45.6%, n=1087) of the endplates assessed had some sort of EPSD in this sample of aged men. Although identifying EPSD is challenging, our study used a double-blinded assessment approach to ensure all EPSD are reliably captured in the assessment. Similarly, previous studies (142,209) have set limits to what will qualify as an EPSD. However, considering that both the cartilaginous and osseous endplates are thin (40,158) and defects of small size or without substantial morphological changes are often missed even with the best available imaging technology (26). Therefore, our assessment ensures that defect size was not a determining factor to qualify an observation as an EPSD, especially, considering one of the hypotheses that we aimed to capture fracture defect (with small AP diameter) among focal defects.

Four EPSD phenotypes including Schmorl's nodes, focal defects, corner defects and erosion were observed on the MRI of the sampled population. Observations from the lumbar endplates (upper T12/L1 to lower L5/S1) MRI reveal that erosion defects were the most common type of EPSD while corner defects were the least common. When all EPSD phenotypes are aggregated, EPSD occur more at the upper lumbar levels and on the caudal endplates and are associated with age but not BMI. However, the trend differs by each EPSD phenotype, except that all EPSD phenotypes are predominant at the caudal endplate. This finding is supported by previous findings (53,132,158,172,189,190) suggesting that the cranial endplate is thicker and stronger than the caudal endplate, making it less susceptible to mechanical failure. Similarly, previous studies (24,26,35,154,169) reported a high prevalence of EPSD in the thoracolumbar and upper lumbar regions, where the endplate may be more fragile due to lower bone density compared to the lower lumbar regions. Conversely, focal defects and Schmorl's nodes occur more at the upper lumbar level and are not associated with BMI.

Also, our findings revealed that age was associated with focal defects but not Schmorl's nodes. Many studies that described Schmorl's nodes as defects containing sclerotic margin are independent of age (122,165,180,182), while Schmorl's nodes defined as defects without sclerotic margins (15,35,145,181) or where Schmorl's nodes are not defined (133,143,183,185,196) are associated with age. Contrarily, erosion and corner defects occur more at the lower lumbar levels. However, erosion is associated with age but not BMI. While corner defects are associated with BMI but not age. The present study disagrees with the traditional theory that supports traumatic or disease causes of Schmorl's nodes (20,21,197). Schmorl's nodes occurrence are probably associated with the vertebra development process during early life (16), through the disc pressing the notochord, the weakest part of the endplate (16). Also, the study attributed spinal axial loading via the BMI on the anterior part of the endplate as the common cause of corner defects and, erosion and focal defect are degenerative aging processes. Furthermore, erosion and corner defects occur most on the caudal endplate and the lower lumbar levels (especially L4/L5) confirming the findings of previous studies (17,33,34) suggesting that the susceptibility of the lower lumbar to the greater range of motion of flexion and extension with the highest range of motion at L4/L5 (201,202) may be responsible for the defects. In conclusion, EPSP is a common spinal finding with possible distinct etiology between the phenotypes.

6.5 Study limitations

Despite the methodological strength of the included studies, some limitations must be noted. First, the use of lower image quality in CT and MRI than currently available. State-of-the-art CT now achieves spatial resolution of approximately 0.25 x 0.5 mm (210), 3T MRI is widespread, and 7T MRI is available in some settings (211). It can therefore be argued that this may not represent the best available technology, and the reliability and validity is expected to improve with image resolutions as technology continue to advance. However, we have reduced the possible effect of image quality by ensuring strong methodology processes in the assessment protocols. Another limitation is the tendency of a spectrum bias associated with the age of the studied population. The data from the Twin Spine Study and cadaveric samples represent an aged population not representative of the

general population. Consequently, there may be a tendency of a higher true positive due to the presumed high prevalence of EPSD and as such detection rate tends to have been higher. Despite the extensive methodology used to develop the new EPSD assessment method, the classification has not been validated for MRI use. Consequently, another limitation relating to the Twin Spine Study dataset is limited ability of MRI relative to CT in identifying the presence of sclerosis/calcification, which inevitably led us to omit this phenotype. Another limitation is the relatively low sample size for some EPSD phenotypes of low prevalence, such as corner defects. Findings related to such EPSD phenotypes, therefore, may have been underpowered.

It is also important to acknowledge that differentiating certain EPSD phenotypes from one another is challenging (e.g., Schmorl's nodes vs. focal defects, erosion vs. wavy/irregular). However, we have attempted to minimize this problem by conducting two independent readings and carefully reconciling discrepancies that may have arisen from challenges in differentiating the phenotypes. Finally, all associations were cross-sectional and, therefore, causal inferences cannot be drawn.

6.6 Conclusions

The research presented in this thesis used multiple methodological approaches, including systematic review and meta-analysis, measurement studies using CT and μ CT of cadaveric spines, and a cross-sectional, epidemiologic study of EPSD prevalence and associations with age and BMI. According to the aggregated data from the literature review, certain EPSD phenotypes are associated with back pain despite several study limitations which include lack of adjustment of potential confounders and the use of non-standardized assessment methods. Also, the common available EPSD assessment methods were limited by certain content needed to provide optimal sensitivity and therefore a novel comprehensive method was developed consisting of six EPSD phenotypes including Schmorl's nodes, focal defects, corner defects, erosion, wavy/irregular defects, and sclerosis/calcification, definitions, and atlases. Using the new assessment method on a large sample of Twin Spine Study dataset, findings confirm EPSD as a common MRI finding with a distinct difference in prevalence and distribution between the EPSD phenotypes.

Similarly, their variability with the association with age and BMI proof further the distinction between the EPSD phenotypes.

6.7 Significance

Overall, this project paved the way for the understanding of the role of EPSD in the pathogenesis of back pain and other spinal imaging findings. Progress has been impeded by the lack of consistent nomenclature and standardized measurement methods that has resulted in wide prevalence rates, diluted associations, and conflicting findings. The systematic review and meta-analysis highlighted the association of EPSD phenotypes, especially focal defects, and sclerosis with back pain, and Schmorl's nodes and back pain in general population. However, those finding were less certain because of a lack of adjustment for confounders and variability in the definition of terms. The use of cadaveric spinal CT and μ CT to study the validity of two common methods of EPSD assessment highlighted the limitations of those methods, which subsequently lead to the development and validation of a new method of EPSD assessment. The use of the new classification system informed the prevalence and distribution of EPSD phenotypes and an understanding to the distinct etiology of each EPSD phenotypes, such as erosion and corner defects and, the distinction between Schmorl's nodes and focal defects. Use of the new standardized classification system can support further studies needed to resolve conflicting findings of the association of EPSD, including specific phenotypes, with other imaging findings and back pain.

6.8 Future directions

The thesis comprised studies involving aged male and female cadavers, and male general populations from the TSS dataset. Therefore, studies involving a wide age range of both sexes would substantially enhance the findings. For example, the Twin Spine Study consists of only male subjects, but findings concerning age and BMI indicate an intricate relationship that may differ by sex. Therefore, studies of female subjects may enhance the generalizability of the findings. Similarly, the findings of the TSS using the novel classification were based on MRI observations. However, the classification has only been validated for clinical CT. Further studies are needed to validate the classification for MRI.

In addition, all observations for the EPSD are macroscopic in this classification and correlated with constitutional factors. Further studies evaluating the microscopic aspect of the EPSD phenotypes including histologic variabilities would inform the basic biologic constituent of each defect. Also, other microstructural components responsible for the physiologic function of the endplate such as the endplate porosity would add further clarity to understanding the field. The etiology and clinical consequences of the EPSD phenotypes remain largely unknown. However, our study has informed the potential differentiation of EPSD phenotypes in prevalence, distribution, and associated variables. Therefore, a comprehensive study using a large dataset is needed to further the understanding of EPSD etiology, association with other imaging findings and clinical outcomes. Also, genetic analysis would open another avenue to understanding the epidemiology and etiology of EPSD. Finally, future studies should focus on longitudinal data to determine the etiology and possible outcomes of each EPSD phenotype.

References

1. Hart LG, Deyo RA, Cherkin DC. Physician office visits for low back pain. Frequency, clinical evaluation, and treatment patterns from a U.S. national survey. *Spine (Phila Pa 1976)*. 1995 Jan;20(1):11–9.
2. Hsiao C-J, Cherry DK, Beatty PC, Rechtsteiner EA. National Ambulatory Medical Care Survey: 2007 summary. *Natl Health Stat Report*. 2010 Nov;(27):1–32.
3. Wu A, March L, Zheng X, Huang J, Wang X, Zhao J, et al. Global low back pain prevalence and years lived with disability from 1990 to 2017: estimates from the Global Burden of Disease Study 2017. *Ann Transl Med*. 2020;8(6):299–299.
4. Hartvigsen J, Hancock MJ, Kongsted A, Louw Q, Ferreira ML, Genevay S, et al. What low back pain is and why we need to pay attention. *Lancet (London, England)*. 2018 Jun;391(10137):2356–67.
5. Mankin HS, Adams RH. Pain in the back and neck. In: R.G. Petersdorf et al. (Eds.), *Principles of Internal Medicine*. 10th ed. New York: McGraw-Hill; 1983. 35–45 p.
6. Gatchel RJ. Introduction to the “Special Issue on Pain Catastrophizing.” *J Appl Biobehav Res*. 2017;22(1):1–5.
7. Battié MC, Videman T, Kaprio J, Gibbons LE, Gill K, Manninen H, et al. The Twin Spine Study: Contributions to a changing view of disc degeneration†. *Spine J [Internet]*. 2009;9(1):47–59. Available from: <http://dx.doi.org/10.1016/j.spinee.2008.11.011>
8. Battié MC, Videman T, Gibbons LE, Fisher LD, Manninen H, Gill K. 1995 Volvo Award in clinical sciences. Determinants of lumbar disc degeneration. A study relating lifetime exposures and magnetic resonance imaging findings in identical twins. *Spine (Phila Pa 1976)*. 1995 Dec;20(24):2601–12.
9. Sambrook PN, MacGregor AJ, Spector TD. Genetic influences on cervical and lumbar disc degeneration: A magnetic resonance imaging study in twins. *Arthritis Rheum*. 1999;42(2):366–72.
10. Munir S, Rade M, Määttä JH, Freidin MB, Williams FMK. Intervertebral Disc Biology: Genetic Basis of Disc Degeneration. *Curr Mol Biol Reports*. 2018;4(4):143–50.
11. Fields AJ, Liebenberg EC, Lotz JC. Innervation of pathologies in the lumbar vertebral end plate and intervertebral disc. *Spine J [Internet]*. 2014;14(3):513–21. Available from: <http://dx.doi.org/10.1016/j.spinee.2013.06.075>
12. Lotz JC, Fields AJ, Liebenberg EC. The Role of the Vertebral End Plate in Low Back Pain. *Glob Spine J*. 2013;3(3):153–63.
13. Lawan A, Leung A, Battié MC. Vertebral endplate defects: nomenclature, classification and measurement methods: a scoping review. *Eur Spine J [Internet]*. 2020;29(6):1397–409. Available from: <https://doi.org/10.1007/s00586-020-06378-8>

14. Hurxthal LM. Schmorl's nodes in identical twins. Their probable genetic origin. *Lahey Clin Found Bull.* 1966;15(3):89–92.
15. Feng Z, Liu Y, Yang G, Battié MC, Wang Y. Lumbar Vertebral Endplate Defects on Magnetic Resonance Images. *Spine (Phila Pa 1976).* 2018;43(13):919–27.
16. Schmorl G, Junghanns H. *The Human Spine in Health and Disease.* 2nd American edition translated and edited by Besemann EF ed. New York: Grune and Stratton. 1971.
17. Hilton RC, Ball J, Benn RT. Vertebral end-plate lesions (Schmorl ' s nodes) in the dorsolumbar spine. 1976;127–32.
18. Vernon-Roberts B, Pirie CJ. Degenerative changes in the intervertebral discs of the lumbar spine and their sequelae. *Rheumatol Rehabil.* 1977 Feb;16(1):13–21.
19. Coventry M, Ghormley RK, Kernohan JW. The Intervertebral Disc: Its Microscopic Anatomy and Pathology. Pathological changes in intervertebral disc. *J Bone Jt Surg.* 1945;27(3):460–74.
20. McCall IW, Park WM, O'Brien JP, Seal V. Acute traumatic intraosseous disc herniation. *Spine (Phila Pa 1976).* 1985;10:134–7.
21. Wagner AL, Murtagh FR, Arrington JA, Stallworth D. Relationship of Schmorl's nodes to vertebral body endplate fractures and acute endplate disk extrusions. *AJNR Am J Neuroradiol.* 2000 Feb;21(2):276–81.
22. Fahey V, Opeskin K, Silberstein M, Anderson R, Briggs C. The pathogenesis of Schmorl's nodes in relation to acute trauma. An autopsy study. *Spine (Phila Pa 1976).* 1998 Nov;23(21):2272–5.
23. Zhang N, Li F-C, Huang Y-J, Teng C, Chen W-S. Possible key role of immune system in Schmorl's nodes. *Med Hypotheses.* 2010;74(3):552–4.
24. Pfirrmann CW, Resnick D. Schmorl Nodes of the Thoracic and Lumbar Spine: Radiographic-Pathologic Study of Prevalence, Characterization, and Correlation with Degenerative Changes of 1,650 Spinal Levels in 100 Cadavers. *Radiology.* 2001;219:368–74.
25. Cheung KMC, Samartzis D, Karppinen J, Mok FPS, Ho DWH, Fong DYT, et al. Intervertebral disc degeneration: New insights based on “skipped” level disc pathology. *Arthritis Rheum.* 2010;62(8):2392–400.
26. Williams FMK, Manek NJ, Sambrook PN, Spector TD, MacGregor AJ. Schmorl's nodes: Common, highly heritable, and related to lumbar disc disease. *Arthritis Care Res.* 2007;57(5):855–60.
27. Hsu KY, Zucherman JF, Derby R, White AH, Goldthwaite N, Wynne G. Painful lumbar end-plate disruptions: a significant discographic finding. *Spine (Phila Pa 1976).* 1988 Jan;13(1):76–8.
28. Saluja G, Fitzpatrick K, Bruce M et al. Schmorl's nodes (intravertebral herniations of intervertebral disc tissue) in two historic British populations. *JAnat.* 1986;145:87–96.

29. Malmivaara A, Videman T, Kuosma E, Troup JD. Malmivaara 1987.pdf. *Spine (Phila Pa 1976)*. 1987;12(5):453–7.
30. Eskola PJ, Kjaer P, Daavittila IM, Solovieva S, Okuloff A, Sorensen JS, et al. Genetic risk factors of disc degeneration among 12-14-year-old Danish children: A population study. *Int J Mol Epidemiol Genet*. 2010;1(2):158–65.
31. Sahoo MM, Mahapatra SK, Kaur S, Sarangi J, Mohapatra M. Significance of vertebral endplate failure in symptomatic lumbar disc herniation. *Glob Spine J*. 2017;7(3):230–8.
32. Wang Y, Videman T, Battié MC. ISSLS prize winner: Lumbar vertebral endplate lesions: Associations with disc degeneration and back pain history. *Spine (Phila Pa 1976)*. 2012;37(17):1490–6.
33. Wang Y, Battie MC, Videman T. A morphological study of lumbar vertebral endplates: radiographic, visual and digital measurements. *Eur spine J*. 2012 Nov;21(11):2316–23.
34. White A, Panjabi M. *Clinical Biochemechanics of the Spine*. 2nd ed. Philadelphia: Lippincott Co; 1990.
35. Wang Y, Videman T, Battié MC. Lumbar vertebral endplate lesions: Prevalence, classification, and association with age. *Spine (Phila Pa 1976)*. 2012;37(17):1432–9.
36. The New York School of Regional Anesthesia. Human spinal column [Internet]. *Spinal Anaesthesia*. 2022 [cited 2022 Oct 18]. Available from: <https://www.nysora.com/techniques/neuraxial-and-perineuraxial-techniques/spinal-anesthesia/>
37. Moore K DA. *Clinically oriented anatomy*. 5th ed. Baltimore: Lippincott Williams & Wilkins,. 2006. 478–519 p.
38. Adams MA, Roughley PJ. What is intervertebral disc degeneration, and what causes it? *Spine (Phila Pa 1976)*. 2006 Aug;31(18):2151–61.
39. Moore RJ. The vertebral endplate: Disc degeneration, disc regeneration. *Eur Spine J*. 2006;15(SUPPL. 3):333–7.
40. Roberts S, Menage J, Urban JPG. Biochemical and Structural Properties of the Cartilage End-Plate and its Relation to the IVD. Vol. 21, *Spine*. 1989. p. 166–74.
41. Urban JPG, Smith S, Fairbank JCT. Nutrition of the intervertebral disc. *Spine (Phila Pa 1976)*. 2004 Dec;29(23):2700–9.
42. Taylor JR. Growth of human intervertebral discs and vertebral bodies. *J Anat*. 1975 Sep;120(Pt 1):49–68.
43. Bernick S, Cailliet R. Vertebral end-plate changes with aging of human vertebrae. *Spine (Phila Pa 1976)*. 1982;7(2):97–102.
44. Oda J, Tanaka H, Tsuzuki N. Intervertebral disc changes with aging of human cervical vertebra. From the neonate to the eighties. *Spine (Phila Pa 1976)*. 1988 Nov;13(11):1205–11.

45. Nachemson A, Lewin T, Maroudas A, Freeman MA. In vitro diffusion of dye through the end-plates and the annulus fibrosus of human lumbar inter-vertebral discs. *Acta Orthop Scand*. 1970;41(6):589–607.
46. Benneker LM, Heini PF, Alini M, Anderson SE, Ito K. 2004 Young Investigator Award Winner: vertebral endplate marrow contact channel occlusions and intervertebral disc degeneration. *Spine (Phila Pa 1976)*. 2005 Jan;30(2):167–73.
47. Dias MS. Normal and abnormal development of the spine. *Neurosurg Clin N Am*. 2007 Jul;18(3):415–29.
48. BICK EM, COPEL JW. Longitudinal growth of the human vertebra; a contribution to human osteogeny. *J Bone Joint Surg Am*. 1950 Oct;32 A(4):803–14.
49. BICK EM, COPEL JW. The ring apophysis of the human vertebra; contribution to human osteogeny. II. *J Bone Joint Surg Am*. 1951 Jul;33-A(3):783–7.
50. Antoniou J, Goudsouzian NM, Heathfield TF, Winterbottom N, Steffen T, Poole AR, et al. The human lumbar endplate. Evidence of changes in biosynthesis and denaturation of the extracellular matrix with growth, maturation, aging, and degeneration. *Spine (Phila Pa 1976)*. 1996 May;21(10):1153–61.
51. Rodriguez AG, Slichter CK, Acosta FL, Rodriguez-Soto AE, Burghardt AJ, Majumdar S, et al. Human disc nucleus properties and vertebral endplate permeability. *Spine (Phila Pa 1976)*. 2011 Apr;36(7):512–20.
52. Fields AJ, Sahli F, Rodriguez AG, Lotz JC. Seeing double: a comparison of microstructure, biomechanical function, and adjacent disc health between double- and single-layer vertebral endplates. *Spine (Phila Pa 1976)*. 2012 Oct;37(21):E1310-7.
53. Zhao F-D, Pollintine P, Hole BD, Adams MA, Dolan P. Vertebral fractures usually affect the cranial endplate because it is thinner and supported by less-dense trabecular bone. *Bone*. 2009 Feb;44(2):372–9.
54. Edwards WT, Zheng Y, Ferrara LA, Yuan HA. Structural features and thickness of the vertebral cortex in the thoracolumbar spine. *Spine (Phila Pa 1976)*. 2001 Jan;26(2):218–25.
55. Silva MJ, Wang C, Keaveny TM, Hayes WC. Direct and computed tomography thickness measurements of the human, lumbar vertebral shell and endplate. *Bone*. 1994;15(4):409–14.
56. Rodriguez AG, Rodriguez-Soto AE, Burghardt AJ, Berven S, Majumdar S, Lotz JC. Morphology of the human vertebral endplate. *J Orthop Res Off Publ Orthop Res Soc*. 2012 Feb;30(2):280–7.
57. Antonacci MD, Mody DR, Heggeness MH. Innervation of the human vertebral body: a histologic study. *J Spinal Disord*. 1998 Dec;11(6):526–31.
58. Fagan A, Moore R, Vernon Roberts B, Blumbergs P, Fraser R. ISSLS prize winner: The innervation of the intervertebral disc: a quantitative analysis. *Spine (Phila Pa 1976)*. 2003 Dec;28(23):2570–6.
59. Bailey JF, Liebenberg E, Degmetich S, Lotz JC. Innervation patterns of PGP 9.5-

- positive nerve fibers within the human lumbar vertebra. *J Anat.* 2011 Mar;218(3):263–70.
60. Laroche M. Intraosseous circulation from physiology to disease. *Jt bone spine.* 2002 May;69(3):262–9.
 61. Crock H V, Yoshizawa H. The blood supply of the lumbar vertebral column. *Clin Orthop Relat Res.* 1976;(115):6–21.
 62. Roberts S, Urban JP, Evans H, Eisenstein SM. Transport properties of the human cartilage endplate in relation to its composition and calcification. *Spine (Phila Pa 1976).* 1996 Feb;21(4):415–20.
 63. Ferguson S, Steffen T. Biomechanics of the aging spine. *Eur Spine J.* 2003;12:S97–103.
 64. Setton LA, Zhu W, Weidenbaum M, Ratcliffe A, Mow VC. Compressive properties of the cartilaginous end-plate of the baboon lumbar spine. *J Orthop Res Off Publ Orthop Res Soc.* 1993 Mar;11(2):228–39.
 65. Arjmand N, Plamondon A, Shirazi-Adl A, Parnianpour M, Larivière C. Predictive equations for lumbar spine loads in load-dependent asymmetric one- and two-handed lifting activities. *Clin Biomech (Bristol, Avon).* 2012 Jul;27(6):537–44.
 66. Wilke HJ, Neef P, Caimi M, Hoogland T, Claes LE. New in vivo measurements of pressures in the intervertebral disc in daily life. *Spine (Phila Pa 1976).* 1999 Apr;24(8):755–62.
 67. Sato K, Kikuchi S, Yonezawa T. In vivo intradiscal pressure measurement in healthy individuals and in patients with ongoing back problems. *Spine (Phila Pa 1976).* 1999 Dec;24(23):2468–74.
 68. Urban JPG, Holm S, Maroudas A, Nachemson A. Nutrition of the Intervertebral Disc. Effect of Fluid Flow on Solute Transport. *Clin Orthop Relat Res.* 1982;170:296–302.
 69. Urban MR, Fairbank JC, Etherington PJ, Loh FRCA L, Winlove CP, Urban JP. Electrochemical measurement of transport into scoliotic intervertebral discs in vivo using nitrous oxide as a tracer. *Spine (Phila Pa 1976).* 2001;26(8):984–90.
 70. Bartels EM, Fairbank JC, Winlove CP, Urban JP. Oxygen and lactate concentrations measured in vivo in the intervertebral discs of patients with scoliosis and back pain. *Spine (Phila Pa 1976).* 1998 Jan;23(1):1–7; discussion 8.
 71. Peshkovsky AS, Peshkovsky SL, Bystryak S. Scalable high-power ultrasonic technology for the production of translucent nanoemulsions. *Chem Eng Process Process Intensif [Internet].* 2013;69:77–82. Available from: <http://dx.doi.org/10.1016/j.cep.2013.02.010>
 72. Brown RA. The Mathematics of Three N-Localizers Used Together for Stereotactic Neurosurgery. *Cureus.* 2015 Oct;7(10):e341.
 73. Elliott JC, Dover SD. X-ray microtomography. *J Microsc.* 1982 May;126(Pt 2):211–3.

74. Flannery BP, Deckman HW, Roberge WG, D'Amico KL. Three-Dimensional X-ray Microtomography. *Science*. 1987 Sep;237(4821):1439–44.
75. Feldkamp LA, Davis LC, Kress JW. Practical cone-beam algorithm. *J Opt Soc Am*. 1984;1(6):612–9.
76. Ritman EL. Current status of developments and applications of micro-CT. *Annu Rev Biomed Eng*. 2011;13:531–52.
77. Choi J-Y, Lee J-M, Sirlin CB. CT and MR imaging diagnosis and staging of hepatocellular carcinoma: part II. Extracellular agents, hepatobiliary agents, and ancillary imaging features. *Radiology*. 2014 Oct;273(1):30–50.
78. Fournier DE, Norley CJD, Pollmann SI, Bailey CS, Al Helal F, Willmore KE, et al. Ectopic spinal calcification associated with diffuse idiopathic skeletal hyperostosis (DISH): A quantitative micro-ct analysis. *J Orthop Res Off Publ Orthop Res Soc*. 2019 Mar;37(3):717–26.
79. Carter R. MRI vs. CT scan; diagnosing spine & neck injuries & degenerative diseases. [Internet]. JosephSpine Institute. 2018 [cited 2022 Oct 11]. Available from: <https://josephspine.com/mri-vs-ct-scan-diagnosing-spine-neck-injuries-degenerative-diseases/>
80. Coppes MH, Marani E, Thomeer RT, Groen GJ. Innervation of “painful” lumbar discs. *Spine (Phila Pa 1976)*. 1997 Oct;22(20):2342–50.
81. Peng B, Hao J, Hou S, Wu W, Jiang D, Fu X, et al. Possible pathogenesis of painful intervertebral disc degeneration. *Spine (Phila Pa 1976)*. 2006 Mar;31(5):560–6.
82. Halvorson KG, Kubota K, Sevcik MA, Lindsay TH, Sotillo JE, Ghilardi JR, et al. A blocking antibody to nerve growth factor attenuates skeletal pain induced by prostate tumor cells growing in bone. *Cancer Res*. 2005 Oct;65(20):9426–35.
83. Weinstein J, Claverie W, Gibson S. The pain of discography. *Spine (Phila Pa 1976)*. 1988 Dec;13(12):1344–8.
84. Peng B, Chen J, Kuang Z, Li D, Pang X, Zhang X. Diagnosis and surgical treatment of back pain originating from endplate. *Eur spine J Off Publ Eur Spine Soc Eur Spinal Deform Soc Eur Sect Cerv Spine Res Soc*. 2009 Jul;18(7):1035–40.
85. Heggeness MH, Doherty BJ. Discography causes end plate deflection. *Spine (Phila Pa 1976)*. 1993 Jun;18(8):1050–3.
86. Hebelka H, Gaulitz A, Nilsson A, Holm S, Hansson T. The transfer of disc pressure to adjacent discs in discography: a specificity problem? *Spine (Phila Pa 1976)*. 2010 Sep;35(20):E1025-9.
87. Esses SI, Moro JK. Intraosseous vertebral body pressures. *Spine (Phila Pa 1976)*. 1992 Jun;17(6 Suppl):S155-9.
88. Bonica JJ. Editorial The need of a taxonomy. *Pain*. 1979;6:247–52.
89. Merskey H. Pain terms: a list with definitions and notes on usage. Recommended

- by the IASP Subcommittee on Taxonomy. *Pain*. 1979;6 3:249.
90. Sherrington CS. Observations on the scratch-reflex in the spinal dog. *J Physiol*. 1906 Mar;34(1-2):1-50.
 91. Ji R-R, Kohno T, Moore KA, Woolf CJ. Central sensitization and LTP: do pain and memory share similar mechanisms? *Trends Neurosci*. 2003 Dec;26(12):696-705.
 92. Woolf CJ, Salter MW. Neuronal plasticity: increasing the gain in pain. *Science*. 2000 Jun;288(5472):1765-9.
 93. Woolf CJ, King AE. Subthreshold components of the cutaneous mechanoreceptive fields of dorsal horn neurons in the rat lumbar spinal cord. *J Neurophysiol*. 1989 Oct;62(4):907-16.
 94. Woolf CJ, King AE. Dynamic alterations in the cutaneous mechanoreceptive fields of dorsal horn neurons in the rat spinal cord. *J Neurosci Off J Soc Neurosci*. 1990 Aug;10(8):2717-26.
 95. Melzack R, Wall PD. Pain mechanisms: A new theory. *Science* (80-). 1965 Nov;150(3699):971-9.
 96. Melzack R, Wall P. *The Challenge of Pain*. New York: Penguin; 1988.
 97. Bonica J. *The management of pain*. Philadelphia: Lea and Fabiger; 1953.
 98. Latremoliere A, Woolf CJ. Central sensitization: a generator of pain hypersensitivity by central neural plasticity. *J pain*. 2009 Sep;10(9):895-926.
 99. Marshall H. *Pain, Pleasure and Aesthetics*. London: Macmillan; 1894.
 100. Dueñas M, Ojeda B, Salazar A, Mico JA, Failde I. A review of chronic pain impact on patients, their social environment and the health care system. *J Pain Res*. 2016;9:457-67.
 101. Cuomo A, Bimonte S, Forte CA, Botti G, Cascella M. Multimodal approaches and tailored therapies for pain management: The trolley analgesic model. Vol. 12, *Journal of Pain Research*. New Zealand; 2019. p. 711-4.
 102. Treede RD, Rief W, Barke A, Aziz Q, Bennett MI, Benoliel R, et al. Chronic pain as a symptom or a disease: The IASP Classification of Chronic Pain for the International Classification of Diseases (ICD-11). *Pain*. 2019 Jan;160(1):19-27.
 103. Meisingset I, Vasseljen O, Vøllestad NK, Robinson HS, Woodhouse A, Engebretsen KB, et al. Novel approach towards musculoskeletal phenotypes. *Eur J Pain (United Kingdom)*. 2020 May;24(5):921-32.
 104. Panella L, Rinonapoli G, Coaccioli S. Where should analgesia lead to? Quality of life and functional recovery with tapentadol. *J Pain Res*. 2019;12:1561-7.
 105. Waddell G. *A New Clinical Model for the Treatment of Low-Back Pain*. 1987. p. 632-44.
 106. Pincus T, Kent P, Bronfort G, Loisel P, Pransky G, Hartvigsen J. Twenty-five years with the biopsychosocial model of low back pain - Is it time to celebrate? *A*

- report from the twelfth international forum for primary care research on low back pain. *Spine (Phila Pa 1976)*. 2013 Nov;38(24):2118–23.
107. Engel GL. The need for a new medical model: a challenge for biomedicine. *Science*. 1977 Apr;196(4286):129–36.
 108. Lall MP, Restrepo E. The biopsychosocial model of low back pain and patient-centered outcomes following lumbar fusion. *Orthop Nurs*. 2017;36(3):213–21.
 109. Cormack B, Stilwell P, Coninx S, Gibson J. The biopsychosocial model is lost in translation: from misrepresentation to an enactive modernization. *Physiother Theory Pract* [Internet]. 2022;00(00):1–16. Available from: <https://doi.org/10.1080/09593985.2022.2080130>
 110. Chan D, Karppinen JI, Ho DWHH, Leong JCY, Cheah KSEE, Luk KDKK, et al. Structural lesions detected by magnetic resonance imaging in the spine of patients with spondyloarthritis - Definitions, assessment system, and reference image set. *Spine (Phila Pa 1976)*. 2017 Feb;17(1):1–7.
 111. Zehra U, Cheung JPY, Bow C, Lu W, Samartzis D. Multidimensional vertebral endplate defects are associated with disc degeneration, modic changes, facet joint abnormalities, and pain. *J Orthop Res*. 2019;37(5):1080–9.
 112. Kaprio J, Koskenvuo M, Langinvainio H, Romanov K, Sarna S, Rose RJ. Genetic influences on use and abuse of alcohol: a study of 5638 adult Finnish twin brothers. *Alcohol Clin Exp Res*. 1987 Aug;11(4):349–56.
 113. Videman T, Battié MC, Gibbons LE, Gill K. A new quantitative measure of disc degeneration. *Spine J*. 2017;17(5):746–53.
 114. Fortin M, Videman T, Gibbons LE, Battié MC. Paraspinal muscle morphology and composition: a 15-yr longitudinal magnetic resonance imaging study. *Med Sci Sports Exerc*. 2014;46(5):893–901.
 115. Crock H V. Internal disc disruption. A challenge to disc prolapse fifty years on. *Spine (Phila Pa 1976)*. 1986;11(6):650–3.
 116. Kuslich SD, Ulstrom CL, Michael CJ. The tissue origin of low back pain and sciatica: a report of pain response to tissue stimulation during operations on the lumbar spine using local anesthesia. *Orthop Clin North Am*. 1991 Apr;22(2):181–7.
 117. Wang Y, Videman T, Battie MC. Morphometrics and lesions of vertebral end plates are associated with lumbar disc degeneration: evidence from cadaveric spines. *J Bone Joint Surg Am*. 2013 Mar;95(5):e26.
 118. Wang Y, Videman T, Battié MC. Modic changes: prevalence, distribution patterns, and association with age in white men. *Spine J* [Internet]. 2012/04/18. 2012 May;12(5):411–6. Available from: <https://pubmed.ncbi.nlm.nih.gov/22515998>
 119. Abbas J, Slon V, Stein D, Peled N, HersHKovitz I, Hamoud K. In the quest for degenerative lumbar spinal stenosis etiology: The Schmorl's nodes model. *BMC Musculoskelet Disord*. 2017;18(1):1–7.
 120. Bailey JF, Fields AJ, Ballatori A, Cohen D. The relationship between endplate

- pathology and patient-reported symptoms for chronic low back pain depends on lumbar paraspinal muscle quality. *SPINE An Int J study spine*. 2019;Publish Ah.
121. Chen L, Battié MC, Yuan Y, Yang G, Chen Z, Wang Y. Lumbar vertebral endplate defects on magnetic resonance images: prevalence, distribution patterns, and associations with back pain. *Spine J*. 2020;20(3):352–60.
 122. Cheung KMC, Karppinen J, Chan D, Ho DWH, Song Y-Q, Sham P, et al. Prevalence and Pattern of Lumbar Magnetic Resonance Imaging Changes in a Population Study of One Thousand Forty-Three Individuals. *Spine (Phila Pa 1976)*. 2009;34(9):934–40.
 123. Zehra U, Cheung JPY, Bow C, Lu W, Samartzis D. Multidimensional vertebral endplate defects are associated with disc degeneration, modic changes, facet joint abnormalities, and pain. *J Orthop Res*. 2019;1080–9.
 124. Sharma A, Parsons M, Pilgram T. Temporal Interactions of Degenerative Changes in Individual Components of the Lumbar Intervertebral Discs. *Spine (Phila Pa 1976)*. 2011;36(21):1794–800.
 125. Iwamoto J, Abe H, Tsukimura Y, Wakano K. Relationship between radiographic abnormalities of lumbar spine and incidence of low back pain in high school rugby players : a prospective study. *Scand J Med Sci Sport*. 2005;15:163–8.
 126. Hamanishi C, Kawabata T YT et al. Schmorl's nodes on magnetic resonance imaging. Their incidence and clinical relevance. *Spine (Phila Pa 1976)*. 1994;19:450–3.
 127. Shamliyan T, Kane RL, Dickinson S. A systematic review of tools used to assess the quality of observational studies that examine incidence or prevalence and risk factors for diseases. *J Clin Epidemiol*. 2010;63(10):1061–70.
 128. Raastad J, Reiman M, Coeytaux R, Ledbetter L, Goode AP. The association between lumbar spine radiographic features and low back pain: A systematic review and meta-analysis. *Semin Arthritis Rheum*. 2015;44(5):571–85.
 129. Viswanathan M, Berkman ND. Development of the RTI item bank on risk of bias and precision of observational studies. *J Clin Epidemiol [Internet]*. 2012;65(2):163–78. Available from: <http://dx.doi.org/10.1016/j.jclinepi.2011.05.008>
 130. Deeks J, Higgins J, Altman D. Analyzing data and undertaking meta-analyses. In: Higgins J, Green S, editors *Cochrane handbook for systematic reviews of intervention version 500*. Chichester: Wiley; 2008.
 131. Guyatt G, Oxman AD, Akl EA, Kunz R, Vist G, Brozek J, et al. GRADE guidelines: 1. Introduction - GRADE evidence profiles and summary of findings tables. *J Clin Epidemiol*. 2011;64(4):383–94.
 132. Munir S, Freidin MB, Rade M, Määttä J, Livshits G, Williams FMK. Endplate Defect Is Heritable, Associated With Low Back Pain and Triggers Intervertebral Disc Degeneration: A Longitudinal Study From TwinsUK. *Spine (Phila Pa 1976)*. 2018;43(21):1496–501.

133. Buttermann GR, Mullin WJ. Pain and disability correlated with disc degeneration via magnetic resonance imaging in scoliosis patients. *Eur spine J Off Publ Eur Spine Soc Eur Spinal Deform Soc Eur Sect Cerv Spine Res Soc*. 2008 Feb;17(2):240–9.
134. Nagashima M, Abe H, Amaya K, Matsumoto H, Yanaihara H, Nishiwaki Y, et al. Risk factors for lumbar disc degeneration in High School American Football Players: A Prospective 2-Year Follow-up Study. *Am J Sports Med*. 2013;41(9):2059–64.
135. Luoma K, Vehmas T, Kerttula L, Grönblad M, Rinne E. Chronic low back pain in relation to Modic changes, bony endplate lesions, and disc degeneration in a prospective MRI study. *Eur Spine J*. 2016;25(9):2873–81.
136. Kjaer P, Leboeuf-Yde C, Korsholm L, Sorensen JS, Bendix T. Magnetic resonance imaging and low back pain in adults: a diagnostic imaging study of 40-year-old men and women. *Spine (Phila Pa 1976)* [Internet]. 2005;30(10):1173–80. Available from: <http://www.ncbi.nlm.nih.gov/pubmed/15897832>
137. Takatalo J, Karppinen J, Niinimäki J, Taimela S, Mutanen P, Sequeiros RB, et al. Association of Modic Changes, Schmorl’s Nodes, Spondylolytic Defects, High-Intensity Zone Lesions, Disc Herniations, and Radial Tears With Low Back Symptom Severity Among Young Finnish Adults. *Spine (Phila Pa 1976)*. 2012;37(14):1231–9.
138. Videman T, Nurminen M, Troup J. Lumbar spinal pathology in cadaveric materials in relation to history of back pain, occupation and physical loading. *Sine*. 1990;15(8):728–40.
139. Miura K, Morita O, Hirano T, Watanabe K, Fujisawa J, Kondo N, et al. Prevalence of and factors associated with dysfunctional low back pain in patients with rheumatoid arthritis. *Eur Spine J* [Internet]. 2019;(0123456789). Available from: <https://doi.org/10.1007/s00586-019-05938-x>
140. Kanna RM, Shetty AP, Rajasekaran S. Patterns of lumbar disc degeneration are different in degenerative disc disease and disc prolapse magnetic resonance imaging analysis of 224 patients. *Spine J* [Internet]. 2014;14(2):300–7. Available from: <http://dx.doi.org/10.1016/j.spinee.2013.10.042>
141. Teraguchi M, Yoshimura N, Hashizume H, Muraki S, Yamada H, Oka H, et al. The association of combination of disc degeneration, end plate signal change, and Schmorl node with low back pain in a large population study: The Wakayama Spine Study. *Spine J* [Internet]. 2015;15(4):622–8. Available from: <http://dx.doi.org/10.1016/j.spinee.2014.11.012>
142. Inaoka M, Yamazaki Y, Hosono N, Tada K, Yonenobu K. Radiographic analysis of lumbar spine for low-back pain in the general population. *Arch Orthop Trauma Surg*. 2000;120(7–8):380–5.
143. Rose PS, Ahn NU, Levy HP, Ahn UM, Davis J, Liberfarb RM, et al. Thoracolumbar spinal abnormalities in Stickler syndrome. *Spine (Phila Pa 1976)*. 2001 Feb;26(4):403–9.

144. Videman T, Battié MC, Gibbons LE, Maravilla K, Manninen H, Kaprio J. Associations between back pain history and lumbar MRI findings. *Spine (Phila Pa 1976)*. 2003;28(6):582–8.
145. Sward L, Hellstrom M, Jacobsson B, Peterson L. Back pain and radiologic changes in the thoraco-lumbar spine of athletes. Vol. 15, *Spine*. 1990. p. 124–9.
146. Iwamoto J, Abe H, Tsukimura Y, Wakano K. Relationship between Radiographic Abnormalities of Lumbar Spine and Incidence of Low Back Pain in High School and College Football Players. *Am J Sports Med [Internet]*. 2004;32(3):781–6. Available from: <http://journals.sagepub.com/doi/10.1177/0363546503261721>
147. Kauppila LI, McAlindon T, Evans S, Wilson PWF, Kiel D, Felson DT. Disc degeneration/back pain and calcification of the abdominal aorta: A 25-year follow-up study in Framingham. Vol. 22, *Spine*. 1997. p. 1642–9.
148. Ogon M, Riedl-Huter C, Sterzinger W, Krismer M, Spratt KF, Wimmer C. Radiologic abnormalities and low back pain in elite skiers. *Clin Orthop Relat Res*. 2001;(390):151–62.
149. Vassilaki M, Hurwitz E. Insights in Public Health: Perspectives on Pain in the Low Back and Neck: Global Burden, Epidemiology, and Management. *Hawaii J Med Public Heal*. 2014;73(4):122–6.
150. Buchbinder R, Blyth F, March, LM Brooks P, Woolf A, Hoy D. Placing the global burden of low back pain in context. *Best Pr Res Clin Rheumatol*. 2013;27(5(5):575–89.
151. Adams M, Dolan P, Luo J, Pollintine P, Landham P, Stefanakis M. Intervertebral disc decompression following endplate damage: implications for disc degeneration depend on spinal level and age. *Spine (Phila Pa 1976)*. 2013;38:1473–81.
152. Eubanks JD, Lee MJ, Cassinelli E AN. Does lumbar facet arthrosis precede disc degeneration? A postmortem study. *Clin Orthop Relat Res*. 2007;464:184–9.
153. Brant-Zawadzki M, Jensen M, Obuchowski N, Ross J, Modic M. Interobserver and intraobserver variability in interpretation of lumbar disc abnormalities. *Spine (Phila Pa 1976)*. 1995;20:1257–64.
154. Brayda-Bruno M, Albano D, Cannella G, Galbusera F, Zerbi A. Endplate lesions in the lumbar spine: a novel MRI-based classification scheme and epidemiology in low back pain patients. *Eur Spine J [Internet]*. 2018 Nov 10 [cited 2019 Feb 22];27(11):2854–61. Available from: <http://link.springer.com/10.1007/s00586-018-5787-6>
155. Ellis D, Virtanen T, Plumbley MD, Raj B. Future perspective. *Comput Anal Sound Scenes Events*. 2017;1(1):401–15.
156. Li Q, Gavrielides MA, Nagaraja S, Hagen MJ, Zeng R, Myers KJ, et al. A micro CT based tumor volume reference standard for phantom experiments. In: *Imaging and Applied Optics [Internet]*. Optical Society of America; 2013. p. QW1G.4. Available from: <http://www.osapublishing.org/abstract.cfm?URI=QMI-2013-QW1G.4>

157. Senck S, Trieb K, Kastner J, Hofstaetter SG, Lugmayr H, Windisch G. Visualization of intervertebral disc degeneration in a cadaveric human lumbar spine using microcomputed tomography. *J Anat.* 2020;236(2):243–51.
158. Wang Y, Battié MC, Boyd SK, Videman T. The osseous endplates in lumbar vertebrae: Thickness, bone mineral density and their associations with age and disk degeneration. *Bone [Internet].* 2011;48(4):804–9. Available from: <http://dx.doi.org/10.1016/j.bone.2010.12.005>
159. Wang Y, Boyd SK, Battié MC, Yasui Y, Videman T. Is greater lumbar vertebral BMD associated with more disk degeneration? A study using μ CT and discography. *J Bone Miner Res.* 2011;26(11):2785–91.
160. Herbert RD. Cohort studies of aetiology and prognosis: They're different. *J Physiother.* 2014;60(4):241–4.
161. Hofmann UK, Keller RL, Gesicki M, Walter C, Mittag F. Interobserver reliability when classifying MR imaging of the lumbar spine: Written instructions alone do not suffice. *Magn Reson Med Sci.* 2020;19(3):207–15.
162. Lawan A, Crites Videman J, Battié MC. The association between vertebral endplate structural defects and back pain: a systematic review and meta-analysis. *Eur spine J Off Publ Eur Spine Soc Eur Spinal Deform Soc Eur Sect Cerv Spine Res Soc.* 2021 Sep;30(9):2531–48.
163. Kuisma M, Karppinen J, Haapea M, Lammentausta E, Niinimäki J, Tervonen O. Modic changes in vertebral endplates: a comparison of MR imaging and multislice CT. *Skeletal Radiol.* 2009 Feb;38(2):141–7.
164. Donescu OS, Battie MC, Videman T. The influence of magnetic resonance imaging findings of degenerative disease on dual-energy X-ray absorptiometry measurements in middle-aged men. *Acta Radiol.* 2007 Mar;48(2):193–9.
165. Hansson T, Roos B. The amount of bone mineral and Schmorl's nodes in lumbar vertebrae. *Spine (Phila Pa 1976).* 1983;8(3):266–71.
166. Harada GK, Tao Y, Louie PK, Basques BA, Galbusera F, Niemeyer F, et al. Cervical spine MRI phenotypes and prediction of pain, disability and adjacent segment degeneration/disease after ACDF. *J Orthop Res.* 2021;39(3):657–70.
167. Samartzis D, Mok F, Karppinen J, Luk K, Cheung K. Is the Morphology and Size of Schmorl's Nodes of the Lumbar Spine Related to Severity of Disk Degeneration? *Glob Spine J.* 2012;02(S 01):1319934.
168. Zehra U, Bow C, Lotz JC, Williams FMK, Rajasekaran S, Karppinen J, et al. Structural vertebral endplate nomenclature and etiology: a study by the ISSLS Spinal Phenotype Focus Group. *Eur Spine J.* 2018;27(1):2–12.
169. Hou Y, Luo Z. A study on the structural properties of the lumbar endplate: histological structure, the effect of bone density, and spinal level. *Spine (Phila Pa 1976).* 2009 May;34(12):E427-33.
170. Boateng GO, Neilands TB, Frongillo EA, Melgar-Quiñonez HR, Young SL. Best Practices for Developing and Validating Scales for Health, Social, and Behavioral

- Research: A Primer. *Front Public Heal.* 2018;6(June):1–18.
171. Karabulut Ö, Tuncer MC, Karabulut Z, Açıköz A, Hatipoğlu ES, Akkuş Z. Relationship between radiographic features and bone mineral density in elderly men. *Folia Morphol (Warsz)* [Internet]. 2010;69(3):170–6. Available from: <http://www.embase.com/search/results?subaction=viewrecord&from=export&id=L359413957>
 172. Tao Y, Galbusera F, Niemeyer F, Samartzis D, Vogele D, Wilke HJ. Radiographic cervical spine degenerative findings: a study on a large population from age 18 to 97 years. *Eur Spine J* [Internet]. 2021;30(2):431–43. Available from: <https://doi.org/10.1007/s00586-020-06615-0>
 173. Lee SH, Son DW, Lee JS, Sung SK, Lee SW, Song GS. Relationship between endplate defects, modic change, facet joint degeneration, and disc degeneration of cervical spine. *Neurospine.* 2020;17(2):443–52.
 174. Modic MT, Ross JS. Lumbar degenerative disk disease. *Radiology.* 2007 Oct;245(1):43–61.
 175. Walsh AJL, Lotz JC. Biological response of the intervertebral disc to dynamic loading. *J Biomech.* 2004 Mar;37(3):329–37.
 176. Rajasekaran S, Babu JN, Arun R, Armstrong BRW, Shetty AP, Murugan S. ISSLS prize winner: A study of diffusion in human lumbar discs: a serial magnetic resonance imaging study documenting the influence of the endplate on diffusion in normal and degenerate discs. *Spine (Phila Pa 1976).* 2004 Dec;29(23):2654–67.
 177. Hauger O, Cotten A, Chateil J, Borg O, Moinard M, Diard F. Giant cystic Schmorl's nodes: imaging findings in six patients. *Am J Roentgenol.* 2001;176:969–72.
 178. Altman DG. *Practical statistics for medical research.* London: Chapman & Hall/CRC press.; 1990.
 179. Zehra U, Flower L, Robson-Brown K, Adams MA, Dolan P. Defects of the vertebral end plate: implications for disc degeneration depend on size. *Spine J* [Internet]. 2017;17(5):727–37. Available from: <http://dx.doi.org/10.1016/j.spinee.2017.01.007>
 180. Dar G, Peleg S, Masharawi Y, Steinberg N, May H, HersHKovitz I. Demographical Aspects of Schmorl Nodes. *Spine (Phila Pa 1976).* 2009;34(9):E312–5.
 181. Mok FPS, Samartzis D, Ebhc D, Karppinen J, Luk KDK, Orth M, et al. Prevalence, determinants, and association of Schmorl nodes of the lumbar spine with disc degeneration: a population-based study of 2449 individuals. *Spine (Phila Pa 1976)* [Internet]. 2010;35(21):1944–52. Available from: <http://www.ncbi.nlm.nih.gov/pubmed/20838277>
 182. Dar G, Masharawi Y, Peleg S, Steinberg N, May H, Medlej B, et al. Schmorl's nodes distribution in the human spine and its possible etiology. *Eur Spine J.* 2010;19(4):670–5.
 183. Hanımoğlu H, Çevik S, Yılmaz H, Kaplan A, Çalış F, Katar S, et al. Effects of

- Modic Type 1 Changes in the Vertebrae on Low Back Pain. *World Neurosurg.* 2019;121:e426–32.
184. Jim JJT, Noponen-Hietala N, Cheung KMC, Ott J, Karppinen J, Sahraravand A, et al. The TRP2 allele of COL9A2 is an age-dependent risk factor for the development and severity of intervertebral disc degeneration. *Spine (Phila Pa 1976)*. 2005;30(24):2735–42.
 185. Li Y, Samartzis D, Campbell DD, Cherny SS, Cheung KMC, Luk KDK, et al. Two subtypes of intervertebral disc degeneration distinguished by large-scale population-based study. *Spine J [Internet]*. 2016;16(9):1079–89. Available from: <http://dx.doi.org/10.1016/j.spinee.2016.04.020>
 186. Lv B, Yuan J, Ding H, Wan B, Jiang Q, Luo Y, et al. Relationship between Endplate Defects, Modic Change, Disc Degeneration, and Facet Joint Degeneration in Patients with Low Back Pain. *Biomed Res Int.* 2019;2019.
 187. van den Heuvel MM, Oei EHG, Renkens JJM, Bierma-Zeinstra SMA, van Middelkoop M. Structural spinal abnormalities on MRI and associations with weight status in a general pediatric population. *Spine J [Internet]*. 2021;21(3):465–76. Available from: <https://doi.org/10.1016/j.spinee.2020.10.003>
 188. Williams FMK, Manek NJ, Sambrook PN, Spector TD, MacGregor AJ. Schmorl's nodes: Common, highly heritable, and related to lumbar disc disease. *Arthritis Care Res.* 2007;57(5):855–60.
 189. Tan CI, Song S, Edmondston SJ, Singer KP. Pattern of thoracic disc degeneration from MRI: Age, Gender and Spinal level influences. *J Musculoskelet Res.* 2001;5(4):269–78.
 190. Grant JP, Oxland TR, Dvorak MF. Mapping the structural properties of the lumbosacral vertebral endplates. *Spine (Phila Pa 1976)*. 2001 Apr;26(8):889–96.
 191. Wong SHJ, Chiu KY, Yan CH. Osteophytes. *J Orthop Surg.* 2016;24(3):403–10.
 192. Xu L, Chu B, Feng Y, Xu F, Zou YF. Modic changes in lumbar spine: Prevalence and distribution patterns of end plate oedema and end plate sclerosis. *Br J Radiol.* 2016;89(1060):1–7.
 193. Arana E, Royuela A, Kovacs FM, Estremera A, Sarasibar H, Amengual G, et al. Lumbar Spine : Agreement in the Interpretation of 1 . 5-T MR Images by Using the Nordic Modic Consensus Purpose : Methods : Results : Imaging [Internet]. 2010;254(3):809–17. Available from: http://www.ncbi.nlm.nih.gov/entrez/query.fcgi?cmd=Retrieve&db=PubMed&dopt=Citation&list_uids=20123897
 194. Khoury MJ, Beaty TH, Cohen BH. Study of Genetic Factors in Diseases. In *Fundamentals of Genetic Epidemiology*. New York: Oxford University press.; 1993. 130 p.
 195. Ala-Kokko L. Genetic risk factors for lumbar disc disease. *Ann Med.* 2002;34(1):42–7.
 196. Hamanishi C, Kawabata T, Yosii T, Tanaka S. Schmorl's nodes on magnetic

- resonance imaging. Their incidence and clinical relevance. *Spine (Phila Pa 1976)*. 1994 Feb;19(4):450–3.
197. Martel W, Seeger JF, Wicks JD, Washburn RL. Traumatic lesions of the discovertebral junction in the lumbar spine. *AJR Am J Roentgenol*. 1976 Sep;127(3):457–64.
 198. Li R, Wang Z, Ma L, Yang D, Xie D, Zhang B, et al. Lumbar Vertebral Endplate Defects on Magnetic Resonance Imaging in Degenerative Spondylolisthesis: Novel Classification, Characteristics, and Correlative Factor Analysis. *World Neurosurg* [Internet]. 2020;141:e423–30. Available from: <https://doi.org/10.1016/j.wneu.2020.05.163>
 199. Baker JD, Sayari AJ, Harada GK, Tao Y, Louie PK, Basques BA, et al. The Modic-endplate-complex phenotype in cervical spine patients: Association with symptoms and outcomes. *J Orthop Res*. 2021;(December 2020).
 200. Rachbauer F, Sterzinger W, Eibl G. Radiographic abnormalities in the thoracolumbar spine of young elite skiers. *Am J Sports Med* [Internet]. 2001;29(4 CC-Musculoskeletal):446-449. Available from: <https://www.cochranelibrary.com/central/doi/10.1002/central/CN-00373366/full>
 201. Cook DJ, Yeager MS, Cheng BC. Range of motion of the intact lumbar segment: A multivariate study of 42 lumbar spines. *Int J Spine Surg* [Internet]. 2015;9:1–8. Available from: <http://dx.doi.org/10.14444/2005>
 202. Korpi J, Poussa M, Heliövaara M. Radiographic mobility of the lumbar spine and its relation to clinical back motion. *Scand J Rehabil Med*. 1988;20(2):71–6.
 203. Zukowski LA, Falsetti AB, Tillman MD. The influence of sex, age and BMI on the degeneration of the lumbar spine. *J Anat*. 2012 Jan;220(1):57–66.
 204. O'Neill TW, McCloskey E V, Kanis JA, Bhalla AK, Reeve J, Reid DM, et al. The distribution, determinants, and clinical correlates of vertebral osteophytosis: a population based survey. *J Rheumatol*. 1999 Apr;26(4):842–8.
 205. Chanapa P, Yoshiyuki T, Mahakkanukrauh P. Distribution and length of osteophytes in the lumbar vertebrae and risk of rupture of abdominal aortic aneurysms: a study of dry bones from Chiang Mai, Thailand. *Anat Cell Biol*. 2014 Sep;47(3):157–61.
 206. Bruno AG, Burkhart K, Allaire B, Anderson DE, Boussein ML. Spinal Loading Patterns From Biomechanical Modeling Explain the High Incidence of Vertebral Fractures in the Thoracolumbar Region. *J Bone Miner Res*. 2017;32(6):1282–90.
 207. Rohlmann A, Pohl D, Bender A, Graichen F, Dymke J, Schmidt H, et al. Activities of everyday life with high spinal loads. *PLoS One*. 2014;9(5):1–9.
 208. Fortin M, Dobrescu O, Jarzem P, Ouellet J, Weber MH. Quantitative Magnetic Resonance Imaging Analysis of the Cervical Spine Extensor Muscles: Intrarater and Interrater Reliability of a Novice and an Experienced Rater. *Asian Spine J*. 2018 Feb;12(1):94–102.
 209. Stabler A, Weiss M, Gartner C, Brossmann J, Reiser F. MR Imaging Intraosseous

(Schmorl's. *Am J Roentgenol.* 1997;168(April):933–8.

210. Kwan AC, Pourmorteza A, Stutman D, Bluemke DA, Lima JAC. Next-generation hardware advances in CT: Cardiac applications. *Radiology.* 2021;298(1):3–17.
211. Park JE, Cheong EN, Jung DE, Shim WH, Lee JS. Utility of 7 Tesla Magnetic Resonance Imaging in Patients With Epilepsy: A Systematic Review and Meta-Analysis. *Front Neurol.* 2021;12(March):1–11.

Appendices

Appendix A:- Table 0-1: Search strategy for each database

1. SCOPUS:

```

(((( "end plate" OR "endplate" OR "schmorl*
node*" ))) AND ((((((( lesion* ) OR defect* ) OR abnormal* ) OR sclerosis ) O
R calcification* ) OR irregular* ) OR erosion* ) ) AND ( ( classif* OR measure* OR
psychometric* OR reliab* OR valid* OR accura* OR reproducib* ) ) ) AND ( EXC
LUDE ( DOCTYPE , "re" ) OR EXCLUDE ( DOCTYPE , "ch" ) OR EXCLUDE ( DOC
TYPE , "bk" ) ) AND ( EXCLUDE ( SUBJAREA , "ENGI" ) OR EXCLUDE ( SUBJAR
EA , "PHAR" ) OR EXCLUDE ( SUBJAREA , "IMMU" ) OR EXCLUDE ( SUBJAREA
, "AGRI" ) OR EXCLUDE ( SUBJAREA , "MATE" ) OR EXCLUDE ( SUBJAREA , "P
HYS" ) OR EXCLUDE ( SUBJAREA , "COMP" ) OR EXCLUDE ( SUBJAREA , "ART
S" ) OR EXCLUDE ( SUBJAREA , "CHEM" ) OR EXCLUDE ( SUBJAREA , "VETE"
) OR EXCLUDE ( SUBJAREA , "MATH" ) OR EXCLUDE ( SUBJAREA , "SOCI" ) O
R EXCLUDE ( SUBJAREA , "ENVI" ) OR EXCLUDE ( SUBJAREA , "ENER" ) OR E
XCLUDE ( SUBJAREA , "EART" ) OR EXCLUDE ( SUBJAREA , "DENT" ) OR EXC
LUDE ( SUBJAREA , "DECI" ) OR EXCLUDE ( SUBJAREA , "BUSI" ) ) AND (
EXCL
UDE ( EXACTSRCTITLE , "Muscle And
Nerve" ) OR EXCLUDE ( EXACTSRCTITLE , "Muscle
Nerve" ) OR EXCLUDE ( EXACTSRCTITLE , "Journal Of
Neuroscience" ) OR EXCLUDE ( EXACTSRCTITLE , "Neuroscience" ) OR EXCLUD
E ( EXACTSRCTITLE , "Experimental
Neurology" ) OR EXCLUDE ( EXACTSRCTITLE , "Journal Of The Neurological
Sciences" ) OR EXCLUDE ( EXACTSRCTITLE , "Neurology" ) OR EXCLUDE ( EXA
CTSRCTITLE , "Journal Of
Neurophysiology" ) OR EXCLUDE ( EXACTSRCTITLE , "Brain
Research" ) OR EXCLUDE ( EXACTSRCTITLE , "Annals Of
Neurology" ) OR EXCLUDE ( EXACTSRCTITLE , "Journal Of
Physiology" ) OR EXCLUDE ( EXACTSRCTITLE , "Acta
Neuropathologica" ) OR EXCLUDE ( EXACTSRCTITLE , "Neuromuscular
Disorders" ) OR EXCLUDE ( EXACTSRCTITLE , "Brain" ) OR EXCLUDE ( EXACTS
RCTITLE , "Human Molecular
Genetics" ) OR EXCLUDE ( EXACTSRCTITLE , "European Journal Of
Neuroscience" ) OR EXCLUDE ( EXACTSRCTITLE , "Journal Of Neuroscience
Research" ) OR EXCLUDE ( EXACTSRCTITLE , "Neuron" ) OR EXCLUDE ( EXACT
SRCTITLE , "Journal Of Neuropathology And Experimental
Neurology" ) OR EXCLUDE ( EXACTSRCTITLE , "Neuroscience
Letters" ) OR EXCLUDE ( EXACTSRCTITLE , "Clinical
Neurophysiology" ) OR EXCLUDE ( EXACTSRCTITLE , "Journal Of Comparative
Neurology" ) OR EXCLUDE ( EXACTSRCTITLE , "Laryngoscope" ) OR EXCLUDE (
EXACTSRCTITLE , "Journal Of
Neurochemistry" ) OR EXCLUDE ( EXACTSRCTITLE , "Neurobiology Of
Disease" ) OR EXCLUDE ( EXACTSRCTITLE , "American Journal Of Human

```

Genetics") OR EXCLUDE (EXACTSRCTITLE , "Electromyography And Clinical Neurophysiology") OR EXCLUDE (EXACTSRCTITLE , "International Review Of Neurobiology") OR EXCLUDE (EXACTSRCTITLE , "Journal Of Neurocytology") OR EXCLUDE (EXACTSRCTITLE , "Journal Of Neuroscience Methods") OR EXCLUDE (EXACTSRCTITLE , "Pain Medicine United States") OR EXCLUDE (EXACTSRCTITLE , "Journal Of Electromyography And Kinesiology") OR EXCLUDE (EXACTSRCTITLE , "Frontiers In Cellular Neuroscience") OR EXCLUDE (EXACTSRCTITLE , "Journal Of Clinical Neurophysiology") OR EXCLUDE (EXACTSRCTITLE , "Journal Of Clinical Neuroscience") OR EXCLUDE (EXACTSRCTITLE , "Molecular Medicine Reports") OR EXCLUDE (EXACTSRCTITLE , "Biochemistry") OR EXCLUDE (EXACTSRCTITLE , "Frontiers In Physiology") OR EXCLUDE (EXACTSRCTITLE , "International Journal Of Molecular Medicine") OR EXCLUDE (EXACTSRCTITLE , "Investigative Ophthalmology And Visual Science") OR EXCLUDE (EXACTSRCTITLE , "Journal Of Biological Chemistry") OR EXCLUDE (EXACTSRCTITLE , "Journal Of Cell Biology") OR EXCLUDE (EXACTSRCTITLE , "Knee Surgery Sports Traumatology Arthroscopy") OR EXCLUDE (EXACTSRCTITLE , "Molecular Neurobiology") OR EXCLUDE (EXACTSRCTITLE , "Neural Regeneration Research") OR EXCLUDE (EXACTSRCTITLE , "Pflugers Archiv European Journal Of Physiology") OR EXCLUDE (EXACTSRCTITLE , "Physiological Reviews") OR EXCLUDE (EXACTSRCTITLE , "Restorative Neurology And Neuroscience") OR EXCLUDE (EXACTSRCTITLE , "Revista De Neurologia") OR EXCLUDE (EXACTSRCTITLE , "Synapse") OR EXCLUDE (EXACTSRCTITLE , "Acta Neurologica Scandinavica") OR EXCLUDE (EXACTSRCTITLE , "American Journal Of Physiology Cell Physiology") OR EXCLUDE (EXACTSRCTITLE , "Cell") OR EXCLUDE (EXACTSRCTITLE , "Frontiers In Neurology") OR EXCLUDE (EXACTSRCTITLE , "Hearing Research") OR EXCLUDE (EXACTSRCTITLE , "International Review Of Cytology") OR EXCLUDE (EXACTSRCTITLE , "Journal Of Neurobiology") OR EXCLUDE (EXACTSRCTITLE , "Journal Of Neurological Sciences") OR EXCLUDE (EXACTSRCTITLE , "Journal Of Reconstructive Microsurgery") OR EXCLUDE (EXACTSRCTITLE , "Journal Of Vascular And Interventional Radiology") OR EXCLUDE (EXACTSRCTITLE , "Molecular And Cellular Neuroscience") OR EXCLUDE (EXACTSRCTITLE , "Neurochemistry International") OR EXCLUDE (EXACTSRCTITLE , "Oncotarget") OR EXCLUDE (EXACTSRCTITLE , "Seminars In Neurology") OR EXCLUDE (EXACTSRCTITLE , "Zhongguo Xiu Fu Chong Jian Wai Ke Za Zhi Zhongguo Xiufu Chongjian Waike Zazhi Chinese Journal Of Reparative And Reconstructive Surgery")) AND (EXCLUDE (EXACTKEYWORD , "Nonhuman") OR EXCLUDE (EXACTKEYWORD , "Animal Experiment") OR EXCLUDE (EXACTKEYWORD , "Animal Tissue") OR EXCLUDE (EXACTKEYWORD , "Animal") OR EXCLUDE (EXACTKEYWORD , "Animal Model") OR EXCLUDE (EXACTKEYWORD , "Nerve Ending") OR EXCLUDE (EXACTKEYWORD , "Rat") OR EXCLUDE (EXACTKEYWORD

WORD , "Rats") OR EXCLUDE (EXACTKEYWORD , "Review") OR EXCLUDE (EXACTKEYWORD , "Disease Models, Animal") OR EXCLUDE (EXACTKEYWORD , "Mice") OR EXCLUDE (EXACTKEYWORD , "Neuromuscular Junction") OR EXCLUDE (EXACTKEYWORD , "Muscle") OR EXCLUDE (EXACTKEYWORD , "Neuromuscular Synapse") OR EXCLUDE (EXACTKEYWORD , "Muscle Contraction")) AND (EXCLUDE (DOCTYPE , "le")) AND (EXCLUDE (SRCTYPE , "k") OR EXCLUDE (SRCTYPE , "b")) AND (EXCLUDE (DOCTYPE , "no"))

2. Pubmed:

((("end plate" OR "endplate" OR "schmorl* node*")) AND ((((((lesion*) OR defect*) OR abnormal*) OR sclerosis) OR calcification*) OR irregular*) OR erosion*)) AND ((classif* OR measure* OR psychometric* OR reliab* OR valid* OR accura* OR reproducib*)) AND (Humans[Mesh])

3. CINAHL:

((((("end plate" OR "endplate" OR "schmorl* node*"))) AND ((((((lesion*) OR defect*) OR abnormal*) OR sclerosis) OR calcification*) OR irregular*) OR erosion*)) AND ((classif* OR measure* OR psychometric* OR reliab* OR valid* OR accura* OR reproducib*)))

4: EMBASE:

((((("end plate" OR "endplate" OR "schmorl* node*"))) AND ((((((lesion*) OR defect*) OR abnormal*) OR sclerosis) OR calcification*) OR irregular*) OR erosion*)) AND ((classif* OR measure* OR psychometric* OR reliab* OR valid* OR accura* OR reproducib*)))

5: Cochrane:

((((("end plate" OR "endplate" OR "schmorl* node*"))) AND ((((((lesion*) OR defect*) OR abnormal*) OR sclerosis) OR calcification*) OR irregular*) OR erosion*)) AND ((classif* OR measure* OR psychometric* OR reliab* OR valid* OR accura* OR reproducib*)))

Appendix B:- Table 0-2: Prisma Checklist

| Section/topic | # | Checklist item | Reported on page # |
|------------------------------------|----|---|--------------------|
| TITLE | | | |
| Title | 1 | Identify the report as a systematic review, meta-analysis, or both. | 19 |
| ABSTRACT | | | |
| Structured summary | 2 | Provide a structured summary including, as applicable: background; objectives; data sources; study eligibility criteria, participants, and interventions; study appraisal and synthesis methods; results; limitations; conclusions and implications of key findings; systematic review registration number. | 19 |
| INTRODUCTION | | | |
| Rationale | 3 | Describe the rationale for the review in the context of what is already known. | 20 |
| Objectives | 4 | Provide an explicit statement of questions being addressed with reference to participants, interventions, comparisons, outcomes, and study design (PICOS). | 20 |
| METHODS | | | |
| Protocol and registration | 5 | Indicate if a review protocol exists, if and where it can be accessed (e.g., Web address), and, if available, provide registration information including registration number. | 23 |
| Eligibility criteria | 6 | Specify study characteristics (e.g., PICOS, length of follow-up) and report characteristics (e.g., years considered, language, publication status) used as criteria for eligibility, giving rationale. | 21 |
| Information sources | 7 | Describe all information sources (e.g., databases with dates of coverage, contact with study authors to identify additional studies) in the search and date last searched. | 21 |
| Search | 8 | Present full electronic search strategy for at least one database, including any limits used, such that it could be repeated. | Appendix 4 |
| Study selection | 9 | State the process for selecting studies (i.e., screening, eligibility, included in systematic review, and, if applicable, included in the meta-analysis). | 21 |
| Data collection process | 10 | Describe method of data extraction from reports (e.g., piloted forms, independently, in duplicate) and any processes for obtaining and confirming data from investigators. | 21 |
| Data items | 11 | List and define all variables for which data were sought (e.g., PICOS, funding sources) and any assumptions and simplifications made. | 21 |
| Risk of bias in individual studies | 12 | Describe methods used for assessing risk of bias of individual studies (including specification of whether this was done at the study or outcome level), and how this information is to be used in any data synthesis. | 22 |
| Summary measures | 13 | State the principal summary measures (e.g., risk ratio, difference in means). | 22 |

| | | | |
|----------------------|----|--|----|
| Synthesis of results | 14 | Describe the methods of handling data and combining results of studies, if done, including measures of consistency (e.g., I^2 for each meta-analysis). | 22 |
|----------------------|----|--|----|

Page 1 of 2

| Section/topic | # | Checklist item | Reported on page # |
|-------------------------------|----|--|---------------------------------------|
| Risk of bias across studies | 15 | Specify any assessment of risk of bias that may affect the cumulative evidence (e.g., publication bias, selective reporting within studies). | 22 |
| Additional analyses | 16 | Describe methods of additional analyses (e.g., sensitivity or subgroup analyses, meta-regression), if done, indicating which were pre-specified. | 25 & 26 |
| RESULTS | | | |
| Study selection | 17 | Give numbers of studies screened, assessed for eligibility, and included in the review, with reasons for exclusions at each stage, ideally with a flow diagram. | 23 |
| Study characteristics | 18 | For each study, present characteristics for which data were extracted (e.g., study size, PICOS, follow-up period) and provide the citations. | 25 & 26 |
| Risk of bias within studies | 19 | Present data on risk of bias of each study and, if available, any outcome level assessment (see item 12). | Figure 2-5: 41 |
| Results of individual studies | 20 | For all outcomes considered (benefits or harms), present, for each study: (a) simple summary data for each intervention group (b) effect estimates and confidence intervals, ideally with a forest plot. | Figure 2-2, 2-3 & 2-4; 38-40 |
| Synthesis of results | 21 | Present results of each meta-analysis done, including confidence intervals and measures of consistency. | 35 & 36, Figure 2-2, 2-3 & 2-4; 38-40 |
| Risk of bias across studies | 22 | Present results of any assessment of risk of bias across studies (see Item 15). | Figure 2-5; 38-40 |
| Additional analysis | 23 | Give results of additional analyses, if done (e.g., sensitivity or subgroup analyses, meta-regression [see Item 16]). | NA |
| DISCUSSION | | | |
| Summary of evidence | 24 | Summarize the main findings including the strength of evidence for each main outcome; consider their relevance to key groups (e.g., healthcare providers, users, and policy makers). | 42 |
| Limitations | 25 | Discuss limitations at study and outcome level (e.g., risk of bias), and at review-level (e.g., incomplete retrieval of identified research, reporting bias). | 43 |
| Conclusions | 26 | Provide a general interpretation of the results in the context of other evidence, and implications for future research. | 443 |

| FUNDING | | | |
|----------------|----|--|----|
| Funding | 27 | Describe sources of funding for the systematic review and other support (e.g., supply of data); role of funders for the systematic review. | vi |

From: Moher D, Liberati A, Tetzlaff J, Altman DG, The PRISMA Group (2009). Preferred Reporting Items for Systematic Reviews and Meta-Analyses: The PRISMA Statement. PLoS Med 6(7): e1000097. doi:10.1371/journal.pmed1000097

For more information, visit: www.prisma-statement.org.

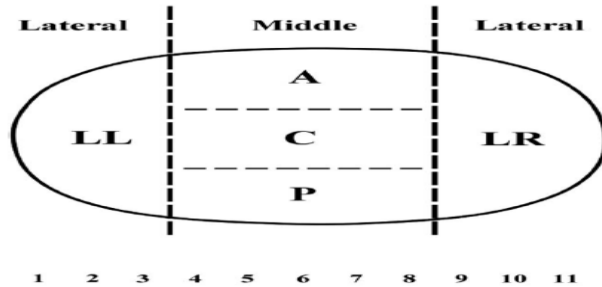
Appendix C: Table 0-3: Evaluation guide comprising the μ CT, reference standard and CT, index test (Feng et al and Brayda-Bruno et al methods) assessments protocol.

A. Definitions of Endplate Defects used on the reference standard (μ CT)

| | |
|-----------------|--|
| Schmorl's Node | A local indentation on the vertebral endplate that has an osseous casing, a smooth and regular margin with an even bottom, and either a round or long appearance ²⁶ . |
| Fracture | A local indentation on the vertebral endplate that is long or irregular in shape with a rough margin. There is no osseous casing and trabecular bone is at least partly exposed. In some cases, osseous callus is present. Includes small fissures, clefts, and fractures. |
| Corner Fracture | An irregular, poorly corticated defect on the epiphyseal rim that may extend to the central endplate. Often, the underlying trabecular bone is widely exposed and may be accompanied by the presence of a limbus vertebra. |
| Erosion | A diffuse breakdown of the endplate where the defect is irregular, shallow, and void of osseous casing. The underlying trabecular bone is widely exposed, and the endplate has a moth-eaten appearance. |
| Jagged | The endplate surface is rough, bumpy, or irregular. Calcium deposition is not significant and trabecular bone is not exposed. |
| Calcification | Intensive calcium deposition upon the endplate with a roughened or irregular appearance with bony outgrowth. Often, the boundary between the epiphyseal rim and central endplate is obliterated. |
| Depression | Significant indentation of the endplate into the vertebral body. Unless accompanied by another defect, the endplate is intact and trabecular bone is not exposed. |

B. Feng et al., method: Endplate defects are defined as a loss or disruption of the smooth appearance of the endplate visible on at least two consecutive sagittal images, regardless of signal changes on the endplate and subchondral trabeculae. Endplates are evaluated for the presence or absence of defects. If present, the endplate defects are further classified using the following classification system. Also, when more than one defect exists on the same endplate, only the larger one will be recorded.

| Feng et al., 2018 | |
|---|--------------------------------------|
| | Diagram Representative Examples |
| Normal endplate is flat (A) or slightly concave (B, C), and smooth in surface. Anterior and posterior vertebral corners could be sharp tips (B) or dull edges (A, C). | <p>Normal endplates</p> |
| Focal defect: Local collapse of the endplate or endplate discontinuity, with or without subchondral bone involvement (D, E, F) | <p>Focal defects</p> |
| Corner defect: Lytic lesions located at the anterior endplate (G, H) or posterior (I) corner of a vertebral body, with apparent disruptions of the subchondral trabeculae | <p>Corner defects</p> |
| Erosive defect: Extensive disruptions or damage of endplate; that is typically an irregular or worm-eaten appearance (J, K, L) | <p>Erosive defects</p> |



Extracted from Feng et al., 2018.

Location and Size of endplate defects

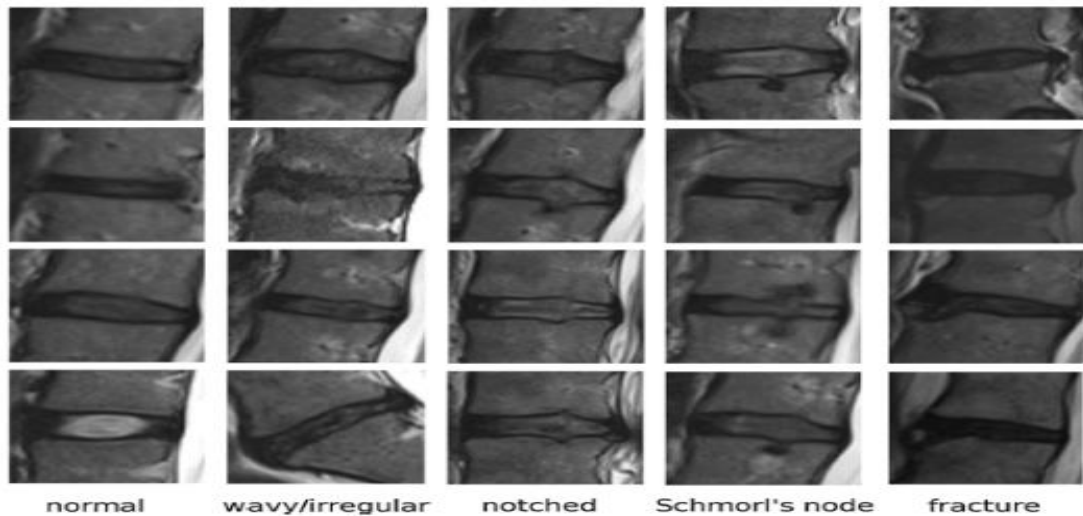
When endplate defects are observed, record spinal level, cranial or caudal location relative to the disc. Based on location, the cross-sectional area of the endplate is divided into four parts. One-fourth of the left and a corresponding one-fourth of the right of the endplate are referred to as the lateral left and lateral right, respectively. While the middle half is further divided into anterior, central and posterior sections.

Anteroposterior diameter of the defect is the ratio of the maximal anteroposterior diameter of an endplate defect to the anteroposterior diameter of the vertebral body measured on the midsagittal image. Anteroposterior diameter of the defect will be estimated by directly measuring the anteroposterior sizes of the defect and the vertebral body at the endplate, using the line function of the DICOM viewer (Horos).

Transverse diameter of the defect is the ratio of the maximal left-right diameter of the endplate defect to the left-right diameter of the vertebral body at the endplate. Endplate defect and vertebrae left-right diameter will be determined by multiplying the image slice thickness and the transitional distance covered by the defect and the vertebral body at the endplate. Axial area of the endplate defect will depend on the location of the defect; area will be rated as none if no defects are present, small if one or two sections are involved, moderate if three sections are involved or large if four or five sections are involved.

C. Brayda-Bruno et al., method: All sagittal slices encompassing the intervertebral space are evaluated to identify defects. If there are two or more defects coexisting on an endplate, the larger one will be recorded. No other measurements of location and size are considered in this system

| Brayda-Bruno et al., method | |
|------------------------------------|--|
| EPSPD phenotypes | Definition |
| Normal | No lesions are visually detected in any of the sagittal MRI slices encompassing the intervertebral space. The curvature of both endplates is physiological |
| Wavy/irregular | No specific lesions but alteration in the shape of physiological curvature |
| Notched | A V-shaped or circular small lesion visible in at least one sagittal MRI slice |
| Schmorl's node | A deep focal defect with a smooth margin and a rounded appearance |
| Fracture | Limbus vertebra, i.e. a well-corticated bone fragment |



Extracted from Brayda-Bruno et al., 2018

Appendix D:- Table 0-4: STARD checklist

| Section & Topic | No | Item | Reported on page # |
|--------------------------|------------|--|--------------------|
| TITLE OR ABSTRACT | | | |
| | 1 | Identification as a study of diagnostic accuracy using at least one measure of accuracy (such as sensitivity, specificity, predictive values, or AUC) | 44 |
| ABSTRACT | | | |
| | 2 | Structured summary of study design, methods, results, and conclusions (for specific guidance, see STARD for Abstracts) | 44 |
| INTRODUCTION | | | |
| | 3 | Scientific and clinical background, including the intended use and clinical role of the index test | 45 |
| | 4 | Study objectives and hypotheses | 46 |
| METHODS | | | |
| <i>Study design</i> | 5 | Whether data collection was planned before the index test and reference standard were performed (prospective study) or after (retrospective study) | 46-49 |
| <i>Participants</i> | 6 | Eligibility criteria | 46 |
| | 7 | On what basis potentially eligible participants were identified (such as symptoms, results from previous tests, inclusion in registry) | 46 |
| | 8 | Where and when potentially eligible participants were identified (setting, location and dates) | 46 |
| | 9 | Whether participants formed a consecutive, random or convenience series | 46 |
| <i>Test methods</i> | 10a | Index test, in sufficient detail to allow replication | 47 |
| | 10b | Reference standard, in sufficient detail to allow replication | 48 |
| | 11 | Rationale for choosing the reference standard (if alternatives exist) | 45-46 |
| | 12a | Definition of and rationale for test positivity cut-offs or result categories of the index test, distinguishing pre-specified from exploratory | 47 |
| | 12b | Definition of and rationale for test positivity cut-offs or result categories of the reference standard, distinguishing pre-specified from exploratory | 47 |
| | 13a | Whether clinical information and reference standard results were available to the performers/readers of the index test | 47 |
| | 13b | Whether clinical information and index test results were available to the assessors of the reference standard | 48-49 |
| <i>Analysis</i> | 14 | Methods for estimating or comparing measures of diagnostic accuracy | 49 |
| | 15 | How indeterminate index test or reference standard results were handled | 49-50 |
| | 16 | How missing data on the index test and reference standard were handled | 49 |
| | 17 | Any analyses of variability in diagnostic accuracy, distinguishing pre-specified from exploratory | 49 |

| | | | |
|--------------------------|------------|---|-------|
| | 18 | Intended sample size and how it was determined | NA |
| RESULTS | | | NA |
| <i>Participants</i> | 19 | Flow of participants, using a diagram | NA |
| | 20 | Baseline demographic and clinical characteristics of participants | NA |
| | 21a | Distribution of severity of disease in those with the target condition | NA |
| | 21b | Distribution of alternative diagnoses in those without the target condition | NA |
| | 22 | Time interval and any clinical interventions between index test and reference standard | NA |
| <i>Test results</i> | 23 | Cross tabulation of the index test results (or their distribution) by the results of the reference standard | 51 |
| | 24 | Estimates of diagnostic accuracy and their precision (such as 95% confidence intervals) | 55 |
| | 25 | Any adverse events from performing the index test or the reference standard | NA |
| DISCUSSION | | | |
| | 26 | Study limitations, including sources of potential bias, statistical uncertainty, and generalisability | 60 |
| | 27 | Implications for practice, including the intended use and clinical role of the index test | 57-60 |
| OTHER INFORMATION | | | |
| | 28 | Registration number and name of registry | 50 |
| | 29 | Where the full study protocol can be accessed | 50 |
| | 30 | Sources of funding and other support; role of funders | |

Curriculum Vitae

| | |
|--|--|
| Name: | Aliyu Lawan |
| Post-secondary Education and Degrees: | <p>University of Maiduguri Maiduguri, Borno, Nigeria 2005-2011 B.M.R. (PT)</p> <p>Bayero University Kano Kano, Kano, Nigeria 2015-2017 M.Sc (PT)</p> <p>The University of Western Ontario London, Ontario, Canada 2019-2022 Ph.D.</p> |
| Honours and Awards: | <p>Oshin and Oyeyemi Awards BMR (PT) Best Graduand Award 2005-2011</p> <p>Nigeria Federal Government Merit Graduate Scholarship M.Sc. Award 2015-2017</p> <p>CMHR Doctoral Fellowship 2019-2021</p> |
| Related Work Experience | <p>Teaching Assistant The University of Western Ontario 1993-1995</p> <p>Lecturer University of Maiduguri 2014-2018</p> <p>Physiotherapist University of Maiduguri Teaching Hospital 2015-2018</p> <p>Physiotherapist Gombe State Ministry of Health 2014-2015</p> |

Publications:

A.Y. Oyeyemi, A.L. Oyeyemi, **A. Lawan**, A. Abubakar, A.A. Rufa’I (2022); Research Productivity of Academics in Medicine and Allied Health Sciences Disciplines in Nigerian Universities: A Cross-sectional Multi-stage Cluster study. *Philippine Journal of Allied Health Sciences* Vol. 6 Iss. 1. [10.36413/pjahs.0601.005](https://doi.org/10.36413/pjahs.0601.005)

A.W. Awotidebe, G.S. Adamu, T.M. Ali, J. Mohammed, I.U. Lawal, **A. Lawan** (2022): Prevalence and Factors Associated with Symptoms of Psychological Distress among Students of Allied Health Sciences in A Nigerian University. *Philippine Journal of Allied Health Sciences* Vol. 6 Iss. 1. [10.36413/pjahs.0601.003](https://doi.org/10.36413/pjahs.0601.003)

U.M. Bello, P. Kannan, M. Chutiyami, D. Salihu, A.M.Y. Cheong, T. Miller, J.W. Pun, A.S. Muhammad, F.A. Mahmud, H.A. Jalo, M.U. Ali, M.A. Kolo, S.K. Sulaiman, **A. Lawan**, I.M. Bello, A.A. Gambo and S.J. Winser (2022) Prevalence of Anxiety and Depression Among the General Population in Africa During the COVID-19 Pandemic: A Systematic Review and Meta-Analysis. *Front. Public Health* 10:814981. doi: 10.3389/fpubh.2022.814981

A. Lawan, J. Crites Videman, M.C. Battié (2021) Association between vertebral endplate structural defects and back pain: A systematic review and meta-analysis. *European Spine Journal*. <https://doi.org/10.1007/s00586-021-06865-6>

A. Lawan, A W Awotidebe, U M Bello, A A Rufa’i, C M Ishaku, M A Masta, A Mukadas (2021): Association between Pregnancy-Related Low Back Pain, Physical Activity and Health-related Quality of Life: A Survey of Pregnant Women in Northern Nigeria. *Philippine Journal of Allied Health Sciences* Vol. 5 Iss. 1. <https://doi.org/10.36413/pjahs.0501.009>

C M Ishaku, B K Jawa, S M Maduagwu, A H Bello, **A Lawan**, A A Rufa’i, A Y Oyeyemi (2021): Pattern and Outcome of Traumatic Spinal Cord Injury Managed at University of Maiduguri Teaching Hospital, Nigeria: A Retrospective Study. *Nigerian Postgraduate Medical Journal*. Volume 28- Issue 1

U.M. Bello, M. Chutiyami, D. Salihu, S. I. Abdu, B. A. Tafida, A. A. Jabbo, A. Gamawa, L. Umar, **A. Lawan**, T. Miller, S. J. Winser (2021) Quality of life of stroke survivors in Africa: a systematic review and meta-analysis. *Quality of Life Research* 30:1–19 <https://doi.org/10.1007/s11136-020-02591-6>

A. Lawan, A. Leung, M.C. Battie (2020): Vertebral Endplate Defects: Nomenclature, Classification and Measurement Methods –A Scoping Review. *European Spine Journal*, DOI:[10.1007/s00586-020-06378-8](https://doi.org/10.1007/s00586-020-06378-8)

A. Lawan, C. Apeyemi, M. Chutiyami, UM. Bello, D. Salihu, BA. Tafida, U. Abubakar, AA. Rufa’i (2020): Impact of Physical Activity and Traumatic Exposure on Occurrence of Gestational Hypertension: A Survey of Pregnant Women in an Armed-conflict Region in Nigeria. *Hypertension in Pregnancy*. <https://doi.org/10.1080/10641955.2020.1765173>

A.Y. Oyeyemi, Z.U. Dahiru, **A. Lawan**, A.L. Oyeyemi, A.A. Akanbi, H.M. Suleiman (2020): Cardiovascular Responses and Perceived Exertion of Young Adults to Head and Shoulder Load Carriage. *Research Journal of Health Science*. 8(1): 45-52

A.A. Rufai, A.L. Oyeyemi, S.M. Maduagwu, A.D. Fredrick, I.A. Saidu, S.U. Aliyu, **A. Lawan** (2019): Work-related musculoskeletal disorders among Nigerian police force. *Niger J Basic Clin Sci*. 16:127-33

A.A. Rufa'i, IA. Saidu, MD. Lawan, AL. Oyeyemi, SU. Aliyu, **A. Lawan**, AM. Jajere, AY. Oyeyem (2019): Outpatients' Satisfaction with the Provision of Physiotherapy Services. *Middle East J Rehabil Health Stud*. 6(1):e69431. doi: [10.5812/mejrh.69431](https://doi.org/10.5812/mejrh.69431)

A. A Rufa'i; AL Oyeyemi; A.F. Kadafa; **A. Lawan**; I.A. Saidu; S.U. Aliyu; A. M. Jajere (2019): Musculoskeletal Pain after Stroke: Prevalence, patterns and distribution among survivors in Maiduguri, North Eastern Nigeria. *Borno Med J.*: 16(1)

A. Lawan, A.W. Awotidebe, A.L. Oyeyemi, A.A. Rufa'i, A.Y. Oyeyemi (2018): Relationship between physical activity and health related quality of life among pregnant women. *African Journal of Reproductive Health*. 22 (3): 80-89, DOI: [10.29063/ajrh2018/v22i3.9](https://doi.org/10.29063/ajrh2018/v22i3.9)

A.L. Oyeyemi, A.Y. Oyeyemi, B.A. Omotara, **A. Lawan**, K.K. Akinroye, R.A. Adedoyin, A. Ramírez (2018): Physical activity profile of Nigeria: implications for research, surveillance and policy. *The Pan African Medical Journal*. 2018; 30:175. doi:[10.11604/pamj.2018.30.175.12679](https://doi.org/10.11604/pamj.2018.30.175.12679)

G. Vincent-Onabajo, H. Daniel, **A. Lawan**, A.M. Usman, M.M. Ali, A. Modu (2018): Musculoskeletal symptoms among family caregivers of community-dwelling stroke survivors in Nigeria. *Journal of Caring Science*. 7 (2): 59-66 doi:[10.15171/jcs.2018.010](https://doi.org/10.15171/jcs.2018.010)

A. Lawan, A.W. Awotidebe, A.L. Oyeyemi, A.Y. Oyeyemi (2017): Patterns and Predictors of Physical Activity among Pregnant Women in Northeast Nigeria. *African Journal for Physical Activity and Health Sciences*, 23(4): 549-562

F.B. Grema, A.Y. Oyeyemi, S.A. Payaneh, **A. Lawan**, A.L. Oyeyemi (2017): Camping Condition and Casual Status of Insurgency Survivors Living with Disability in Internally Displaced Persons Camp in Northeastern Nigeria: a Case Series. *BAJEBAP*. 3 (1): 28-32

A.Y. Oyeyemi, **A. Lawan**, G.J. Akpeli, A.L. Oyeyemi (2016): Comparison of cardiovascular responses following self-selected maximal effort in forward, backward and sideways walking. *Achieves of Medical and Biomedical research*. 2016;3(2): doi: [10.4314/ambr.v3i2.x](https://doi.org/10.4314/ambr.v3i2.x)

A.L. Oyeyemi, C.M. Ishaku, J. Oyekola, H.D. Wakawa, **A. Lawan**, S. Yakubu, A. Y. Oyeyemi (2016): Patterns and associated factors of physical activity among adolescents in Nigeria, *PLoS ONE* 11(2): e0150142. doi: [10.1371/journal.pone.0150142](https://doi.org/10.1371/journal.pone.0150142)

A.Y. Oyeyemi, T.I. Atama, **A.Lawan**, A.L. Oyeyemi (2015): Cardiovascular Parameters of Nigerian Physiotherapy Students During an End of Semester Examination. *Journal of Medical and Biomedical Sciences*. 4(2): 14-20, doi: <http://dx.doi.org/10.4314/jmbs.v4i2.3>

A.Y. Oyeyemi, A.A. Rufa'i, **A. Lawan** (2013): Low Back Pain Incidence, Anthropometric Characteristics and Activities of Daily Living In pregnant women in a Teaching Hospital Center Antenatal clinic, *Tropcal J. Obs Gynae* 30(1)

A.Y. Oyeyemi, U.B. Yero, A.L. Oyeyemi, **A. Lawan** (2012): Cardiovascular Responses following Sweeping in the Recumbent and Straight Standing Positions, *Sahel Medic J*. 15(2): 73-79

Conference Presentations

Bello, U.M., Kannan, P., Chutiyami, M., Salihu, D., Cheong, A.M.Y., Miller, T., Pun, J.W., Muhammad, A.S., Mahmud, F.A., Jalo, H.A., Ali, M.U., Kolo, M.A., Sulaiman, S.K., **Lawan, A.**, Bello, I.M., Gambo, A.A. & Winsler, S.J. Depression and Anxiety Among the General Population in Africa During the COVID-19 Pandemic: A Systematic Review and Meta-Analysis - Nigeria Society of Physiotherapy 62nd Scientific Conference 2022 (Virtual), Enugu, Nigeria, 9-15 October 2022. [Poster presentation]

A Lawan, James Faul, Andrew Leung, Stephanie Leung, Joseph Umoh, David Holdsworth, Michele C. Battié (2022): Detection and Characterization of Vertebral Endplate Structural Defects on Clinical Imaging and Micro-CT: A Diagnostic Test Validity Study. Live Poster Presentation for the London Health Sciences Research Day, May 31, 2022, Virtual

A Lawan, James Faul, Andrew Leung, Stephanie Leung, Joseph Umoh, David Holdsworth, Michele C. Battié (2022): Detection and Characterization of Vertebral Endplate Structural Defects on Clinical Imaging and Micro-CT: A Diagnostic Test Validity Study. Live Poster Presentation for the Canadian Bone and Joint Conference, April 20-22, 2022, Virtual

A Lawan. Leung, S. Leung, M. C. Battié (2022): Detection and Characterization of Vertebral Endplate Structural Defects on Clinical Imaging and Micro-CT: A Diagnostic Test Validity Study. Oral/Podium Presentation for the International Society for Study of Lumbar Spine, May 9-13, 2022, at Boston, MA. USA

A Lawan, Jackson Crites Videman, Michele C. Battié (2021): Association between vertebral endplate structural defects and back pain: A systematic review and meta-analysis. Oral Presentation at the 2021 Back and Neck Pain Forum, Global Virtual Conference, November 11-13, 2021

A Lawan, Anna Belay, Shaima Behery, Suzan Ibrahim, Tiana Ulrich, Kishanthiny Varatharaja, Michael C. Battié (2021): Are paraspinal muscle morphology and composition associated with lumbar spinal stenosis: A systematic review. Poster Presentation at the 2021 Back and Neck Pain Forum, Global Virtual Conference, November 11-13, 2021

A. Lawan, J. Crites Videman, M.C. Battié. Association between vertebral endplate structural defects and back pain: A systematic review and meta-analysis. Presented at the International Society of the Study of the Lumbar Spine annual meeting (virtual). June 1-4, 2021

A. Lawan, J. Crites Videman, M.C. Battié. Association between vertebral endplate structural defects and back pain: A systematic review and meta-analysis. Presented at London Health Sciences Research Day (virtual). May 11, 2021

U.M. Bello, M. Chutiyami, D. Salihu, S. I. Abdu, B. A. Tafida, A. A. Jabbo, A. Gamawa, L. Umar, **A. Lawan**, T. Miller, S. J. Winser (2021) Quality of life of stroke survivors in Africa: a systematic review and meta-analysis. Presented at the World Physiotherapy Congress (Virtual).

A. Lawan, A. Leung, M.C. Battie (2020): Vertebral Endplate Defects: Nomenclature, Classification and Measurement Methods –A Scoping Review. Presented as a Virtual Poster Paper In MSK Rehab Strategies for Now & the Future, at the Canadian Bone and Joint Conference 2020

A. Lawan, A. Leung, M.C. Battie (2020): Vertebral Endplate Defects: Nomenclature and Measurement Methods. Accepted for a Special Poster Presentation for the International Society for Study of Lumbar Spine at the Spine Week scheduled for April 27, 2020 in Melbourne, Australia

A. Lawan, A.W. Awotidebe, A.L. Oyeyemi, A. A. Rufa'i, A. Y. Oyeyemi (2017): Pattern and Associated factors of Physical Activity among Pregnant women in a Tertiary Health Care Hospital. Presented at the 57th Annual General meeting and Scientific Conference of the Nigerian Society of Physiotherapy, Abakaliki, Ebonyi State, Nigeria

A.L. Oyeyemi, A.Y. Oyeyemi, B. A. Omotara, **A. Lawan**, K.K. Akinroye, Andrea Ramírez (2016): A glance at the Nigerian Physical Activity Country Card for Adults. Paper presented at the 6th ISPAH congress in Bangkok, Thailand

A. Lawan, A.Y. Oyeyemi, Z.U. Dahiru, A. L. Oyeyemi, A.A. Akanbi (2016): Cardiovascular responses between load carriage on the head and shoulder. Paper presented at the 56th Annual Scientific Conference and General Meeting of the Nigerian Society of Physiotherapy, Kaduna, Nigeria

A.Y. Oyeyemi, F. Jajimaji, O. A. Jaiyeola, A. L. Oyeyemi, **A. Lawan** (2016): Cardiovascular responses between habitual and non-habitual millet pounder, Paper presented at the 56th Annual Scientific Conference and General Meeting of the Nigerian Society of Physiotherapy, Kaduna, Nigeria

A. Lawan, A.L. Oyeyemi, C.M. Ishaku, J. Oyekola, H. D. Wakawa, S. Yakubu, A.Y. Oyeyemi (2016): Pattern and associated factors of physical activity among Adolescence in Nigeria. Presented at The 2nd International Conference on Physical Activity and Sport for Health and Development in Africa. Kenyatta University, Nairobi, Kenya

A. Lawan (2015): Clinical Auditing; Perspective of the Clinician, Patient and the Community. General Hospital Presentation at State Specialist Hospital Gombe.

S.M. Maduagwu, K. Abdulazeez, A.Y. Oyeyemi, O.A. Jaiyeola, B.J. Aremu, O.A. Akanbi, A.M. Jajere, R.A. Isyaku & **A. Lawan** (2012): Knowledge of effect of exercise on persons living with HIV among health care professionals at the University of Maiduguri Teaching Hospital, Maiduguri. Paper presented at the 22nd Conference of the Nigerian Society of Physiotherapy